JGERI
Journal of Green Energy Research and Innovation
ISSN: 3041-9018

Journal of Green Energy Research and Innovation

Volume 1, Issue 4, Autumn 2024

PUBLISHER
Arak University

Journal of Green Energy Research and Innovation (JGERI)

Publisher: **Arak University**

Director-in-Charge: **Dr. Ali Asghar Ghadimi**

Editor-in-Chief: **Prof. Gevork B. Gharehpetian**

Deputy Editor: **Dr. Abolghasem Daeichian**

Executive Editor**: Dr. Mahyar Abasi**

Coverage area: **International**

Journal Type: **Scientific and technical**

Language: **English**

Frequency: **Quarterly**

Review Time: **4-8 Weeks**

Publication Type: **Electronic, Print**

Open Access: **Yes**

Policy: **Peer-Reviewed**

DOI**: 10.61186/jgeri**

E-mails: **jgeri@araku.ac.ir**

Website: **https://jgeri.araku.ac.ir/**

Address: **Department of Electrical Engineering, Faculty of Engineering, Arak University, Arak, Iran.**

P.O. Box: **38156-8-8349**

Tel: **086-32625099**

Editorial Board

About Journal

JGERI is interested in the results of research in the field of green and renewable energies. The scope of publications of this journal in the field of green energy is extensive and it welcomes novel and innovative studies. Due to the increasing influence of renewable energy in power systems, studies, research, and reports resulting from scientific achievements in this specific area have risen compared to previous decades. This journal is ready to publish specialized articles in all fields related to green energy and interdisciplinary topics related to this scientific branch in the form of open access, which is published annually in four issues as free and open access by Arak University, Iran. **JGERI** is ready to receive the latest research results ranging from analytical methods, numerical simulation, experimental research, and development studies concerning the knowledge and application of green energy.

The following articles are acceptable:

- **Research articles** are expected to present innovative solutions, new concepts, or creative ideas that can help solve existing or emerging technical challenges in the field of green and renewable energy.
- **Review articles** are expected to provide enlightening and specialized reviews, trainings, or case studies on an important topic, timely and widely in the field of green and renewable energies.
- **Applied articles** are expected to share the results of the industry's valuable experiences in dealing with challenging technical issues, developing/adopting new standards, applying new technologies or solving complex problems in the field of green and renewable energies. These articles can have a significant impact on the strategic plans of the industry in the coming years.

Aims and Scope

JGERI is interested on the qualified international multidisciplinary research results related to all aspects of green energy. The scope of **JGERI** is very broad, and welcomes original, novel fundamental and engineering research. We also publish reviews and industrial reports of green energy and its impact on the eco-environment.

We welcome research papers that focus on, but are not limited to, the following areas:

- Policies and Strategies for Green Energy Systems
- Fundamental And Industrial Applications for Green Energy Systems
- Energy Conversion, Control Techniques, and Grid Interactive Systems for Green Energy Systems
- Environmental Impacts of Energy Technologies and Pollution Control
- Materials And Catalysis for Green Energy Systems
- Green Energy Consumption
- Artificial Intelligence, Machine Learning, and Computational Methods in Green Energy Systems
- Public Awareness and Education for Green Energy Systems
- Solar Energy and Photovoltaic
- Wind Energy
- Hydrogen Energy and Energy Storage
- Biofuel and Bioenergy

Each manuscript will go through a rigors peer-review process. you can visit our Instructions for Authors page for information on preparing your manuscript.

Guide for Authors

1. Important points and rules for manuscript submission and publication

-Submitting a manuscript to a journal means that the manuscript is not under review or has not been published anywhere in any other language before.
-The submission of the manuscript for publication by the author, implicitly or explicitly, implies the approval of the organization or body where the author works and has used its affiliation.
-By submitting the manuscript, all authors officially declare their agreement to grant the copyright of the manuscript in case of acceptance to Arak University and **JGERI**. However, the authors are responsible for all the contents published in the manuscript, and the journal is only a reviewer and publisher.
- All authors are required to declare any actual or potential conflicts of interest, including financial, personal, or relationships with individuals or organizations that could affect their work.
- Each of the authors must declare their contribution and role in the manuscript on the Title Page to the journal. The statement of approval of all authors and their role in the manuscript is the responsibility of the corresponding author.
- Authors should note that all manuscripts sent to **JGERI** are checked with Authenticate's CrossCheck software to analyze the authenticity of the content. In this analysis, the overlap and similar texts presented in the submitted manuscripts will be determined.
- **JGERI** makes its manuscripts open to access after publication and there is no charge (APC) for reviewing and publication of manuscripts, and readers can download and use the articles for free.
- All authors, if they had financial support in conducting research related to this manuscript, should briefly state their role. If financial source(s) have no role in the results of the research published by the article, this should also be mentioned by the authors.
- Acknowledgments to individuals and institutions can be mentioned in a separate section at the end of the manuscript before References, and they must not be included as footnotes or in any other form. In this section, it is recommended to mention the names of those who have collaborated during the research (such as those helping in the language correctness aspect of the manuscript, assisting in writing the manuscript or proofreading it, and other cases).
- Non-commercial use of the manuscript will be governed by the Creative Commons Attribution-NonCommercial 4.0 International License, which is currently available at the link (https://creativecommons.org/licenses/by-nc/4.0/). This certificate allows others to use the authors' work in a non-commercial way and utilize it in their research work, although in the new work, they need to acknowledge the authors and mention its non-commercial nature.

2. Initial submission of the manuscript

Submission to this journal is online and you will be accompanied in all the steps of creating a user account and uploading files. All correspondence, including notification of the editor's decision and request for revision, will be made via email. To submit your manuscript, just click on the **Submit Manuscript** option on the journal page. Then, click on **Register** to create an author account. A message will be sent to your email containing your username and password. Then, log in to the manuscript submission system on the Users login page, where you need to enter the username and password and submit your new manuscript. Once you are logged in, you can change your password by clicking on My Home in the top menu. For the next time, just log in to your account. Please include the names, addresses, and email addresses of at least three potential academic reviewers with the paper. Please include reviewers' names and their academic rank, affiliation, and contact information (mail address is mandatory). However, only the editor has the right to decide on the use of suggested reviewers. All the submitted manuscripts undergo the process of plagiarism check with IThenticate software and the review process begins. According to the journal policy, there is a difference between the requirements for initial and revised submission files. Required files for initial submission include three files: **JGERI_Main_Manuscript**, **JGERI_Form_for_Copyright_Transfer_Statement and Conflict_ of_ Interest_ Disclosure** and **JGERI_Cover_Letter**, all three of which must be sent to the journal in PDF format. You can use the links below to download the requirements and suggestions files of these three files.

- JGERI_Guideline_for_Main_Manuscript
- JGERI_Guideline_for_Cover_Letter
- JGERI_Form_for_Copyright_Transfer_Statement and Conflict_ of_ Interest_ Disclosure

3. Submission of the revised manuscript

If the submitted manuscript, after going through the initial review process, is evaluated by the officials and reviewers of the journal and a decision is made to make corrections and revisions in the form of minor or major, the authors are obliged to make the corrections and prepare the response letter to the reviewers within the time specified by the journal. Three files must be sent to the journal at this stage: WORD and PDF files of the revised manuscript (changes should be highlighted), PDF file of the response to the reviewers (including the comments and responses of each of the reviewers separately), Title Page and Authorship file in WORD format (containing two main forms: Title Page and Authorship). The link to download the necessary files along with their requirements and instructions is given below. Points raised in the file **JGERI_Revised_Manuscript** must be followed for compiling the revised manuscript. The authors are obliged to submit the revised file in PDF and WORD format to the journal. Also, different parts of the file **JGERI_Form_for_Title_Page_ and_ Authorship** needs to be completed and signed by the corresponding author, but **JGERI_Response_to_the_Reviewers_Comments** is suggested by the journal and it is not necessary to follow all the points of that file. It should be noted that all the stages of page layout and editing in the form of final publication are the responsibility of the journal. In the completion stages of this process, the cooperation of the authors is needed, and we will inform you at each stage. Thus, the minimum requirements for file compilation are provided in the template file.

- JGERI_Guideline_for_Revised_Manuscript
- JGERI_Form_for_Title_Page_ and_ Authorship
- JGERI_Guideline_for_Response_to_the_Reviewers_Comments

4. **After the final acceptance of the manuscript**

After announcing the final acceptance of the manuscript (reviews may happen several times), the files **JGERI_Revised_Manuscript** and **JGERI_Form_for_Title_Page_ and_ Authorship** will be sent to the paging unit for page layout and final editing. After the final acceptance announcement, the authors will be asked to send a graphic abstract included in a single file. Then, the process of compilation of the manuscript will be completed by the journal and finally, the proof version of the manuscript will be sent to the authors. The authors are obliged to check the proof file completely and report to the journal if they find any ambiguity or error in the final file. In some cases, along with the final proof file of the manuscript, there may be a series of errors and ambiguities in the manuscript, which are sent to the author in the form of comments along with the proof version of the manuscript. The corresponding author is obliged to clarify and resolve these problems and ambiguities in the specified time.

5. **After publication on the journal's website**

After announcing the initial acceptance, the information of the article without its content will be indexed in the Articles in the Press section of the website. After including the article in the issue selected by the journal, the desired article will be indexed in the Current Issue unit along with Vol, No, and pp. Also, the electronic file of the article can be introduced in all scientific references through the DOI link. The important point is that, after acceptance and indexing, the names of the authors cannot be changed, that is, it will not be possible to add, delete, or change the order of the names of the authors and their organizational affiliations.

Cooperative Publication Organization

Renewable Energy Research Institute of Arak University
http://araku.ac.ir/web/riren

Iranian Wind Energy Association
https://www.irwea.org/fa/

Indexing Databases and Social Networks

Google Scholar: https://scholar.google.com/citations?user=47bsJFoAAAAJ&hl=en

Linkedin: https://www.linkedin.com/in/jgeri-arak-university-0818872b9

Academia:https://independent.academia.edu/JournalofGreenEnergyResearchandInnovationJGERI

PaperHive: https://paperhive.org/users/jgeri

GrowKudos: https://www.growkudos.com/profile/j._green_energy_res._innov._jgeri

MyScineceWork: https://www.mysciencework.com/profile/j.green.energy.res.innov.jgeri

SciExplore: https://sciexplore.ir/profiles/author/987-081-740

Magiran: https://www.magiran.com/magazine/8484

Contents

Journal of Green Energy Research and Innovation

Optimal Capacitor Placement in Distributed Networks Polluted with Harmonics in the Presence of Wind Energy-based Distributed Generation Sources

Narges Bagheri, Mohammad Amin Bahramian, Ali Asghar Ghadimi

Highlight

- Minimize losses while meeting voltage and harmonic constraints is proposed
- Proper capacitor size and location selection to improve voltage deviations with low harmonics is suggested.
- Optimally-sized and located parallel capacitors reduce losses, improve voltage profile and stability, and address issues with inductive loads.

Graphical Abstract

Use your device to scan and read the article online

Citation
N. Bagheri, M. A. Bahramian, and A. A. Ghadimi, "Optimal Capacitor Placement in Distributed Networks Polluted with Harmonics in the Presence of Wind Energy-based Distributed Generation Sources," *Journal of Green Energy Research and Innovation*, vol. 1, no. 4, pp. 1-16, 2024.

https://doi.org/10.61186/jgeri.1.4.1

JGERI Journal of Green Energy Research and Innovation

Online ISSN: 3041-9018

Journal of Green Energy Research and Innovation

Journal Homepage: www.jgeri.araku.ac.ir

Optimal Capacitor Placement in Distributed Networks Polluted with Harmonics in the Presence of Wind Energy-based Distributed Generation Sources

Narges Bagheri [1], Mohammad Amin Bahramian *[2,3], Ali Asghar Ghadimi [2,3]

[1] *Department of Electrical Engineering, Payam Golpayegan Institute of Higher Education, Golpayegan, Iran.*
[2] *Department of Electrical Engineering, Faculty of Engineering, Arak University, Arak 38156-8-8349, Iran.*
[3] *Research Institute of Renewable Energy, Arak University, Arak 38156-8-8349, Iran.*

* ***Corresponding Author:*** *a-bahramian@msc.araku.ac.ir*

ARTICLE INFO

Keywords:
Renewable energy,
Capacitor placement,
Harmonics,
Loss reduction,
Distributed generation,
Genetic algorithm.

Article history:
Received: 18 March 2024;
Revised: 20 April 2024;
Accepted: 22 April 2024;

Article type:
Research Article

ABSTRACT

In electrical distribution networks, inefficiencies and instabilities often arise from inductive loads like motors and transformers, which exhibit a lagging power factor. This reduces system capacity, increases losses, and can lead to lower voltage levels. To address these issues, integrating parallel capacitors proves effective, enhancing the power factor, improving voltage profiles, and reducing overall system losses and costs. This research explores the optimal placement of parallel capacitors within a distribution network to manage reactive power effectively, thereby minimizing losses and improving voltage stability and system efficiency. Utilizing DigSILENT Power Factory and MATLAB, a genetic algorithm optimizes the location and sizing of capacitors in a 33-bus distribution network, considering scenarios with and without distributed generation (DG) and the impact of harmonic currents. The study finds that incorrect sizing or placement of capacitors can worsen voltage deviations when higher harmonic levels are present. However, the optimization method accurately determines the best parameters for capacitor installation, ensuring compliance with voltage and harmonic constraints. Deploying more than three to four capacitors does not significantly affect outcomes, while a single busbar capacitor often fails to meet operational standards. In conclusion, strategic capacitor placement and sizing can significantly reduce losses, enhance voltage stability, and mitigate inefficiencies caused by inductive loads. Attention to harmonics is crucial to avoid negative impacts on the network. This approach offers a replicable framework for similar optimizations in other distribution systems, advancing smart grid technology implementation.

1. Introduction

The integration of wind turbine DGs into the electrical grid represents a sustainable energy advancement, albeit accompanied by significant technical challenges. Notably, the power converters within these turbines are sources of harmonic distortion that may jeopardize grid stability and damage electrical equipment [1]. Harmonics can be conceptualized as undesirable electrical "noise" that interferes with the seamless flow of

power, analogous to static on a radio signal. The severity of this distortion is influenced by multiple factors such as the type of converter, its control mechanisms, and the inherent robustness of the grid [2, 3]. A weak grid, akin to a fragile clothesline, might sustain light winds (low wind power) but could falter under strong gusts (high wind power), leading to instability. Additionally, the intrinsic variability of wind energy contributes to further challenges, as inconsistent wind speeds can lead to fluctuations in grid frequency and voltage [4].

The issue of optimal capacitor placement within distribution systems has also garnered considerable attention due to the diverse benefits that capacitors offer, including reduction in power losses [5], enhancement of voltage profiles, augmentation of system capacity and reliability, and improvement of power factor. To address this complex problem, a variety of analytical, heuristic, and metaheuristic methods have been employed to effectively site and size capacitors. Early research efforts centered on articulating the core problem using simplified system models and constraints [5-7]. Sensitivity analyses were employed to pinpoint potential capacitor locations [5], and methods such as gravitational search algorithms were utilized to determine near-optimal capacitor sizes. Additionally, innovative heuristic techniques based on interior point nonlinear programming relaxation have been developed to swiftly identify high-potential buses for capacitors [6].

Further advances have seen the integration of analytical screening with metaheuristic global search strategies, such as the use of loss sensitivity factor analysis for selecting capacitor sites and ant colony optimization for determining optimal sizes [7]. These hybrid methodologies have effectively narrowed the search space, yielding high-quality solutions. Moreover, various metaheuristic approaches tailored for the capacitor placement challenge have been proposed, including particle swarm optimization [8], simulated annealing [9], genetic algorithms [10], discrete particle swarm optimization [11], ant colony search [12], clustering-based optimization [13], and teaching-learning-based optimization [14]. Despite their intensive computational demands, these methods are adept at handling complex, nonconvex constraints across extensive, multidimensional solution spaces.

Recent research has increasingly focused on integrating practical considerations into problem formulations, such as the incorporation of existing capacitors, discrete capacitor sizes, time-varying loads, harmonics, and the costs associated with installation and operation [15]. Other considerations include reliability indices [16], voltage regulation [17], loss reduction [18], and multiobjective trade-offs [19]. Advanced power flow analysis techniques, such as backward/forward sweep and radial distribution power flow, have been pivotal in evaluating complex problem formulations under realistic operating conditions. Test scenarios range from standard IEEE benchmark systems with 13 and 33 buses to large-scale distribution networks with over 200 buses, demonstrating the effectiveness of optimized approaches on extensive operational infrastructures.

In sum, the quality of electricity delivery is generally assessed by ensuring that frequency, waveform, and voltage level parameters remain within standardized and

acceptable limits. Disturbances or harmonic effects primarily manifest through voltage harmonics, although harmonic currents can also induce issues like telephone interference and may influence the network remotely [20]. Although the frequency of electricity supplied by power plants is controllable and unaffected by consumers, the waveform and voltage levels are directly influenced by the loads within the network, especially nonlinear loads that introduce harmonics [21].

This research develops an advanced optimization framework for strategically placing capacitors in distributed networks, particularly those integrating wind energy-based DG sources and experiencing harmonic distortions. The study introduces a multi-objective optimization problem, targeting both power loss reduction and voltage profile enhancement, while also considering voltage limits and harmonic levels. A genetic algorithm, implemented in DigSILENT software, is employed to address this complex problem, enabling detailed evaluation of various scenarios including those without DGs or harmonic impacts, and others focusing solely on loss reduction or voltage improvement.

The evaluation highlights the crucial role of harmonics in capacitor placement. It finds that incorrect capacitor sizing or location can lead to worse voltage deviations when harmonics are present, underscoring the need for incorporating harmonic mitigation in the optimization process. Additionally, the study establishes that installing more than three to four capacitors offers diminishing returns in a 33-bus test system, providing practical insights for system operators on the limits of capacitor utility.

The paper is organized into several sections: Section 1 provides an introduction, background, and motivation for the research; Section 2 details the formulation of the optimization problem, including definitions of variables, objective functions, and constraints; Section 3 describes the solution methodology using a genetic algorithm and the software tools employed; Section 4 discusses the results of simulations under various scenarios, including those without DGs/harmonics and those focusing on loss or voltage profiles, as well as scenarios incorporating DGs/harmonics. Finally, Section 5 summarizes the key findings and conclusions of the study.

2. Problem formulation

2.1. Optimization problem variables

The variables of the optimization problem include the size of capacitor units, the maximum number of capacitor units that can be installed at each busbar or node, and the maximum number of busbars or nodes considered for capacitor placement.

2.2. Objective function

The objective function of this program is to reduce losses and improve the voltage profile. Although users can also input their desired objective function, voltage, and harmonic constraints are added to the objective function by large penalty coefficients.

2.3. Optimization problem constraints

The constraints of the optimal capacitor placement problem include the permissible voltage range of busbars, the maximum loading limit of distribution network lines, and the permissible harmonic range of voltage at network busbars. If the capacitor is installed at the consumer's location, the power loss reduction after installation in the feeder is obtained from Equation (1):

$$LR = R[2I_L(RLF)I_c - I_C^2] \quad (1)$$

In this equation, (I_L) represents the load current, (I_C) denotes the capacitor current, and (RLF) is the reactive load factor. Reducing losses has the following advantages:

- Reduction of maximum load (demand) losses
- Energy savings thanks to energy loss reduction
- Reduction of maximum reactive load
- Voltage improvement

By employing capacitors in a system, an increase in system voltage will be achieved from the installation to the generation points. In a system with a leading power factor, the voltage increases because capacitors can reduce the reactive current transfer of the system. As a result, the reactive and resistive voltage drop in the system decreases [22]. Several formulae are available to estimate the voltage increase caused by capacitors, but typically the following formula is used:

$$\Delta V = \frac{(Kvar)(X_1)}{10(kv)^2} \quad (2)$$

ΔV: The amount of voltage increase at capacitor point

kv: Line-to-line voltage of the system without using a capacitor

$Kvar$: Three-phase nominal reactive power of the capacitor bank

X_1: Inductive reactance of the system at the place of installation of the capacitor, Ohm

Voltage constraint can be expressed as in Equation (3):

$$V_{min} \leq V_i \leq V_{max}: i = 1 \dots N_n \quad (3)$$

N_n is the number of buses or nodes.

The condition of the allowed line currents can be expressed as follows in Equation (4):

$$I_{min} \leq I_j \leq I_{max}: j = 1 \dots N_b \quad (4)$$

Where N_b is the number of lines or branches.

3. Solution methodology

3.1. Genetic algorithm

In this study, a genetic algorithm and DigSILENT are used. The algorithm is a random search method based on natural selection. This algorithm consists of a population, where each individual in the population (chromosomes) represents a sample solution, and each

component of the chromosomes (genes) represents a specific variable of the problem. A new generation is produced by considering the fitness function of individuals and using genetic operators (crossover and mutation), and the fitness function improves over the iterations of the algorithm [23].

In the first step of solving the problem, a random population is used. The genetic algorithm improves the initial population by applying operators on chromosomes and provides it to the next generation. These operators include evolution, crossover, mutation, and shuffling. Through the evolution operator, chromosomes with the highest fitness in each generation are selected and sent to the next generation. Exchange of multiple points is performed among the chromosomes that have reached the previous generation, such that a certain percentage of similar genes between two parent chromosomes are randomly selected and exchanged, creating two new chromosomes. As a result, no defective chromosomes are created due to the crossover operation [24].

A mutation is performed on a limited number of random bits of the chromosomes that have reached the previous generation, and these bits are randomly changed to new, random numbers. This way, the likelihood of the optimization algorithm getting stuck in local optimum points is reduced. In this study, the genetic algorithm available in the MATLAB software is used.

3.2. Software packages

In this work, DigSILENT software is used, and communication with MATLAB is established through a DigSILENT programming language (DPL) program. Initially, the MATLAB program is executed, which receives initial information, including the number of candidate busbars for capacitor locations, the number of considered busbars, and the size of capacitor units, from the user. Then, the genetic algorithm is invoked. After receiving the capacitor placement vector containing the location and size of capacitors, it calls the second DPL file.

In this file, the capacitor placement vector is exported to DigSILENT in the form of a data file and waits for the response. After receiving the software response, which includes the value of the objective function, the results are stored for the next iteration in the first DPL file.

After receiving the file containing the information about the location and size of capacitors in the software, it performs capacitor placement in the network, calculates the objective function, and sends it to MATLAB. The objective function of this program is to reduce losses while considering voltage and harmonic constraints. Although the user can also input their desired objective function, voltage, and harmonic constraints are added to the objective function by large penalty coefficients. This approach ensures that the genetic algorithm distances itself from capacitor placement in busbars that may lead to severe voltage drop or worse harmonic conditions.

The second DPL is used to calculate losses. This program calculates losses and the objective function after optimal capacitor placement. It is worth mentioning that in the DigSILENT software, the total network losses or losses of individual lines are not

calculated in the presence of harmonics. Therefore, these calculations need to be programmed. Figure 1 shows the flowchart of problem-solving steps.

4. Simulation and results

4.1. Base case analysis

In this section, simulation results of optimal capacitor placement in a standard distribution network are presented. The set of software and developed programs is capable of determining the location and number (size) of capacitor banks for a hypothetical network with harmonics in a way that minimizes the objective function. The objective function is a combination of user-defined coefficients for losses and voltage profiles.

The network under study is a standard IEEE 33-bus distribution network with a base voltage of 11 kV. The linear single-line diagram of the IEEE 33-bus network and the locations of each busbar are illustrated in Figure 2.

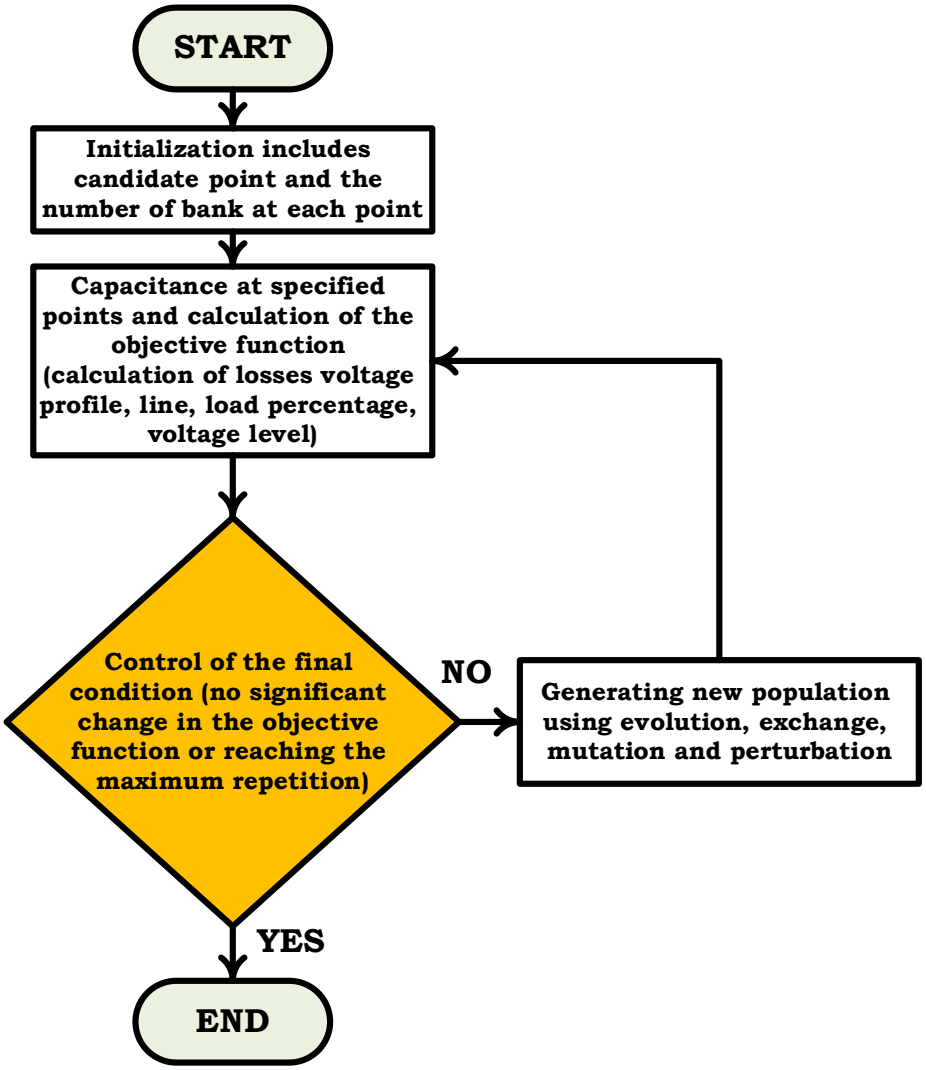

Figure 1. The flowchart of problem-solving steps.

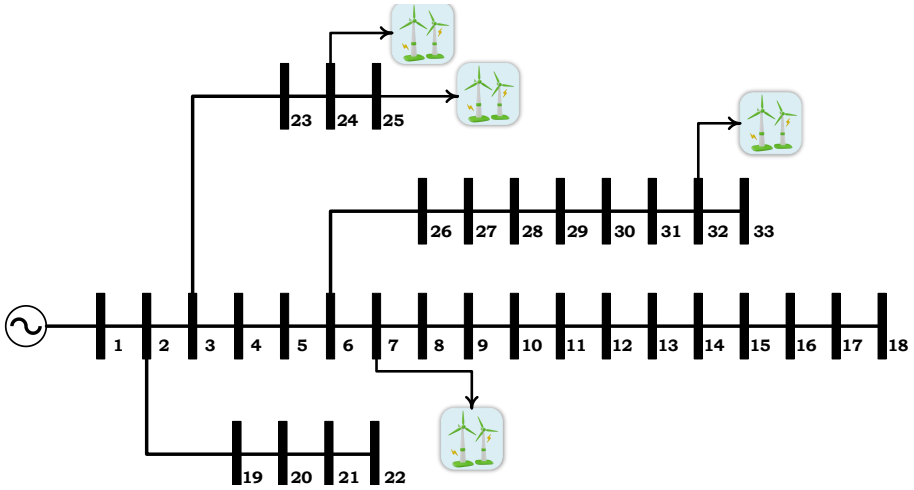

Figure 2. Single-line view of the 33-bus network.

Total System Summary					Study Case: Study Case				Annex: / 1
No. of Substations	0		No. of Busbars	33	No. of Terminals	0		No. of Lines	32
No. of 2-w Trfs.	0		No. of 3-w Trfs.	0	No. of syn. Machines	0		No. of asyn.Machines	0
No. of Loads	32		No. of Shunts/Filters	0	No. of SVS	0			
Generation	=	0.00 kW	0.00 kvar		0.00 kVA				
External Infeed	=	3917.68 kW	2435.16 kvar		4612.83 kVA				
Load P(U)	=	3715.00 kW	2300.00 kvar		4369.35 kVA				
Load P(Un)	=	3715.00 kW	2300.00 kvar		4369.35 kVA				
Load P(Un-U)	=	0.00 kW	0.00 kvar						
Motor Load	=	0.00 kW	0.00 kvar		0.00 kVA				
Grid Losses	=	202.68 kW	135.16 kvar						
Line Charging	=		0.00 kvar						
Compensation ind.	=		0.00 kvar						
Compensation cap.	=		0.00 kvar						
Installed Capacity	=	0.00 kW							
Spinning Reserve	=	0.00 kW							
Total Power Factor:									
Generation	=	0.00 [-]							
Load/Motor	=	0.85 / 0.00 [-]							

Figure 3. Summary of the standard 33-bus network.

In this study, the standard distribution network is modelled in DigSILENT Power Factory software. Additionally, MATLAB software is used for optimization calculations and the genetic algorithm. A program is written in the DPL to establish communication between the network and the genetic algorithm. A summary of the standard network report is shown in Figure 3. As illustrated, the total losses of the network are equal to 202.68 kW.

To consider the effects of DG and harmonics resulting from nonlinear loads, the following modifications, according to reference [25], were applied to the standard network. These modifications include adding DG at busbars 7, 24, 25, and 32, and replacing the existing linear load with a nonlinear (harmonic) load at busbars 6 and 27.

Simulation results indicate that in the first stage, with the introduction of DG and a total generation of 800 kW, network losses decrease to 172.8 kW. In the next stage, with an increase in load, network losses increase to 510.45 kW. To consider the effects of harmonics, according to Table 1, the harmonic model of the six-pulse converter was added to DG and nonlinear loads. The harmonics of the six-pulse converter are illustrated in Figure 4. The network losses with harmonics present will be 518.18 kW, indicating an increase of 8 kW compared to the harmonic-free condition.

Table 1. Test network changes compared to the standard network.

Type of change	Type of Harmonic	Q (kVar)	P (kW)	Busbar No.
Adding a DG	6 pulse converter	97	200	7
	6 pulse converter	97	200	24
	6 pulse converter	97	200	25
	6 pulse converter	97	200	32
Alternative Load	6 pulse converter	750	1000	6
	6 pulse converter	750	1000	27

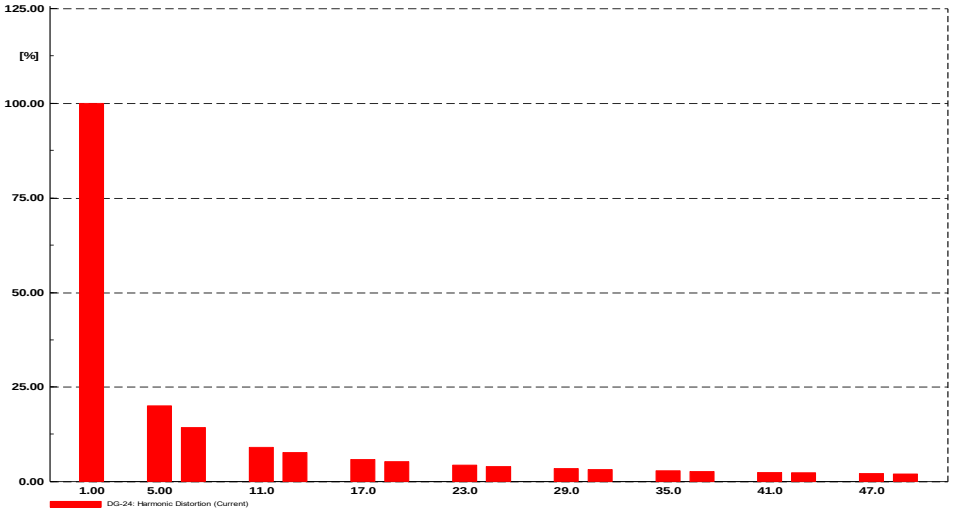

Figure 4. Spectrum of current harmonics of six-pulse converter.

```
==========================================
Capacitor Position Bus  = 30
==========================================
Capacitor Capacity KVAR  = 1400
==========================================
Cost Function = 143.6136
==========================================
```

Figure 5. Sample output of a MATLAB program for a capacitor-compensated busbar.

To place capacitors using the genetic algorithm, MATLAB software has been employed. For program execution, the number of candidate capacitor busbars and the size of capacitor units are specified as inputs. In this study, simulations were performed assuming 1 to 4 capacitor busbars.

4.2. Capacitor placement without harmonic load

Without considering harmonic loads and DG, capacitor placement is performed to reduce losses and improve voltage profile. In the first stage, capacitor placement is done solely with the objective of loss reduction. The output of the program is illustrated in Figure 5. Therefore, if there is one candidate busbar capacitor with the loss reduction objective, then busbar number 30, with a size of 1400 kVA, will be the optimal busbar. In this case, network losses will decrease from 202.68 kW to 143.6 kW. The complete results are shown in Table 2. Each of the solutions converged to an answer after approximately 6000 iterations.

Next, capacitor placement to improve the voltage profile has been carried out. In this case, the percentage of voltage drop or rise in all network busbars has been selected as the objective function. A decrease in this value implies that the voltage at busbars is approaching unity. The results of running the program are shown in Table 3.

According to Figure 6, using the objective function to improve the voltage profile (reduce the distance of voltages from unity) has been achieved successfully through capacitor placement. However, a crucial point to consider is the comparison of network losses before and after capacitor placement. The network losses with this capacitor placement approach have reached approximately 540 kW, showing an increase close to 170% compared to network losses without capacitors. Therefore, it can be concluded that the voltage index alone may not be sufficient.

Table 2. Capacitor placement for loss reduction in test network without dg and harmonic loads.

Number of candidate busbars for capacitor placement	Losses (kW)	Total capacitance placement (kVAR)	Capacitance placement per busbar in each order (kVAR)	Capacitor-placed busbars
0	68/202	0	-	-
1	6/143	1400	1400	30
2	7/135	1700	550-1150	11-30
3	2/132	2150	550-500-1100	24-13-30
4	2/132	2150	1000-500-250-400	5-24-12-30

Table 3. Results of capacitor placement for voltage profile improvement in test network without DG and harmonic loads.

Number of candidate busbars for capacitor placement	Voltage profile index	Total capacitance placement (kVAR)	Capacitance placement per busbar in each order (kVAR)	Capacitor-placed busbars
0	1/170	0	-	-
1	5/45	5000	5000	8
2	7/14	5850	1500-4350	13-28
3	4/12	8490	3650-2300-2450	12-24-30
4	0/9	7900	1650-4250-1100-900	25-26-31-16

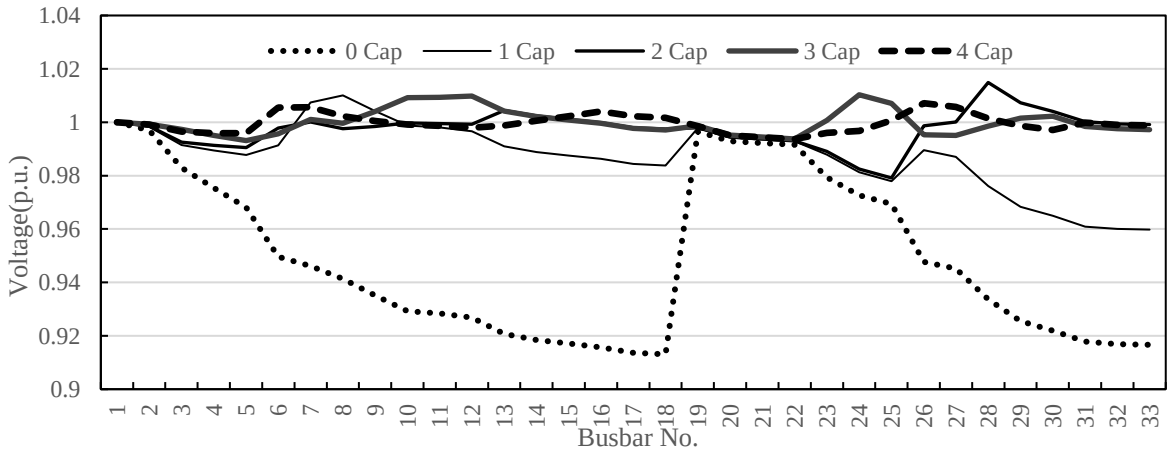

Figure 6. Standard network bus voltages after capacitor placement to improve voltage profile.

Considering that the proximity of busbar voltages can create a good margin of confidence for network utilization, it is possible to use the sum of two indices, losses, and voltage profile, for optimal capacitor placement. It should be noted that in some research, the voltage placement index within the normal range (0.5 to 0.95 per unit (p.u.)) has been considered as the voltage share in the objective function. This index, considering load variations, will not provide a suitable safe range for the operator. In Table 4, simulation results considering both loss and voltage indices simultaneously are presented.

As shown in Figure 7, considering the objective function with a combined index, in addition to reducing losses, the voltage is also within the permissible range (above 0.95 p.u.). In this case, network losses amount to 145 kW, which is a reduction compared to the base case (202 kW). In Figure 7, the voltage profile status is depicted for two scenarios with the objective function of loss index and the objective function of voltage index.

Table 4. Results of capacitor placement to reduce losses and improve voltage profile in the test network without the presence of DG and harmonic loads.

Number of candidate busbars for capacitor placement	Total index (losses + 100 times the sum of voltage deviations)	Total capacitance placement (kVAR)	Capacitance placement per busbar in each order (kVAR)	Capacitor-placed busbars
0	8/372	0	-	-
1	9/291	3750	3750	7
2	244	2300	800-1500	14-30
3	9/235	2800	1150-500-1150	7-30-14
4	8/232	3250	600-900-1200-550	24-7-30-14

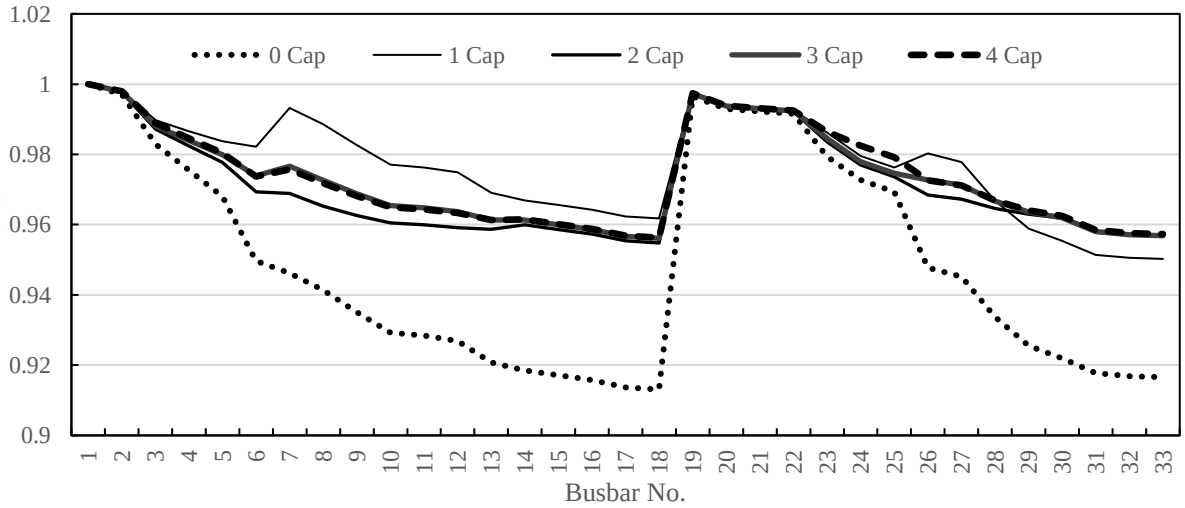

Figure 7. Comparison of bus voltages to simultaneously reduce losses and improve voltage profile in the standard network.

4.3. Capacitor placement with harmonic loads and DG

Taking harmonic loads into account in the network, harmonic reduction can be added to other capacitor placement objectives. If capacitor placement is done incorrectly in a harmonic-rich network, it can worsen harmonic distortion conditions. For example, Figure 8 shows the result of incorrectly placing a capacitor in the test network at only 50 kW at busbar number 6. As illustrated, harmonic distortion has significantly increased after capacitor placement. In practice, such a situation can lead to the fuse of the capacitor bank burning out.

The occurrence of intensification is near harmonic number 49. Also, the change in the behavior of the impedance observed from busbar number 6 with the presence of 50, 100, and 1000 kVar capacitor banks in this busbar, based on the change in the frequency coefficient, is shown.

Given the mentioned content, it can be concluded that capacitor placement in harmonic networks should be done with precision and sufficient study. Therefore, reducing harmonic distortion can also be added to the objective function of optimal capacitor placement. Considering the direct relationship between losses and harmonics, if the objective function is chosen as losses, it is expected that harmonic distortion in the network will decrease. Thus, the level of harmonic distortion and bus voltages can be considered as constraints, and the objective function can be selected as losses. Table 5 presents the results of optimal capacitor placement to reduce losses, with a constraint on voltage drop or increase not exceeding 5% and a maximum overall voltage distortion of 5%.

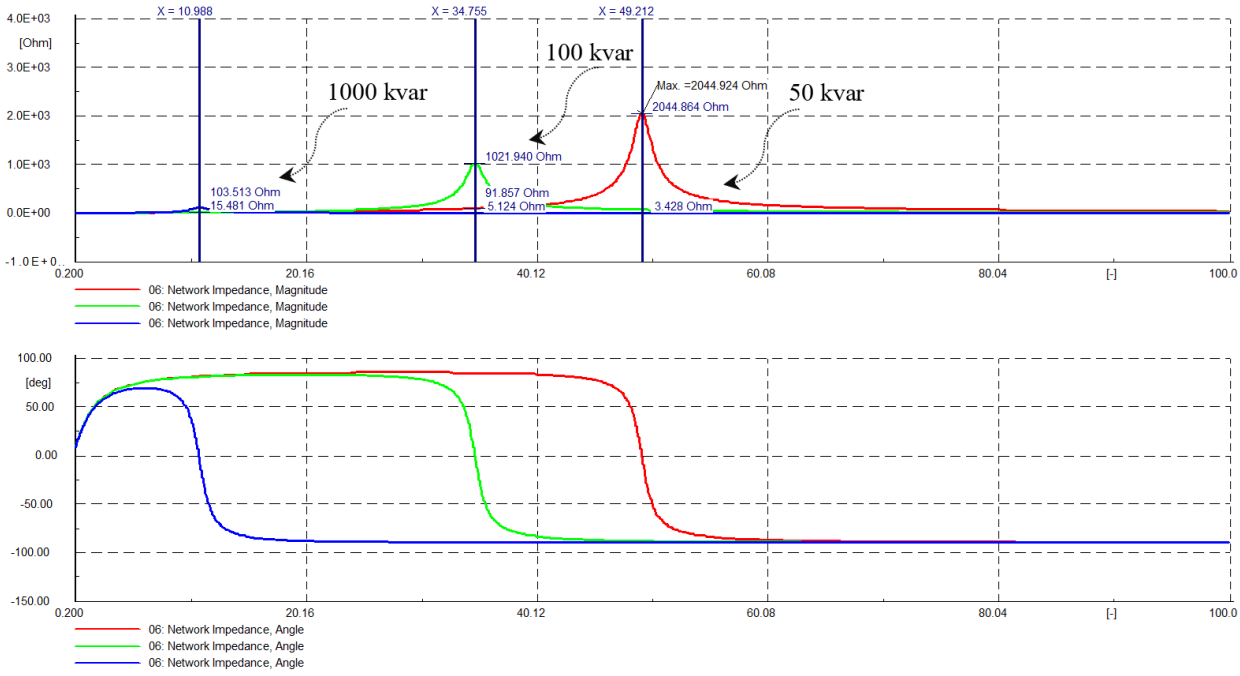

Figure 8. Frequency scan of the impedance of bus No. 6 for various capacitor sizes.

The examination of Table 5 indicates that using a single capacitor bank does not provide the possibility of reducing losses. However, employing two or more capacitors for installation can reduce losses in the harmonic network. The voltage and harmonic status of the capacitors are illustrated in Figures 9 and 10, respectively. As shown in Figure 9, it was not possible to meet the voltage constraint in buses 26 to 33 using a single capacitor. In other cases (utilizing more than one capacitor), the voltage constraint has been achieved. The results in Figure 10 demonstrate that, despite having a single capacitor for capacitive placement, the reduction of total voltage distortion in buses 26 to 33 was not feasible.

Table 5. Capacitor placement to reduce losses and constraints on harmonic distortion in the presence of DG.

Number of candidate busbars for capacitor placement	Total Losses Index (kW)	Total capacitance placement (kVAR)	Capacitance placement per busbar in each order (kVAR)	Capacitor-placed busbars
0	18/518	0	-	-
1	17/558	4750	4750	9
2	400	5050	2800-2250	11-29
3	5/347	5350	2350-1050-1950	30-13-7
4	6/325	5000	800-1400-2050-750	15-32-7-29

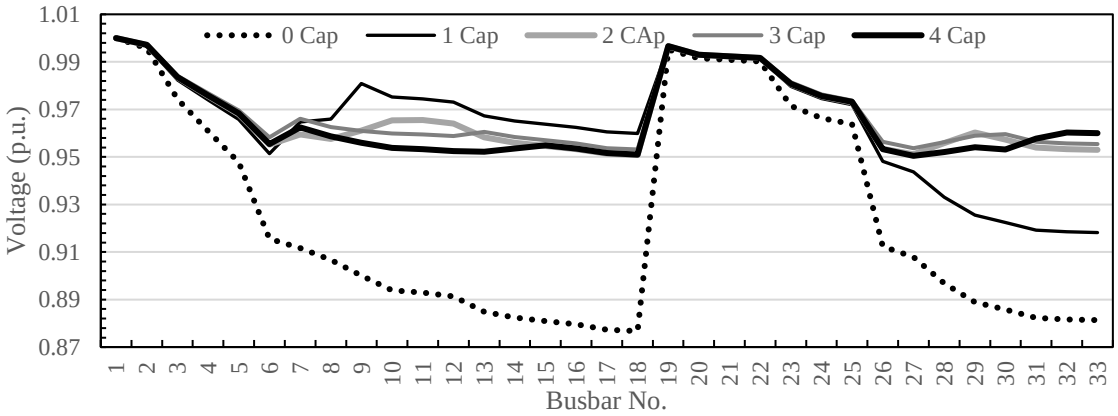

Figure 9. Busbar voltages to reduce losses and constraints on voltage and harmonic distortion.

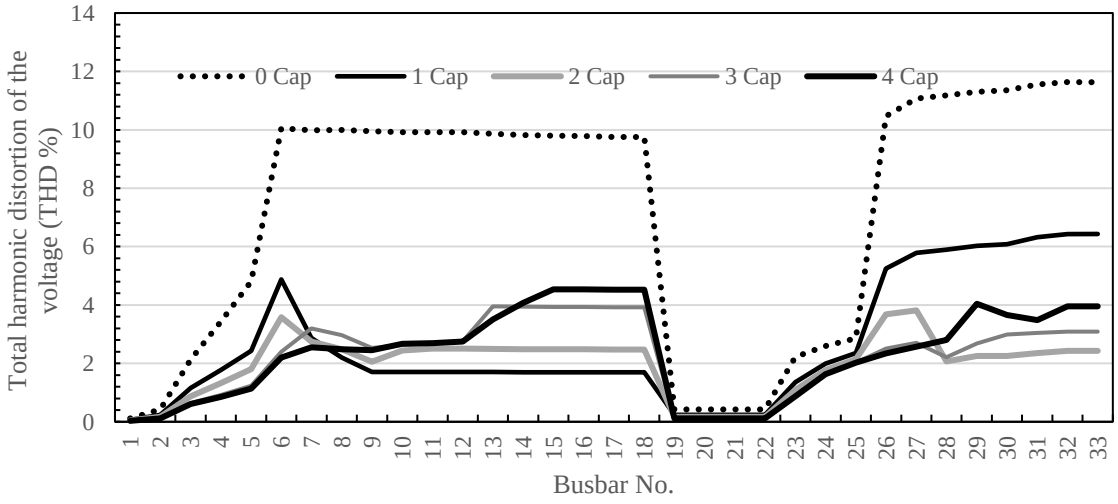

Figure 10. Total voltage distortion in network busbars with the presence of harmonic sources and DG.

However, in other capacitor placement scenarios, the overall voltage distortion remained below the standard limit (5%). Simulation results in this study have been compared with the reference [25], and the comparison is presented in Table 6.

5. Conclusion

The key achievements and findings from this study on the optimal placement of capacitors in distributed networks, particularly those incorporating wind energy-based DGs and experiencing harmonic distortions, are significant. Notably, the study found that when harmonic loads were not considered, optimization could effectively reduce network losses by up to 33% compared to baseline scenarios. However, targeting capacitors solely to enhance voltage profiles led to increased network losses, underscoring the necessity of integrating both loss reduction and voltage stabilization in the optimization objectives.

Employing a combined index objective function that addressed both losses and voltage deviations enabled the optimization to secure a 28% reduction in losses while maintaining voltage levels above 0.95 p.u. This highlights the effectiveness of a multi-objective approach in achieving comprehensive system enhancements. In scenarios involving harmonic-generating loads and wind-based DGs, inappropriate capacitor placement significantly exacerbated harmonic distortions, which could damage equipment.

The optimization methodology developed in this research successfully identified capacitor locations and sizes that minimized losses and maintained both voltage and harmonic distortion within acceptable limits. The analysis showed that using a single capacitor bank was inadequate for meeting both voltage and harmonic constraints. Conversely, the deployment of two or more optimally placed capacitors led to a 37% reduction in losses relative to the baseline with harmonics, while keeping voltages above 0.95 p.u. and the THD below 5%.

These outcomes affirm the robustness of the proposed optimization framework in determining optimal capacitor placements that balance the critical objectives of reducing losses, regulating voltage, and mitigating harmonic disturbances in distributed networks with renewable energy sources. Ultimately, this research delivers substantial advancements in addressing the complexities of capacitor placement in modern distribution grids amid growing DG penetration and power electronic loads, offering network operators a viable, efficient, and reliable solution to improve system performance, efficiency, and quality.

Table 6. Comparison of simulation results with the results of the reference [25].

Results	Proposed method		Reference [25]	
	Before Capacitor Placement	After Capacitor Placement	Before Capacitor Placement	After Capacitor Placement
$P_{Loss}(KW)$	518	325	452	250
$THD_{max}(\%)$	10	4.8	7.41	4.98
$V_{max}(pu)$	1.05	1.05	1.05	1.0500
$V_{min}(pu)$	0.88	0.95	0.957	0.992

References

[1] A. Argüello, R. Torquato, and W. Freitas, "Passive Filter Tuning for Harmonic Resonance Mitigation in Wind Parks," *IEEE Transactions on Power Delivery*, vol. 38, no. 6, pp. 3834-3846, 2023.

[2] A. M. Eltamaly, Y. S. Mohamed, A. -H. M. El-Sayed, and A. N. A. Elghaffar, "Analyzing of Wind Distributed Generation Configuration in Active Distribution Network," *8th International Conference on Modeling Simulation and Applied Optimization (ICMSAO)*, pp. 1-5, 2019.

[3] P. Catalán, Y. Wang, J. Arza, and Z. Chen, "A Comprehensive Overview of Power Converter Applied in High-Power Wind Turbine: Key Challenges and Potential Solutions," *IEEE Transactions on Power Electronics*, vol. 38, no. 5, pp.6169-6195, 2023.

[4] D. A. Ciupăgeanu, G. Lăzăroiu, and L. Barelli, "Wind Energy Integration: Variability Analysis and Power System Impact Assessment," *Energy*, vol. 185, pp.1183-1196, 2019.

[5] Y. M. Shuaib, M. S. Kalavathi, and C. C. Rajan, "Optimal Capacitor Placement in Radial Distribution System using Gravitational Search Algorithm," *International Journal of Electrical Power & Energy Systems,* vol. 64, pp. 384-397, 2015.

[6] S. Segura, R. Romero, and M. J. Rider, "Efficient Heuristic Algorithm Used for Optimal Capacitor Placement in Distribution Systems," *International Journal of Electrical Power & Energy Systems*, vol. 32, no. 1, pp. 71-78. 2010.

[7] A. A. Abou El-Ela, R. A. El-Sehiemy, A. M. Kinawy, and M. T. Mouwafi, "Optimal Capacitor Placement in Distribution Systems for Power Loss Reduction and Voltage Profile Improvement," *IET Generation, Transmission & Distribution*, vol. 10, no. 5, pp. 1209-1221, 2016.

[8] A. Elsheikh, Y. Helmy, Y. Abouelseoud, and A. Elsherif, "Optimal Capacitor Placement and Sizing in Radial Electric Power Systems," *Alexandria Engineering Journal*, vol. 53, no. 4, pp. 809-816, 2014.

[9] A. H. Etemadi, and M. Fotuhi-Firuzabad, "Distribution System Reliability Enhancement using Optimal Capacitor Placement," *IET Generation, Transmission & Distribution*, vol. 2, no. 5, pp. 621-631, 2008.

[10] S. Lohia, O. P. Mahela, and S. R. Ola, "Optimal Capacitor Placement in Distribution System using Genetic Algorithm," *IEEE 7th Power India International Conference (PIICON),* pp. 1-6, 2016.

[11] A. A. Eajal, and M. E. El-Hawary, "Optimal Capacitor Placement and Sizing in Unbalanced Distribution Systems with Harmonics Consideration Using Particle Swarm Optimization," *IEEE Transactions on Power Delivery*, vol. 25, no. 3, pp. 1734-1741, 2010.

[12] C. T. Su, C. F. Chang, and J. P. Chiou, "Optimal Capacitor Placement in Distribution Systems Employing Ant Colony Search Algorithm," *Electric Power Components and Systems*, vol. 33, no. 8, pp. 931-946, 2005.

[13] M. E. Baran, and F. F. Wu, "Optimal Capacitor Placement on Radial Distribution Systems," *IEEE Transactions on Power Delivery*, vol. 4, no. 1, pp. 725-734, 1989.

[14] A. Z. Abass, D. A. Pavlyuchenko, and Z. S. Hussain, "Methods Comparison for Optimal Capacitor Placement in Distribution System," *International Multi-Conference on Industrial Engineering and Modern Technologies (FarEastCon),* pp. 1-6, 2020.

[15] Y. Xu, Z. Y. Dong, K. P. Wong, E. Liu, and B. Yue, "Optimal Capacitor Placement to Distribution Transformers for Power Loss Reduction in Radial Distribution Systems," *IEEE Transactions on Power Systems*, vol. 28, no. 4, pp. 4072-4079, 2013.

[16] J. Vuletić, and M. Todorovski, "Optimal Capacitor Placement In Radial Distribution Systems using Clustering Based Optimization," *International Journal of Electrical Power & Energy Systems*, vol. 62, no. 1, pp. 229-236, 2014.

[17] S. Sultana, and P. K. Roy, "Optimal Capacitor Placement in Radial Distribution Systems using Teaching Learning Based Optimization," *International Journal of Electrical Power & Energy Systems*, vol. 54, pp. 387-398, 2014.

[18] A. A. El-Fergany, "Optimal Capacitor Allocations using Evolutionary Algorithms," *IET Generation, Transmission & Distribution*, vol. 7, no. 6, pp. 593-601, 2013.

[19] R. S. Rao, S. V. Narasimham, and M. Ramalingaraju, "Optimal Capacitor Placement in a Radial Distribution System using Plant Growth Simulation Algorithm," *International Journal of Electrical Power & Energy Systems*, vol. 33, no. 5, pp. 1133-1139, 2011.
[20] A. Kazemi, and A. M. Dezfuli, "Optimal Placement of Distributed Energy Resources to Reduce Losses, Improve Voltage Profile, and Convert it into a Self-healing Smart Grid," *Journal of Green Energy Research and Innovation*, vol. 1, no. 1, pp. 1-33, 2024.
[21] S. D. Kermani, A. Morsagh Dezfuli, R. Behvandi, and M. Kankanan," Voltage Sag Reduction by ANFIS in Wind Turbine Generation Units," *Journal of Green Energy Research and Innovation*, vol. 1, no. 3, pp. 49-76, 2024.
[22] Institute of Electrical and Electronics Engineers, "IEEE Guide for Application of Shunt Power Capacitors," IEEE Std 1036-1992, 1992.
[23] B. T. Luke, "Genetic algorithms and beyond," *Data Handling in Science and Technology*, vol. 23, pp. 3-54, 2003.
[24] D. E. Goldberg, and K. Deb, "A Comparative Analysis of Selection Schemes Used in Genetic Algorithms," *Foundations of genetic algorithms*, vol. 1, pp. 69-93, 1991.
[25] S. A. Taher, M. Hasani, and A. Karimian, "A Novel Method for Optimal Capacitor Placement and Sizing in Distribution Systems with Nonlinear Loads and DG using GA," *Communications in Nonlinear Science and Numerical Simulation*, vol. 16, no. 4, pp. 851-862, 2011.

Declaration of Competing Interest

The authors declare that they have no known competing financial interests or personal relationships that could have appeared to influence the work reported in this paper. The ethical issues, including plagiarism, informed consent, misconduct, data fabrication and/or falsification, double publication and/or submission, redundancy, have been completely observed by the authors.

Credit Authorship Contribution Statement

Narges Bagheri: Conceptualization, Software, Roles/Writing - original draft. **Mohammad Amin Bahramian:** Resources, Roles/Writing - original draft. **Ali Asghar Ghadimi:** Conceptualization, Formal analysis, Methodology, Roles/Writing - original draft.

Bibliography

Narges Bagheri was born in Shahrekord, Iran, in 1988. She received her associate's degree in Electronics Engineering from Khorramabad Girls' Technical and Vocational School, Lorestan, Iran, in 2007, her bachelor's degree in Electronics Engineering from Shahrekord Islamic Azad University, Shahrekord, Iran, in 2011, and her master's degree in Power Systems Engineering from Payam Golpayegan Institute of Higher Education, Golpayegan, Iran, in 2017. She is currently working as a building electrical supervisor engineer in the Construction Engineering Organization of Chaharmahal-o-Bakhtiari province. Her special interests are operation, energy management, renewable energy and stability of power systems.

Mohammad Amin Bahramian received a B.Sc. degree in electrical engineering from Arak University, Arak, Iran, in 2020. He is now an M.Sc. graduate in electrical engineering from Arak University, having completed his degree in 2022. He also is currently employed at "Camellia Electronics Industry Innovators," where he contributes to the field of power electronics, specializing in DC-DC converters and LED drivers. His research interests include Power Converters, Renewable Energy Systems, Smart Grid Technologies and Digital Control Systems.

Ali Asghar Ghadimi received his M.Sc. and Ph.D. degree in Power Engineering from Tehran Polytechnich University, Tehran, Iran in 2002 and 2008 respectively. He is currently Associate Professor and research member in Department of Electrical Engineering at Arak University, Arak, IRAN. His current research interests are in the area of MicroGrid, Renewable Energy, and Power system optimal planning.

Journal of Green Energy Research and Innovation

Robust Control of Load Voltage in an Islanded Wind Energy Conversion System Using Nonlinear Methods

Adel Sotoudeh, Mohammad Mahdi Rezaei, Mohammadreza Moradian

Highlight

- Using input-output controller and sliding mode simultaneously
- Load side voltage control using voltage converter
- Two-stage control of squirrel cage induction generator (SCIG)

Graphical Abstract

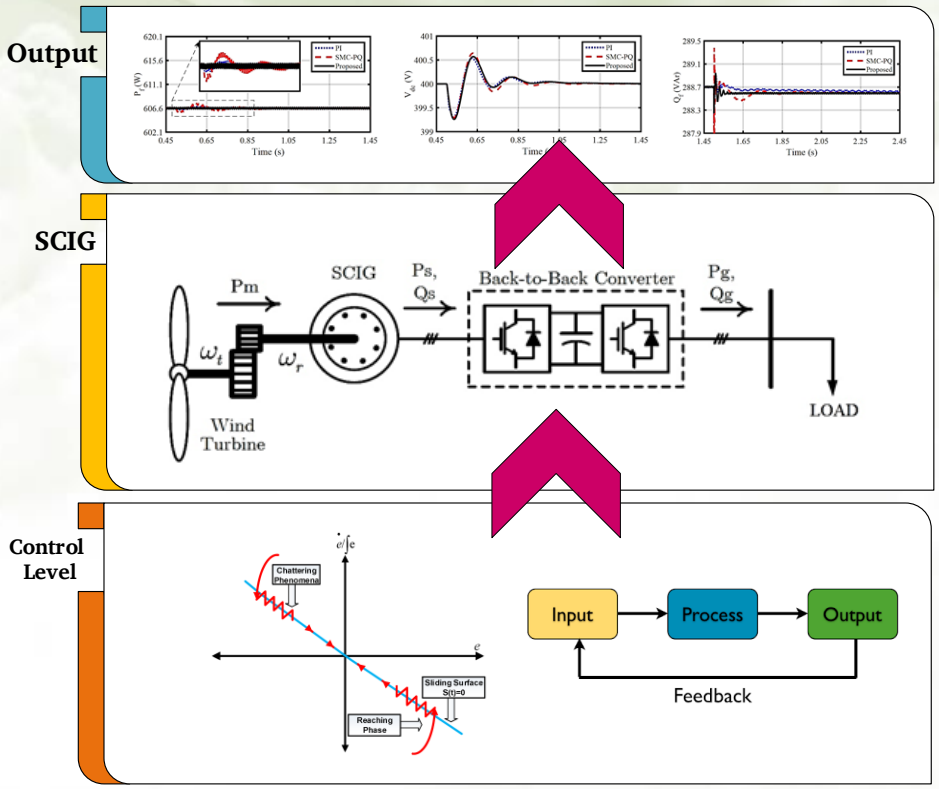

Use your device to scan and read the article online

Citation

A. Sotoudeh, M. M. Rezaei, and M. Moradian, "Robust Control of Load Voltage in an Islanded Wind Energy Conversion System Using Nonlinear Methods," *Journal of Green Energy Research and Innovation*, vol. 1, no. 4, pp. 17-34, 2024.

https://doi.org/10.61186/jgeri.1.4.17

JGERI Journal of Green Energy Research and Innovation

Online ISSN: 3041-9018

Journal of Green Energy Research and Innovation

Journal Homepage: www.jgeri.araku.ac.ir

Robust Control of Load Voltage in an Islanded Wind Energy Conversion System Using Nonlinear Methods

Adel Sotoudeh [1], Mohammad Mahdi Rezaei [1*], Mohammadreza Moradian[2]

[1] *Department of Electrical Engineering, Khomeinishahr Branch, Islamic Azad University, Khomeinishahr, Isfahan, Iran.*
[2] *Department of Electrical Engineering, Najafabad Branch, Islamic Azad University, Najafabad, Isfahan.*

* ***Corresponding Author:*** *mm.rezaei@iaukhsh.ac.ir*

ARTICLE INFO

Keywords:
Wind energy,
Induction generator,
Nonlinear control,
Feedback linearization,
Sliding mode control.

Article history:
Received: 26 April 2024;
Revised: 13 May 2024;
Accepted: 21 May 2024;

Article type:
Research Article

ABSTRACT

Renewable wind energy is a significant source of green energy supply that has gained considerable attention and development in numerous countries in recent years. These systems are utilized as islanded units in circumstances where it is not feasible to establish a connection to the network. Various structures exist for these systems, but the focus of many studies has been on wind energy conversion systems based on a squirrel cage induction machine with back-to-back converters. When operating in islanded mode, this structure necessitates specific control requirements, with the most crucial being the supplying of the desired voltage and frequency of the load. In this paper, two control structures are proposed and constructed to regulate the load voltage by controlling the load-side converter. Two control loops have been implemented in the first control structure. The inner loop utilizes the state feedback input-output method to control the voltage, while the outer loop employs the sliding mode method to control the power components. The objective is to derive the control law for the reference biaxial voltage of the load-side converter. The second proposed structure incorporates the voltage controller sliding mode control method in the inner loop and then the state feedback input-output method is employed in the outer loop to control the current components of the load-side converter, thus designing the system control input. The simulation results of both structures in MATLAB software have been compared by introducing various disturbances to assess the control systems' resilience to each other and the common proportional-integral linear control structure. In the suggested method, voltage and current variations manifest concurrently in the control structure predicated on power components.

1. Introduction

1.1. Problem Statement

The widespread utilization of fossil fuels during the 20th and 21st centuries has led to both climate change and global warming. The provision of electrical energy from renewable sources such as solar, hydro, wind, etc. as green energy has consistently been regarded as such [1]. Over the previous years, the utilization of wind energy to generate

clean power for countries has experienced significant growth. It is projected that by the end of 2030, at least 50% of the world's electricity demand will be met by this method [2]. Currently, wind energy conversion systems (WECS) are implemented in diverse structures as depicted in Figure 1 [3]. Each of these constructions can be operated either onshore or offshore. Meanwhile, the squirrel cage induction generator (SCIG), while requiring power converters with full capability, has significantly reduced maintenance costs, a smaller size, and a more affordable price compared to doubly-fed induction machines [4, 5]. The use of type F of these buildings, particularly in onshore WECS, has gained significant acceptance in recent years (Figure 2) [6].

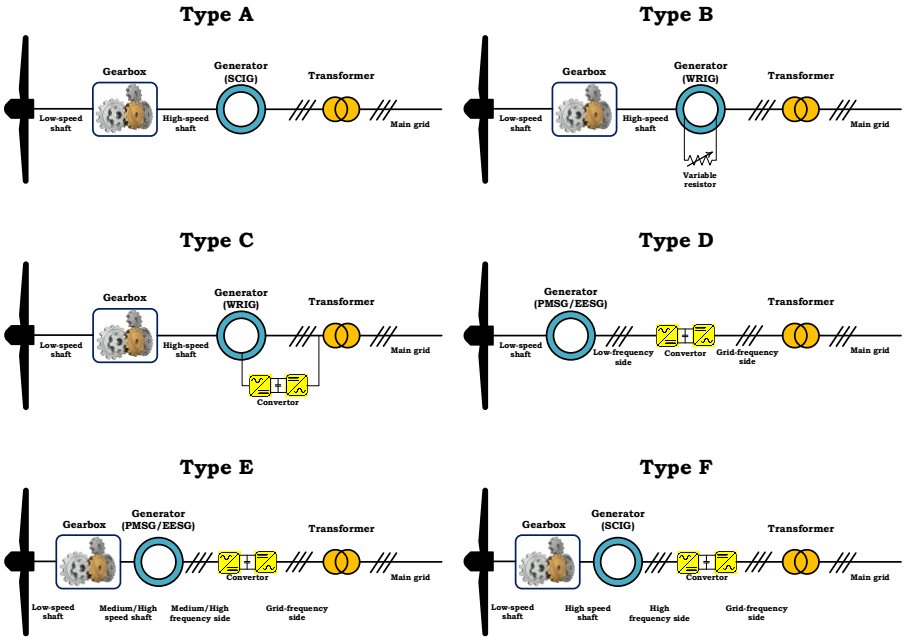

Figure 1. Types of structures used in WECS [3].

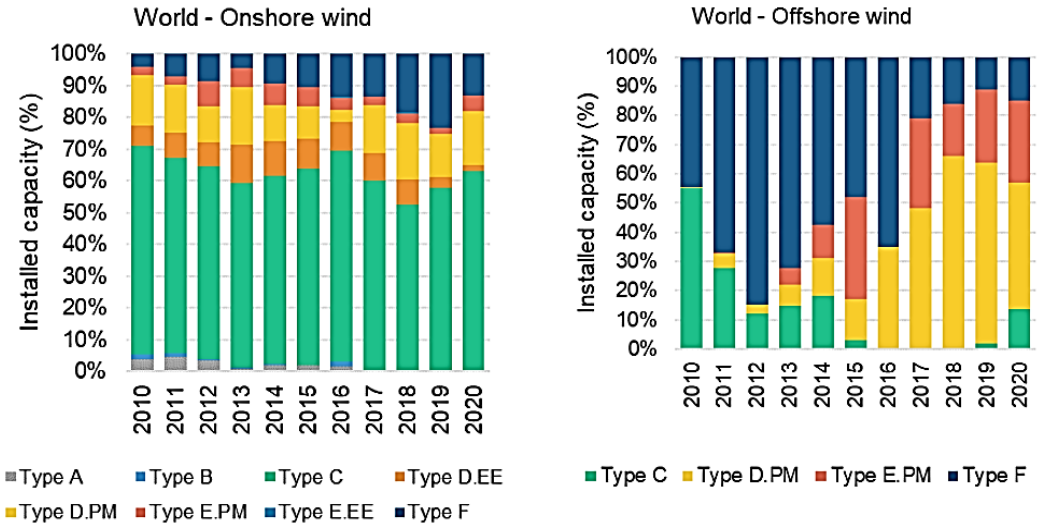

Figure 2. The rate of adoption of various wind turbine structures by the end of 2020 worldwide [6].

1.2. Literature review

The design of a control structure that aligns with the control objectives for both the machine-side converter (MSC) and network-load side converters becomes crucial in systems with back-to-back converters. These control objectives can vary in each of the modes, whether grid-connected or grid-disconnected modes. One objective that has been the focus of numerous studies in grid-connected mode is to maximize the power generated by the WECS [7] or control the power injected into the grid. The authors of this paper provided a robust control design for the mentioned objectives [8]. During islanded mode, a primary objective of the MSC is to effectively regulate the state variables of the generator to meet the energy demands of the load. Conversely, voltage and frequency controls are a highly important control target for the load side converter, as stated in [9-11]. These objectives are particularly crucial when dealing with nonlinear and unbalanced loads, as well as transient conditions [12]. In recent research, a variety of control approaches, such as linear, nonlinear, a combination of linear and nonlinear methods, and techniques based on artificial intelligence, have been employed to accomplish the stated objectives [13]. The proportional-integral (PI) linear control approach is widely utilized in research because of its simplicity. However, identifying the ideal coefficients for this method is a significant difficulty [14,15]. This method can be transformed into a nonlinear method called fractional-order PI by changing the order of its integral part. Similar to the PI method, the fractional-order PI method can be used in conjunction with other linear and nonlinear control methods. It has been observed to exhibit superior performance in transient states compared to traditional PI methods [16]. In the context of nonlinear control systems, it is worth noting the existence of sliding mode control, which can be further categorized into sub-branches such as high-order sliding mode control or fractional-order sliding mode control [17-20]. Also, in some articles, the discussion of wind turbines has been discussed only from the point of view of steady-state and efficiency improvement and cost reduction [21,22]. In addition, numerous research studies have also explored the use of input-output feedback linearization (IOFL) methods and the backward control approach [8,20]. The primary differentiation between linear and nonlinear approaches lies in their treatment of transient states. Generally, linear control methods have a straightforward design, but their ability to respond to different dynamic transient states is significantly less compared to nonlinear control systems. Moreover, linear methods often function just as regulators and exhibit a resistant behavior towards states. The lack of robust transitivity in many circumstances leads to the loss of system stability [16].

1.3. Research gaps

According to the reviewed references, there are the following research gaps in the past research:

- Most of the proposed methods have not given appropriate responses to different modes of fluctuations in the network.

- Most of the references have used methods based on the PID control method, which does not perform well against transient changes.

1.4. Innovations and research contributions

To solve the disadvantages and gaps stated in the previous part, in this article, a two-stage control method is presented, the innovations of which are as follows:

- Using the sliding mode control method to control the outer loop,
- Using the input-output method to control the inner loop,

The following text presents an introduction to the system being studied. Subsequently, two control systems are constructed for the load-side converter, to control the load voltage using nonlinear approaches. The stability of these control systems is also demonstrated. In Section 4, the performance of these structures has been evaluated by simulation in the MATLAB software coding environment. The comparison was made between the structures themselves and the linear PI technique [14] in various transient states.

2. Modeling of the system under study

This paper examines a WECS operating in off-grid mode, utilizing a SCIG as shown in Figure 3. Within this configuration, back-to-back converters operate to supply electrical power to the load through an LC filter to minimize the presence of output harmonics. The MSC and load-side converter (LSC) are interconnected via a capacitor known as the DC-link capacitor. To optimize data storage and enhance simulation speed, the average model of converters is utilized. Furthermore, this system assumes that the load's power demand is consistently lower than the wind system's power generation and that any losses incurred during the switching process are disregarded for the converters. The wind turbine is modeled using a direct current (DC) mechanical prime mover.

2.1. Squirrel-cage Induction Generator (SCIG)

The dynamic equations of the generator based on the state variables of flux and stator current in the *dq* synchronous reference frame are as follows [23]:

$$\begin{cases} \frac{d}{dt}\lambda_{sd} = V_{sd} - R_s I_{sd} + \omega_e \lambda_{sq} \\ \frac{d}{dt}\lambda_{sq} = V_{sq} - R_s I_{sq} - \omega_e \lambda_{sd} \end{cases} \quad (1)$$

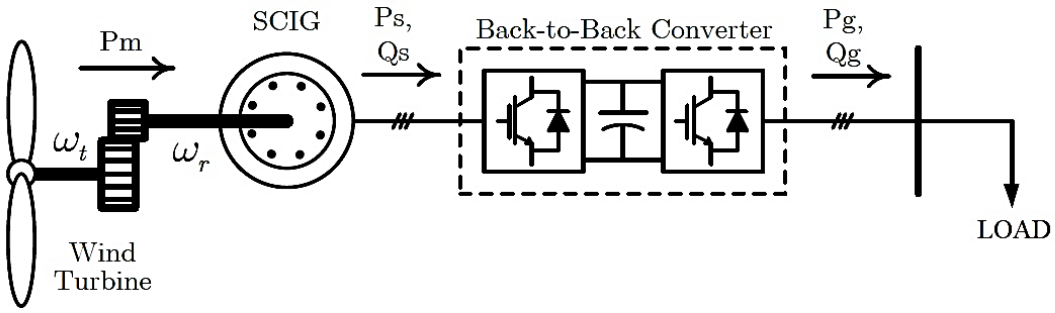

Figure 3. The schematic diagram of an off-grid WECS based on SCIG.

$$\begin{cases} \frac{d}{dt} I_{sd} = \frac{1}{\sigma L_m} \left[V_{rd} - \frac{R_r}{L_m} \left(\lambda_{sd} - L_s I_{sd} \right) + \left(\omega_e - \omega_r \right) \left(\frac{L_r}{L_m} \lambda_{sq} + L_m \sigma I_{sq} \right) \right] \\ \quad - \frac{L_r}{L_m} \left(V_{sd} - R_s I_{sd} + \omega_e \lambda_{sq} \right) \\ \frac{d}{dt} I_{sq} = \frac{1}{\sigma L_m} \left[V_{rq} - \frac{R_r}{L_m} \left(\lambda_{sq} - L_s I_{sq} \right) - \left(\omega_e - \omega_r \right) \left(\frac{L_r}{L_m} \lambda_{sd} + L_m \sigma I_{sd} \right) \right] \\ \quad - \frac{L_r}{L_m} \left(V_{sq} - R_s I_{sq} - \omega_e \lambda_{sd} \right) \end{cases} \quad (2)$$

where λ_{sdq}, V_{sdq}, I_{sdq}, and V_{rdq} are the fluxes, voltages, stator biaxial currents, and rotor biaxial voltages, respectively. Also, the ohmic resistances and inductances of the stator windings are defined as R_s, R_r, L_s, and L_r, respectively. Also, L_m is known as the mutual inductance of the rotor and stator and $\sigma = 1 - L_s L_r / L_m^2$ is the leakage factor. ω_e is the synchronous speed and ω_r is the electrical speed of the rotor, for which the dynamic equation is as follows similar to the last state variable of the machine:

$$\frac{d}{dt} \omega_r = \frac{P}{2} \frac{1}{J} \left(T_e - T_m - D \omega_r \right) \quad (3)$$

T_m, T_e, J, D and P are respectively the mechanical torque and the electromagnetic torque of the generator, the accumulated moment of inertia (including the moment of inertia of the generator and the mechanical prime mover), the accumulated damping factor, and the poles of the generator.

2.2. Load and DC Link

At the load terminal, due to the use of the RC filter, the dynamic equations of the load voltage in the biaxial *dq* synchronous frame can be written as follows in Equation (4):

$$\begin{cases} \frac{d}{dt} V_{fd} = \frac{1}{C_f} \left[I_{fd} - I_{Ldq} + \omega_e C_f V_{fq} + \xi_{vd} \right] \\ \frac{d}{dt} V_{sq} = \frac{1}{C_f} \left[I_{fq} - I_{Lq} - \omega_e C_f V_{fd} + \xi_{vq} \right] \end{cases} \quad (4)$$

In the above equations, V_{fdq}, I_{fdq}, and I_{Ldq} are the output biaxial voltage and currents of the LSC and the biaxial currents of the load connected to the system. Also, ξ_{vdq} denotes the cumulative uncertainty vectors affecting the voltage dynamics, which are caused by parametric and modeling uncertainties, and C_f is the filter capacitor. On the other hand, the following dynamic equations can be derived for the biaxial currents of the output convertera as in Equation (5):

$$\begin{cases} \frac{d}{dt} I_{fd} = \frac{1}{L_f} \left[V_{id} - R_f I_{fd} - V_{fd} + \omega_e L_f I_{fq} + \xi_{id} \right] \\ \frac{d}{dt} I_{fq} = \frac{1}{L_f} \left[V_{iq} - R_f I_{fq} - V_{fq} - \omega_e L_f I_{fd} + \xi_{iq} \right] \end{cases} \quad (5)$$

Similar to the load voltage vectors, for the biaxial currents of the LSC, ξ_{idq} are defined as uncertainty vectors. Also, R_f and L_f are the resistance and inductance of the filter. V_{idq} are the output biaxial voltages of the LSC. On the other hand, for the DC link, according to the dynamics of the capacitor C placed between the two LSC and MSC the following equation can be written as Equation (6):

$$\frac{d}{dt}V_{dc} = \frac{1}{C}(I_{dc} - I_o) \tag{6}$$

I_{dc} is the input current to the DC link through the MSC and I_o is the output current from the DC link to the LSC. If the real and reactive power of the load is represented by P_f and Q_f , we can write Equation (7) as:

$$\begin{bmatrix} P_f \\ Q_f \end{bmatrix} = \frac{3}{2}\begin{bmatrix} V_{fd} & V_{fq} \\ V_{fq} & -V_{fd} \end{bmatrix}\begin{bmatrix} I_{fd} \\ I_{fq} \end{bmatrix} \tag{7}$$

and the instantaneous active power produced by the generator ($-P_g$) can be calculated as Equation (8):

$$P_g = 1.5\left(V_{sd}I_{sd} + V_{sq}I_{sq}\right) \tag{8}$$

The currents used in Equation (6) can be calculated through the following equations:

$$\begin{cases} I_{dc} = -P_g / V_{dc} \\ I_o = P_L / V_{dc} \end{cases} \tag{9}$$

3. Design of the Control Structure

This study utilizes the control structure described in [23] for the MSC. The objective of this research is to build the control design for the LSC using two different approaches. The primary objective on the load side is to control the voltage magnitude and frequency delivered to the load. To fulfill the control objectives described above, the converter in this section should be controlled accordingly.

3.1. Load voltage controller using the first proposed method

This approach utilizes two cascade controllers. The primary objective of the first controller is to control the magnitude of the load voltage by employing the state feedback input-output technique.

$$\begin{aligned} e_{vd} &= V_{fd}^{*} - V_{fd} \\ e_{vq} &= V_{fq}^{*} - V_{fq} \end{aligned} \tag{10}$$

The synchronous dq frame on the load side is considered in such a way that the voltage vector is only in the direction of the *d* axis, and for this purpose V_{fd}^{*} is 239 V and V_{fq}^{*} is zero. In the following, the design process of a positive definite Lyapunov function is designed and defined as follows:

$$W_{V_{fdq}} = \frac{1}{2}\begin{bmatrix} e_{V_{fd}}^2 \\ e_{V_{fq}}^2 \end{bmatrix} + \frac{1}{2}\gamma_v \begin{bmatrix} \tilde{\xi}_{vd}^{\,2} \\ \tilde{\xi}_{vq}^{\,2} \end{bmatrix} \tag{11}$$

In Equation (11), γ_v is an always-positive coefficient. The difference vector of the actual value of the accumulated uncertainties affecting the voltage dynamics with their estimated value, shown by $\tilde{\xi}_{vdq}$, is calculated according to Equation (12):

$$\begin{cases} \tilde{\xi}_{vd} = \xi_{vd} - \hat{\xi}_{vd} \\ \tilde{\xi}_{vq} = \xi_{vq} - \hat{\xi}_{vq} \end{cases} \tag{12}$$

$\hat{\xi}_{vdq}$ is the estimated value of biaxial voltage uncertainties. Next, the derivative of the Lyapunov function defined in Equation (11) can be written in the following form:

$$\frac{d}{dt}W_{V_{fdq}} = \frac{d}{dt}\begin{bmatrix} V_{fd}^* \\ V_{fq}^* \end{bmatrix} - \frac{d}{dt}\begin{bmatrix} V_{fd} \\ V_{fq} \end{bmatrix} + \gamma_i \frac{d}{dt}\begin{bmatrix} \tilde{\xi}_{vd} \\ \tilde{\xi}_{vq} \end{bmatrix}\begin{bmatrix} \tilde{\xi}_{vd} \\ \tilde{\xi}_{vq} \end{bmatrix} \tag{13}$$

Considering that the derivative of the voltage reference values is zero and on the other hand $\frac{d}{dt}\tilde{\xi}_{vdq} = -\frac{d}{dt}\hat{\xi}_{vdq}$, by choosing the estimation rules according to [24] from Equation (14):

$$\frac{d}{dt}\begin{bmatrix} \hat{\xi}_{Vfd} \\ \hat{\xi}_{Vfq} \end{bmatrix} = -\frac{\sqrt{\gamma_v}}{C_f}\begin{bmatrix} e_{Vfd} \\ e_{Vfq} \end{bmatrix} \tag{14}$$

and by inserting Equation (4) into Equation (13), the control input, which is the reference currents of the LSC, can be designed as follows with a positive coefficient k_v:

$$\begin{bmatrix} I_{fd}^* \\ I_{fq}^* \end{bmatrix} = \begin{bmatrix} I_{Ld} - \omega_e C_f V_{fq} - \xi_{vd} + k_v e_{vd} \\ I_{Lq} + \omega_e C_f V_{fd} - \xi_{vq} + k_v e_{vq} \end{bmatrix} \tag{15}$$

With this control law, the derivative of the designed Lyapunov function becomes negative semi-definite, and in this way, according to Barbalat's lemma [25], the asymptotic stability of the control system of the first part can be proved. The second controller in this cascade system is supposed to be designed to control the power components and legally extract control for the reference voltage of the LSC. Having the reference currents from Equation (15), the reference values of active and reactive powers can be calculated using Equation (7):

$$\begin{bmatrix} P_f^* \\ Q_f^* \end{bmatrix} = \frac{3}{2}\begin{bmatrix} V_{fd} & V_{fq} \\ V_{fq} & -V_{fd} \end{bmatrix}\begin{bmatrix} I_{fd}^* \\ I_{fq}^* \end{bmatrix} \tag{16}$$

Now, by defining the error of the power components through Equation (17), the process of designing the control system of this section begins:

$$\begin{bmatrix} e_{P_f} \\ e_{Q_f} \end{bmatrix} = \begin{bmatrix} P_f^* \\ Q_f^* \end{bmatrix} - \begin{bmatrix} P_f \\ Q_f \end{bmatrix} \tag{17}$$

In this section, the design of the controller is done using the sliding mode method. Thus, the sliding surfaces are selected as follows:

$$\begin{bmatrix} S_P \\ S_Q \end{bmatrix} = \begin{bmatrix} e_{P_f} \\ e_{Q_f} \end{bmatrix} + k_{spq} \int_0^t \begin{bmatrix} e_{P_f} \\ e_{Q_f} \end{bmatrix} \mathrm{d}\tau \tag{18}$$

In this equation, k_{spq} is an always-positive coefficient. In the following, if the derivative of Equation (18) is taken, we have:

$$\frac{d}{dt}\begin{bmatrix} S_P \\ S_Q \end{bmatrix} = \frac{d}{dt}\begin{bmatrix} P_f^* - P_f \\ Q_f^* - Q_f \end{bmatrix} + k_{spq}\begin{bmatrix} e_{P_f} \\ e_{Q_f} \end{bmatrix} = \frac{d}{dt}\begin{bmatrix} P_f^* \\ Q_f^* \end{bmatrix} - \frac{d}{dt}\begin{bmatrix} P_f \\ Q_f \end{bmatrix} + k_{spq}\begin{bmatrix} e_{P_f} \\ e_{Q_f} \end{bmatrix} \tag{19}$$

In Equation (19), to simplify the relations of the control system, the instantaneous derivative of the reference power values is considered equal to zero. For the derivative of power components, it can be derived from Equation (7) as follows:

$$\frac{d}{dt}\begin{bmatrix} P_f \\ Q_f \end{bmatrix} = \frac{3}{2}\frac{d}{dt}\begin{bmatrix} V_{fd} & V_{fq} \\ V_{fq} & -V_{fd} \end{bmatrix}\begin{bmatrix} I_{fd} \\ I_{fq} \end{bmatrix} + \frac{3}{2}\begin{bmatrix} V_{fd} & V_{fq} \\ V_{fq} & -V_{fd} \end{bmatrix}\frac{d}{dt}\begin{bmatrix} I_{fd} \\ I_{fq} \end{bmatrix} \tag{20}$$

By placing Equations (4) and (5) in the above equation, we can write:

$$\frac{d}{dt}\begin{bmatrix} P_f \\ Q_f \end{bmatrix} = \begin{bmatrix} G_P \\ G_Q \end{bmatrix} + \begin{bmatrix} H_P \\ H_Q \end{bmatrix} + \frac{3}{2L_f}\begin{bmatrix} V_{fd} & V_{fq} \\ V_{fq} & -V_{fd} \end{bmatrix}\begin{bmatrix} V_{id} \\ V_{iq} \end{bmatrix} \tag{21}$$

where G_P, G_Q, H_P, and H_Q are defined as follows:

$$G_P = \frac{3}{2C_f}\left(\left(I_{fd} - I_{Ld} + \omega_e C_f V_{fq} + \xi_{vd}\right)I_{fd} + \left(I_{fq} - I_{Lq} - \omega_e C_f V_{fd} + \xi_{vq}\right)I_{fq}\right) \tag{22}$$

$$G_Q = \frac{3}{2C_f}\left(\left(I_{fq} - I_{Lq} - \omega_e C_f V_{fd} + \xi_{vq}\right)I_{fd} - \left(I_{fd} - I_{Ld} + \omega_e C_f V_{fq} + \xi_{vd}\right)I_{fq}\right) \tag{23}$$

$$H_P = \frac{3}{2L_f}\left(\left(-R_f I_{fd} - V_{fd} + \omega_e L_f I_{fq} + \xi_{id}\right)V_{fd} + \left(-R_f I_{fq} - V_{fq} - \omega_e L_f I_{fd} + \xi_{iq}\right)V_{fq}\right) \tag{24}$$

$$H_Q = \frac{3}{2L_f}\left(\left(-R_f I_{fd} - V_{fd} + \omega_e L_f I_{fq} + \xi_{id}\right)V_{fq} - \left(-R_f I_{fq} - V_{fq} - \omega_e L_f I_{fd} + \xi_{iq}\right)V_{fd}\right) \tag{25}$$

By inserting Equation (21) into Equation (19), the derivative of the sliding surfaces of the power components will change as follows:

$$\frac{d}{dt}\begin{bmatrix} S_P \\ S_Q \end{bmatrix} = -\begin{bmatrix} G_P \\ G_Q \end{bmatrix} - \begin{bmatrix} H_P \\ H_Q \end{bmatrix} - \frac{3}{2L_f}\begin{bmatrix} V_{fd} & V_{fq} \\ V_{fq} & -V_{fd} \end{bmatrix}\begin{bmatrix} V_{id} \\ V_{iq} \end{bmatrix} + k_{spq}\begin{bmatrix} e_{P_f} \\ e_{Q_f} \end{bmatrix} \tag{26}$$

In this way, a certain positive definite Lyapunov function is expressed as follows in the continuation of the design process:

$$W_{PQ} = \frac{1}{2}\begin{bmatrix} S_P \\ S_Q \end{bmatrix}^T \begin{bmatrix} S_P \\ S_Q \end{bmatrix} > 0 \tag{27}$$

The derivative of this function is:

$$\frac{d}{dt}W_{PQ} = \begin{bmatrix} S_P \\ S_Q \end{bmatrix}^T \frac{d}{dt}\begin{bmatrix} S_P \\ S_Q \end{bmatrix} \tag{28}$$

By inserting Equation (26) into Equation (28), the derivative of the function W_{PQ} is extracted according to Equation (29):

$$\frac{d}{dt}W_{PQ}=\begin{bmatrix}S_P\\S_Q\end{bmatrix}^T\left\{-\begin{bmatrix}G_P\\G_Q\end{bmatrix}-\begin{bmatrix}H_P\\H_Q\end{bmatrix}-\frac{3}{2L_f}\begin{bmatrix}V_{fd}&V_{fq}\\V_{fq}&-V_{fd}\end{bmatrix}\begin{bmatrix}V_{idq}\\V_{iq}\end{bmatrix}+k_{spq}\begin{bmatrix}e_{P_f}\\e_{Q_f}\end{bmatrix}\right\} \tag{29}$$

Now, to guarantee the stability of the control system, the control inputs V_{idq} are designed as the reference voltages of the LSC in such a way that the derivative of the negative semi-definite function W_{PQ} is obtained:

$$\begin{bmatrix}V_{id}^*\\V_{iq}^*\end{bmatrix}=\frac{2L_f}{3}\begin{bmatrix}V_{fd}&V_{fq}\\V_{fq}&-V_{fd}\end{bmatrix}^{-1}\left\{k_{spq}\begin{bmatrix}e_{P_f}\\e_{Q_f}\end{bmatrix}-\begin{bmatrix}G_P\\G_Q\end{bmatrix}-\begin{bmatrix}H_P\\H_Q\end{bmatrix}+k_{satpq}\begin{bmatrix}sat(S_P)\\sat(S_Q)\end{bmatrix}\right\} \tag{30}$$

k_{satpq} is also a control positive gain coefficient in Equation (30). With the above control law, the asymptotic stability of the controller can be guaranteed following Barblat's lemma, and as a result, the derivative of the designed Lyapunov function will be equal to:

$$\frac{d}{dt}W_{PQ}=-\begin{bmatrix}S_P\\S_Q\end{bmatrix}^T\left\{k_{satpq}\begin{bmatrix}sat(S_P)\\sat(S_Q)\end{bmatrix}\right\}=-k_{satpq}S_P\left\{sat(S_P)\right\}-k_{satpq}S_Q\left\{sat(S_Q)\right\}\le 0 \tag{31}$$

The voltage obtained from Equation (30) will be applied to the LSC with synchronous frequency, and thus the load frequency will be set at its nominal value.

3.2. Load voltage controller using the second proposed method

In this method, two cascade controllers are used. The first controller of this method is designed to control the size of the load voltage. Therefore, considering Equation (10), the design of the control system with the sliding mode control method is described below. For this purpose, two sliding surfaces (S_{vd} and S_{vq}) are considered as follows:

$$\begin{bmatrix}S_{vd}\\S_{vq}\end{bmatrix}=\begin{bmatrix}e_{vd}\\e_{vq}\end{bmatrix}+k_{sv}\int_0^t\begin{bmatrix}e_{vd}\\e_{vq}\end{bmatrix}\mathrm{d}\tau \tag{32}$$

where k_{sv} is a positive control gain coefficient. By Equation (32), we can write:

$$\frac{d}{dt}\begin{bmatrix}S_{vd}\\S_{vq}\end{bmatrix}=\frac{d}{dt}\begin{bmatrix}V_{fd}^*-V_{fd}\\V_{fq}^*-V_{fq}\end{bmatrix}+k_{sv}\begin{bmatrix}e_{vd}\\e_{vq}\end{bmatrix}=\frac{d}{dt}\begin{bmatrix}V_{fd}^*\\V_{fq}^*\end{bmatrix}-\frac{d}{dt}\begin{bmatrix}V_{fd}\\V_{fq}\end{bmatrix}+k_{sv}\begin{bmatrix}e_{vd}\\e_{vq}\end{bmatrix} \tag{33}$$

Considering that the derivative of voltage reference values is zero, by inserting Equation (4) into Equation (33), the derivative of sliding surfaces will be equal to:

$$\frac{d}{dt}\begin{bmatrix}S_{vd}\\S_{vq}\end{bmatrix}=-\begin{bmatrix}\left(I_{fd}-I_{Ld}+\omega_e C_f V_{fq}+\xi_{vd}\right)\\\left(I_{fq}-I_{Lq}-\omega_e C_f V_{fd}+\xi_{vq}\right)\end{bmatrix}+k_{sv}\begin{bmatrix}e_{vd}\\e_{vq}\end{bmatrix} \tag{34}$$

According to the sliding mode control method, a positive definite Lyapunov function is selected for the sliding surfaces as follows:

$$W_{Vdq}=\frac{1}{2}\begin{bmatrix}S_{vd}\\S_{vq}\end{bmatrix}^T\begin{bmatrix}S_{vd}\\S_{vq}\end{bmatrix}>0 \tag{35}$$

By taking the derivation of function W_{Vdq} and inserting Equation (34) into it:

$$\frac{d}{dt}W_{Vdq}=\begin{bmatrix}S_{vd}\\S_{vq}\end{bmatrix}^{T}\left\{-\begin{bmatrix}\left(I_{fd}-I_{Ld}+\omega_e C_f V_{fq}+\xi_{vd}\right)\\\left(I_{fq}-I_{Lq}-\omega_e C_f V_{fd}+\xi_{vq}\right)\end{bmatrix}+k_{sv}\begin{bmatrix}e_{vd}\\e_{vq}\end{bmatrix}\right\} \tag{36}$$

Now, if the biaxial reference currents of the LSC as the control input are designed as follows, the stability of the controller can be guaranteed:

$$\begin{bmatrix}I_{fd}^{*}\\I_{fq}^{*}\end{bmatrix}=\begin{bmatrix}I_{Ld}-\omega_e C_f V_{fq}-\xi_{vd}+k_{sv}e_{vd}+k_{satv}sat(S_{vd})\\I_{Lq}+\omega_e C_f V_{fd}-\xi_{vq}+k_{sv}e_{vq}+k_{satv}sat(S_{vq})\end{bmatrix} \tag{37}$$

As a result, Equation (36) will be changed as follows by inserting Equation (37) into it:

$$\frac{d}{dt}W_{Vdq}=-\begin{bmatrix}S_{vd}\\S_{vq}\end{bmatrix}^{T}\begin{bmatrix}k_{satv}sat(S_{vd})\\k_{satv}sat(S_{vq})\end{bmatrix}=-k_{satv}S_{vd}sat(S_{vd})-k_{satv}S_{vq}sat(S_{vq})\le 0 \tag{38}$$

In Equations (37) and (38), k_{satv} is the positive gain coefficient of the control. In this way, since W_{Vdq} is a positive definite function and its derivative is negative semi-definite and continuous, according to Barblat's lemma, the asymptotic stability of the designed controller can be guaranteed [25].

Now it is time to design the second controller using the IOFL method. Having the reference currents from Equation (37), the biaxial currents error of the LSC can be defined as follows:

$$\begin{bmatrix}e_{I_{fd}}\\e_{I_{fq}}\end{bmatrix}=\begin{bmatrix}I_{fd}^{*}\\I_{fq}^{*}\end{bmatrix}-\begin{bmatrix}I_{fd}\\I_{fq}\end{bmatrix} \tag{39}$$

Next, a positive definite Lyapunov function is designed:

$$W_{I_{fdq}}=\frac{1}{2}\begin{bmatrix}e_{I_{fd}}^{2}\\e_{I_{fq}}^{2}\end{bmatrix}+\frac{1}{2}\gamma_i\begin{bmatrix}\tilde{\xi}_{id}^{2}\\\tilde{\xi}_{iq}^{2}\end{bmatrix} \tag{40}$$

In the above equation, γ_i is a positive number and $\tilde{\xi}_{idq}$ shows the difference between the actual value (ξ_{idq}) of the accumulated uncertainty vectors affecting the flow dynamics and their estimated value ($\hat{\xi}_{idq}$):

$$\tilde{\xi}_{idq}=\xi_{idq}-\hat{\xi}_{idq} \tag{41}$$

In this way, the derivative of Equation (40) can be written as follows:

$$\frac{d}{dt}W_{I_{fdq}}=\frac{d}{dt}\begin{bmatrix}I_{fd}^{*}\\I_{fq}^{*}\end{bmatrix}-\frac{d}{dt}\begin{bmatrix}I_{fd}\\I_{fq}\end{bmatrix}+\gamma_i\frac{d}{dt}\begin{bmatrix}\tilde{\xi}_{id}\\\tilde{\xi}_{iq}\end{bmatrix}\begin{bmatrix}\tilde{\xi}_{id}\\\tilde{\xi}_{iq}\end{bmatrix} \tag{42}$$

Table 1. Values of studied system parameters and control coefficients.

Rated power of the machine and converters (P_n)	746 W	DC-link voltage	400 v	k_{sv}	0.245
Rated voltage of the system (V_n)	415 V	DC-link capacitor (C)	1650 µF	k_{satv}	0.05
Stator resistance (R_s)	9.919 Ω	Filter resistance (R_f)	0.25 Ω	k_{spq}	1000
Rotor resistance (R_r)	4.628 Ω	Filter inductance (L_f)	0.006 H	k_{satpq}	5
Stator inductance (L_s)	0.9291 H	Filter capacitance (C_f)	41 µF	k_v	0.245
Rotor inductance (L_r)	0.9291 H	Resistive load	173 W	k_i	180
Magnetizing inductance (L_m)	0.8895 H	Resistive-inductive load	70W+546 VAR	γ_v	1.681×10^{-7}
Number of poles (P)	4	Inertia moment (J)	0.0525 kg.m^2	γ_i	0.0036

Considering that $\frac{d}{dt}\tilde{\xi}_{idq} = -\frac{d}{dt}\hat{\xi}_{idq}$ and choosing the estimation rule from the following equations [24]:

$$\frac{d}{dt}\begin{bmatrix}\hat{\xi}_{Ifd}\\ \hat{\xi}_{Ifq}\end{bmatrix} = -\frac{\sqrt{\gamma_i}}{L_f}\begin{bmatrix}e_{Ifd}\\ e_{Ifq}\end{bmatrix} \tag{43}$$

If the reference voltages of the LSC (V_{idq}) are designed as the control input of the second controller to control the output currents of the LSC, as follows:

$$\begin{bmatrix}V_{id}^*\\ V_{iq}^*\end{bmatrix} = R_f\begin{bmatrix}I_{fd}\\ I_{fq}\end{bmatrix} + \begin{bmatrix}V_{fd}\\ V_{fq}\end{bmatrix} + \omega L_f\begin{bmatrix}-I_{fq}\\ I_{fd}\end{bmatrix} + L_f\frac{d}{dt}\begin{bmatrix}I_{fd}^*\\ I_{fq}^*\end{bmatrix} + k_i\begin{bmatrix}e_{Ifd}\\ e_{Ifq}\end{bmatrix} - \begin{bmatrix}\hat{\xi}_{Ifd}\\ \hat{\xi}_{Ifq}\end{bmatrix} \tag{44}$$

and are placed in Equation (42) together with Equation (43), it can be shown that $\frac{d}{dt}W_{I_{fdq}} \le 0$ and, according to Barbalat's lemma [23], the asymptotic stability of the controller is guaranteed. It should be noted that in the above control law, k_i is a positive control coefficient.

As in the previous part, the voltage obtained from Equation (44) will be applied to the LSC with the synchronous frequency, and in this way, the load frequency will be set at the desired nominal value.

4. Simulation and analysis of results

In this section, the initial settings of system parameters are presented based on Table 1. The specified parameters are selected from [14]. Given that the control system structures designed in the previous section are nonlinear, three disturbances have been taken into account to assess the robustness of these structures.

These disturbances include uncertainty in the system parameter, change in the operating point of the system, and a disturbance with a large amplitude, each is

individually scrutinized. However, to assess the effectiveness of proposed method 1 and proposed method 2, the simulation results were compared with each other and with the results of the traditional PI linear control system mentioned in [14]. In simulation results, the term "Proposed" refers to the proposed control structure 2, "PI" refers to the PI control structure [14], and "SMC-PQ" refers to the proposed structure 1.

The simulations were conducted using the MATLAB software coding environment on a personal computer equipped with an Intel® Core™i7 processor operating at a frequency of 2.5GHz. The computer had 8 GB of RAM and ran on a 64-bit operating system version 10.

4.1. Parametric uncertainty

At the 0.5 s mark, a 10% rise is regarded as an uncertainty in the stator resistance. It is important to mention that this uncertainty is just applicable to the system model. Figure 4 (a) depicts the load voltage changes graph, which demonstrates that all three approaches exhibited robust behavior. However, the proposed method 2 displayed far fewer transient states and returned to its previous value at a faster rate. Furthermore, as depicted in this diagram, the power components are determined by the multiplication of the output voltage and current of the LSC. Consequently, any changes in the voltage directly impact the performance of the internal power control loop. As a result, the fluctuations observed in the proposed method 1 are more pronounced compared to the other two methods.

Figures 4(b) and (c) depict the variations in the active and reactive output power of the LSC. The uncertainty in the parameter has resulted in a temporary change in the output power components of the grid-side converter. Although the transitory state of the findings from proposed method 2 is not particularly important, the results from PI techniques and proposed method 1 have returned to their prior value after a transient state. Figure 4(d) illustrates the variations in the DC-link voltage. The introduction of parameter uncertainty does not have a substantial impact on the output active power.

The voltage quickly returns to its initial value after a satisfactory transient state in all three methods. However, the results from proposed method 2 demonstrate a faster convergence rate. Figures 4(e) and (f) display the flux and torque of the machine, respectively. The results obtained from nonlinear methods 1 and 2 are indistinguishable, whereas the PI method exhibits a distinct transient state.

The findings from Figures 4(a) to (f) validate that the proposed method 2, apart from its robustness against parameter uncertainties, exhibits superior efficiency compared to both the linear PI technique and the proposed method 1.

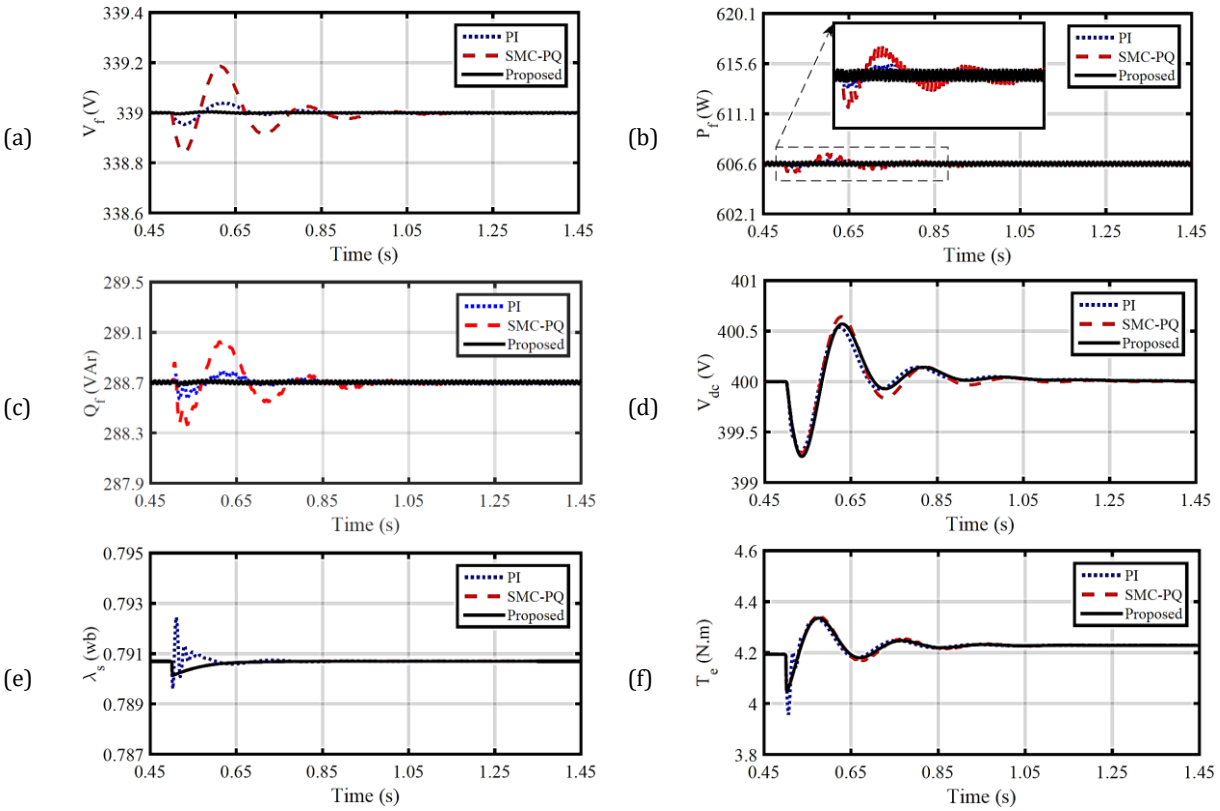

Figure 4. Simulation results when applying parametric uncertainty, respectively, for load terminal voltage, active power injected into the load, load reactive power, DC-link voltage, stator flux and electromagnetic torque of the machine for three control structures.

4.2. Changing the system's operating point

In this scenario, the impedance of the balanced resistive load increases by 5% from the moment of 1.5 s. Figure 5 shows the behavior of important system parameters on the load side and the machine side. Figure 5(a) demonstrates that the load voltage in proposed method 2 exhibits a reduced transient state and a greater convergence speed.

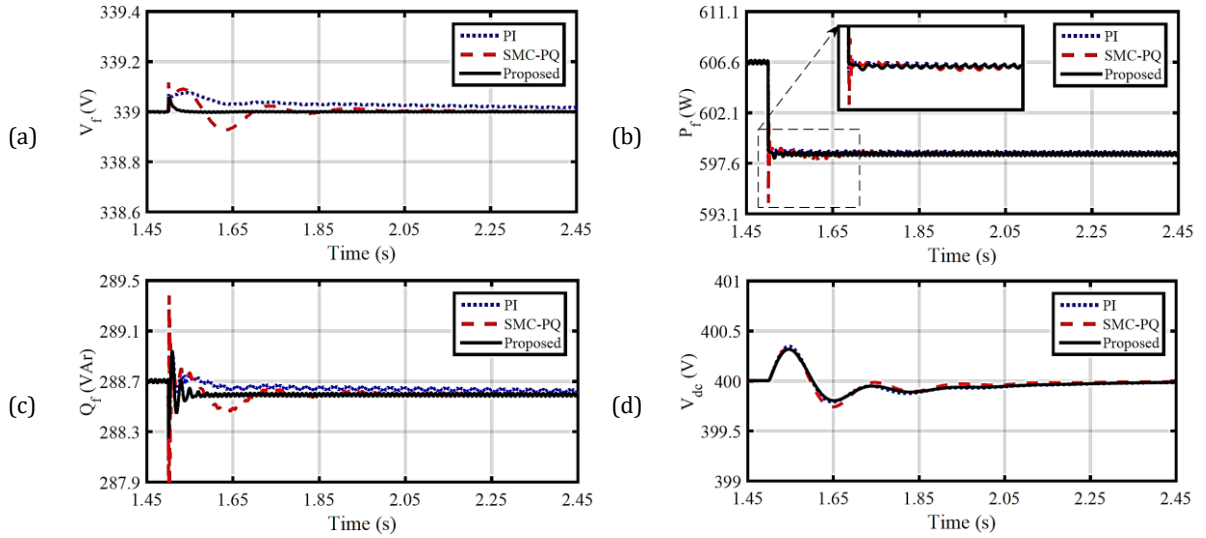

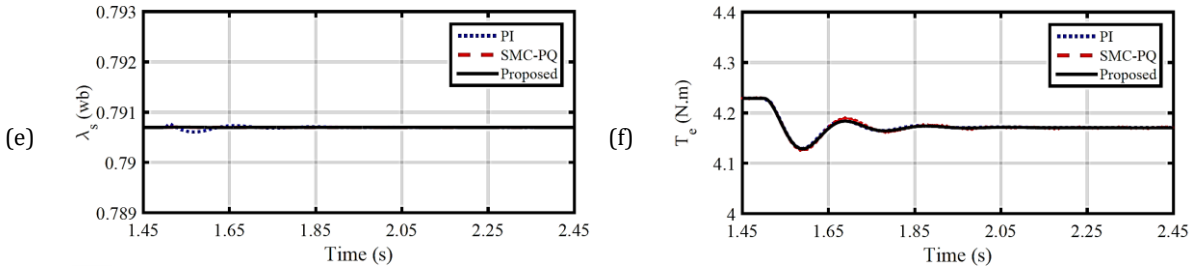

Figure 5. Simulation results when changing the operating point of the system, respectively, for the load terminal voltage, active power injected into the load, load reactive power, DC-link voltage, stator flux and electromagnetic torque of the machine for three control structures.

Furthermore, due to its suitability for adjustment rather than tracking, the PI technique has not yet reached its final value within the range of the given shape. While the suggested control method 1 shows a faster convergence speed compared to the PI technique, its transient state is more severe than that of proposed method 2. Figures 5(b) and (c) depict the variations in the active and reactive powers of the LSC. It is evident that in all three approaches, the power components reach their new reference values after a temporary period. However, the suggested method 2 demonstrates superior speed and transient state performance compared to the other techniques. Figure 5(d) displays the variations in the DC-link voltage. The outcomes of all three approaches are nearly identical to one another. Nevertheless, approach 2 has superior transitivity. Figures 5(e) and (f) additionally illustrate the alterations in the flux and torque of the machine. It is evident that there have been no substantial fluctuations in the machine flux, and the outcomes of both suggested nonlinear approaches are in agreement with each other. The torque of the machine is decreased in all three approaches to restore the equilibrium between power production and consumption in response to load variations.

4.3. Large disturbance

In this section, at the moment of 2.5 s, the total impedance of the load reaches 30% of its nominal value and returns to its normal state after half a power cycle (0.01 s). This situation can be considered similar to a symmetrical three-phase short circuit at the load terminal.

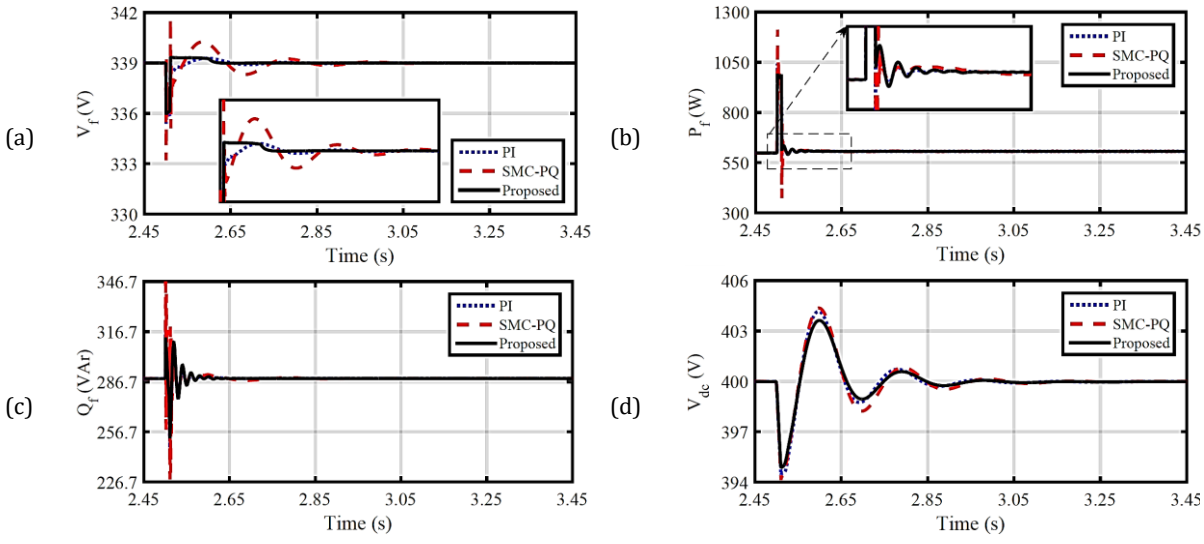

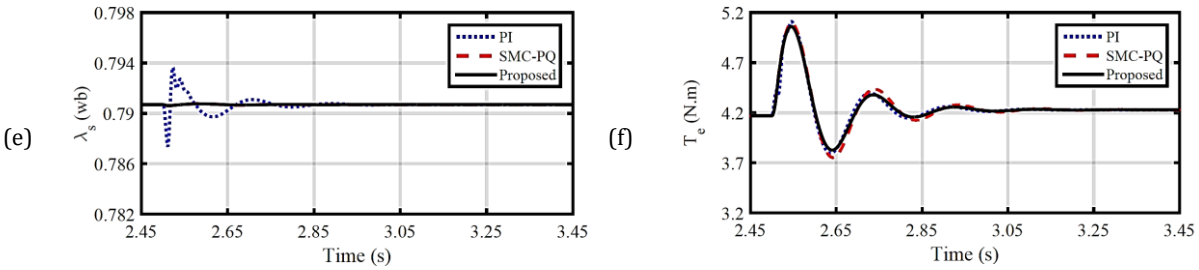

Figure 6. Simulation results during large disturbances in the system for load terminal voltage, active power injected to load, load reactive power, DC-link voltage, stator flux and machine electromagnetic torque for three control structures.

Figure 6(a) illustrates the variations in load voltage following the application of short circuit conditions. Despite experiencing a significant decrease during short circuits, all three methods exhibit this behavior. However, in proposed method 2, the load voltage reaches its nominal value more efficiently and rapidly, displaying a more appropriate transient state and speed. Figures 6(b) to (d) depict the output power components of the LSC and the DC-link voltage, respectively. These figures illustrate that the occurrence of short-circuit circumstances has resulted in a significant transient state in all three ways. However, the proposed technique 2 has achieved faster convergence of the indicated variables to their previous levels. Figures 6(e) and (f) display the flux and torque of the machine. There are no substantial alterations in the flux of the machine in proposed techniques 1 and 2. The machine's torque has returned to its original value after a transient state in all three techniques. However, the proposed method 2 exhibits a faster rate of convergence compared to the other two methods.

5. Conclusion

This work presents two nonlinear robust control architectures for the LSC of a SCIG-based WECS operating in off-grid mode. A comparison has been made between the simulation results of the two suggested systems and the PI technique under three common disturbances: parametric uncertainty, system operating point change, and major disturbance. Both proposed structures exhibit superior suitability and resilience compared to the PI technique. However, the performance of control structure 2 demonstrates a more favorable reaction in transient states induced by disturbances, in contrast to method 1. The cause for this can be elucidated as follows: in suggested method 1, voltage and current variations manifest concurrently in the control structure predicated on power components, but in proposed method 2, these fluctuations manifest solely in each control loop individually. In summary, the obtained results are as follows:

- Designing and implementing a hybrid control method to control SCIG-based WECS operating in off-grid mode.
- Optimal and flexible control to balance and stabilize the load voltage.

References

[1] A. Gatto, "The Energy Futures We Want: A Research and Policy Agenda for Energy Transitions," *Energy Research & Social Science*, vol. 89, 102639, 2022.

[2] S. Frank, H. Böttcher, et al., "Dynamics of the Land Use, Land Use Change, and Forestry Sink in the European Union: The Impacts of Energy and Climate Targets for 2030," *Climatic Change*, vol. 138, pp. 253-266, 2016.

[3] C. Vázquez-Hernández, J. Serrano-González, and G. Centeno, "A Market-Based Analysis on the Main Characteristics of Gearboxes Used in Onshore Wind Turbines," *Energies*, vol. 10, no. 11, p. 1686, 2017.

[4] M. M. Ahmed, W. S. Hassanein, and M. A. Enany, "Proposing and Evaluation of SC Techniques for Variable Speed High-Power Operation of SEIG," *IEEE Access*, vol. 8, pp. 20666-20675, 2020.

[5] M. Shiraliyan, P. Sharma, and C. Sharma, "Automatic Reactive Power Control of Isolated Wind–Diesel Hybrid Power System using Artificial Bee Colony and Gray Wolf Optimization," *International Journal of Green Energy*, vol. 15, no. 14-15, p. 889-904, 2018.

[6] T. Telsnig, A. Georgakaki, et al., "Clean Energy Technology Observatory: Wind Energy in the European Union–2022 Status Report on Technology Development, " *Trends, Value Chains and Markets*, 2022.

[7] M. M. Rezaei, "A Nonlinear Maximum Power Point Tracking Technique for DFIG-Based Wind Energy Conversion Systems," *Engineering science and technology, an international journal*, vol. 21, no. 5, pp. 901-908, 2018.

[8] A. Sotoudeh, J. Soltani, and M. M. Rezaei, "A Robust Control for SCIG-Based Wind Energy Conversion Systems Based on Nonlinear Control Methods," *Journal of Control, Automation and Electrical Systems*, vol. 32, pp. 735-746, 2021.

[9] S. K. Tiwari, B. Singh, and P. K. Goel, "Design and Control of Microgrid Fed by Renewable Energy Generating Sources," *IEEE Transactions on Industry Applications*, vol. 54, no. 3, pp. 2041-2050, 2018.

[10] M. El Achkar, R. Mbayed, G. Salloum, N. Patin, and E. Monmasson, "Voltage Control of a Stand-Alone Cascaded Doubly Fed Induction Generator," *IEEE Transactions on Industrial Electronics*, vol. 66, no. 1, pp. 762-771, 2018.

[11] R. Mishra, and T. K. Saha, "Control of SCIG Based Constant Voltage Generation Scheme for Distributed Power Supply," *International Journal on Electrical Engineering and Informatics*, vol. 10, no. 3, pp. 513-525, 2018.

[12] R. Mishra, and T. K. Saha, "Control of A Stand-Alone Distributed Generation System with Unbalanced and Nonlinear Load," *International Transactions on Electrical Energy Systems*, vol. 30, no. 4, pp. e12286, 2020.

[13] M. Abdelrahem, C. M. Hackl, R. Kennel, and J. Rodriguez, "Efficient Direct-Model Predictive Control with Discrete-Time Integral Action for PMSGs," *IEEE Transactions on Energy Conversion*, vol. 34, no. 2, pp. 1063-1072, 2019.

[14] R. Mishra, and T. K. Saha, "Combined Control of Stand-Alone Energy Conversion Scheme for Distributed Sources: Development and Performance Analysis," *International Journal of Electrical Power & Energy Systems*, vol. 115, 105480, 2020.

[15] R. Mishra, and T. K. Saha, "Modelling and Analysis of Distributed Power Generation Schemes Supplying Unbalanced and Nonlinear Load," *International Journal of Electrical Power & Energy Systems*, vol. 119, 105878, 2020.

[16] A. Sotoudeh, and M. M. Rezaei, "Robust Control of Isolated SCIG-Based WECS Feeding Constant Power Load using Adaptive Backstepping and Fractional Order PI Methods," *International Journal of Dynamics and Control*, vol. 12, no. 2, pp. 452-462, 2024.

[17] L. Xiong, P. Li, and J. Wang, "High-Order Sliding Mode Control of DFIG under Unbalanced Grid Voltage Conditions," *International Journal of Electrical Power & Energy Systems*, vol. 117, 105608, 2020.

[18] S. Huang, J. Wang, et al., "A Fixed-Time Fractional-Order Sliding Mode Control Strategy for Power Quality Enhancement of PMSG Wind Turbine," *International Journal of Electrical Power & Energy Systems*, *vol.* 134, 107354, 2021.

[19] H. H. Mousa, A. R. Youssef, and E. E. Mohamed, "Optimal Power Extraction Control Schemes for Five-Phase PMSG Based Wind Generation Systems," *Engineering science and technology, an international journal*, vol. 23, no. 1, pp. 144-155, 2020.

[20] Z. Jai Andaloussi, A. Raihani, A. El Magri, R. Lajouad, and A. El Fadili, "Novel Nonlinear Control and Optimization Strategies for Hybrid Renewable Energy Conversion System," *Modelling and simulation in engineering*, vol. 2021, no. 1, p. 3519490, 2021.

[21] J. Ebrahimi, and M. Abasi, "Design of a Power Management Strategy in Smart Distribution Networks with Wind Turbines and EV Charging Stations to Reduce Loss, Improve Voltage Profile, and Increase Hosting Capacity of the Network," *Journal of Green Energy Research and Innovation*, vol. 1, no. 1, pp. 1-15, 2024.

[22] A. A. Karimi Taleb, H. Makvandi, and A. Oraee , "The Impact of Wind Direction on Wind Farms' Output Power and Income," *Journal of Green Energy Research and Innovation*, vol. 1, no. 1, pp. 34-47, 2024.

[23] A. Sotoudeh, and M. M. Rezaei, "An Adaptive Control Strategy for Grid-Forming of SCIG-Based Wind Energy Conversion Systems," *Energy Reports*, vol. 10, pp. 114-122, 2023.

[24] M. M. Rezaei, and J. Soltani, "A Robust Control Strategy for a Grid-Connected Multi-Bus Microgrid under Unbalanced Load Conditions," *International Journal of Electrical Power & Energy Systems*, vol. 71, pp. 68-76, 2015.

[25] M. Abasi, M. Falah Nezhadnaeini, M. Karimi, and N. Yousefi "A Novel Meta heuristic Approach to Solve Unit Commitment Problem in The Presence of wind Farms" *Revue roumaine des sciences techniques Serie Electrotechnique et Energetique*, vol. 60, no. 3, pp. 253–262, 2015.

Declaration of Competing Interest

The authors declare that they have no known competing financial interests or personal relationships that could have appeared to influence the work reported in this paper. The ethical issues, including plagiarism, informed consent, misconduct, data fabrication and/or falsification, double publication and/or submission, redundancy, have been completely observed by the authors.

Credit Authorship Contribution Statement

Adel Sotoudeh: Conceptualization, Data curation, Formal analysis, Investigation, Roles/Writing - original draft, Writing-review & editing. **Mohammad Mahdi Rezaei:** Methodology, Project administration, Writing-review & editing. **Mohammadreza Moradian:** Methodology, Validation, Visualization, Roles/Writing-original draft, Writing-review & editing.

Bibliography

Adel Sotoudeh was born in Iran in 1989. He received his Ph.D. degree in Electrical Engineering (Power system) from Khomeinishahr Branch, Islamic Azad University, Khomeinishahr /Isfahan, Iran, in 2023. Also, he has taught for ten years at Khorasgan Islamic Azad University and sama college. He has published 4 research papers. His research interests include power quality, smart grids, design, optimization and implementation of electrical drives, and microgrids.

Mohammad Mahdi Rezaei received the M.Sc. degree in electrical engineering from Amirkabir University of Technology (Tehran Polytechnic), Tehran, Iran, in 2007, and the Ph.D. degree in electrical engineering from the Science and Research Branch, Islamic Azad University, Tehran, Iran, in 2015. He is currently an Associated Professor in the Department of Electrical and Computer Engineering, Khomeinishahr Branch, Islamic Azad University, Isfahan, Iran. His main areas of research are control of microgrids, distributed generations, and design, optimization and implementation of electrical drives.

Mohammadreza Moradian received the M.Sc. degree in electrical engineering from Isfahan University of Technology, Isfahan, Iran, in 2001, and the Ph.D. degree in electrical engineering from the Science and Research Branch, Islamic Azad University, Tehran, Iran, in 2016. He is currently an Associated Professor in the Department of Electrical and Computer Engineering, Najafabad Branch, Islamic Azad University, Isfahan, Iran. His main areas of research are electrical machines and drives, distributed generations, and design, power system reliability.

Journal of Green Energy Research and Innovation

Optimizing Reactive Power for DG Units to Minimize Power System Losses Using Stochastic Modeling

Majid Najjarpour, Behrouz Tousi, Amir Hossein Karamali

Highlight

- Optimal distribution of reactive power in presence of DG units
- Genetic algorithm
- Minimize Power System Losses
- statistical-quality based Taguchi method

Graphical Abstract

Use your device to scan and read the article online

Citation
M. Najjarpour, B. Tousi, and A. H. Karamali, "Optimizing Reactive Power for DG Units to Minimize Power System Losses Using Stochastic Modeling," *Journal of Green Energy Research and Innovation*, vol. 1, no. 4, pp. 35-46, 2024.

https://doi.org/10.61186/jgeri.1.4.35

JGERI Journal of Green Energy Research and Innovation

Online ISSN: 3041-9018

Journal of Green Energy Research and Innovation

Journal Homepage: www.jgeri.araku.ac.ir

Optimizing Reactive Power for DG Units to Minimize Power System Losses Using Stochastic Modeling

Majid Najjarpour [1], Behrouz Tousi [2*], Amir Hossein Karamali[1]

[1]*Department of Electrical Engineering, Iran University of Science and Technology (IUST), Tehran, Iran.*
[2]*Electrical Engineering Department, Faculty of Electrical and Computer Engineering, Urmia University, Urmia, Iran.*

* ***Corresponding Author:*** *b.tousi@urmia.ac.ir*

ARTICLE INFO

Keywords:
Genetic algorithm,
Wind turbine,
Orthogonal arrays,
Optimal reactive power distribution.

Article history:
Received: 09 March 2024;
Revised: 18 April 2024;
Accepted: 21 April 2024;

Article type:
Research Article

ABSTRACT

In recent decades, because of some main and principle world problems such as increasing the population, global warming, climate changes, and fossil fuel sources reduction, the using of renewable energies has impressively increased that can solve and reduce the caused problems by traditional power plants, and also can control power system the important indexes such as losses, voltage drop, transferring capacity. Reactive power has an important role in controlling and minimizing of losses, the optimal distribution of reactive power in presence of Distributed generation (DG) units in distribution networks is an important and key problem. In this paper, for uncertainties modelling of DG units and optimizing the reactive power, the statistical-quality based Taguchi method and Genetic algorithm are used, respectively. The simulation of this paper is checked and done in MATLAB and MINITAB using IEEE 57-bus standard network, and simulation results show 5.5 MW reduction of the distribution network losses.

1. Introduction

In addition to the active power, optimal reactive power distribution (ORPD) and voltage control are some of the most important issues in the power system that play a key role in the economic operation and loss control of the network, that means the set of the voltage of the generators, the position of the taps, and also the number of reactive compensators of the network, set at the best values then the amount of losses in the network reaches its minimum value [1]. In the normal and steady state of the network, determining the optimal state of these elements is sufficient to have the optimal answer. But when uncertainties are applied to the network, the state of uncertainty affects the final answer and the position of the network elements to the extent that this problem must be resolved again, taking into account the sources of uncertainty. This issue is non-convex and non-linear in nature. Hence, many classical methods such as the gradient method have been used [2]. In [2], reactive and active powers are separated and then the optimization problem is solved. Dynamic programming [3], Lagrange function and Cohen-Tucker conditions [4], linear programming [5], marine predators' algorithm (MPA) [6], modified

jellyfish search optimizer (MJSO) [7], African Vultures Optimization Algorithm (AVOA) [8] and modified version of Artificial Hummingbird Algorithm (MAHA) [9] for the ORPD problem are also presented. In addition, in [10] a multi-objective ORPD is proposed for an IEEE 69-bus distribution network, considering different load levels and the uncertainty of load models and demand. It introduces an optimization approach based on a modified grey wolf optimizer and multi-level Pareto analysis, demonstrating its effectiveness. In [11-13] the problem is done in the form of a programming mixed with integer and using GAMS software. Also, using the above software in [14,15], it has performed the two objectives of reactive power programming in order to reduce losses and voltage deviations and in [16], the voltage remains stable by active power control. In addition, uncertainties due to load and wind are considered in it. Also, in [17] a stochastic programming method is presented for coordinated operation of distributed energy resources in an unbalanced IEEE 34-bus three-phase active distribution network (ADN), effectively reducing system cost and co-optimizing active and reactive power. Allocation and sizing are also very important to reduce losses. In [18] a two-layer methodology that utilizes a two-stage stochastic programming algorithm is proposed for the allocation and sizing of Static Var Compensators (SVCs) in IEEE 33 and 69 radial distribution systems, effectively addressing uncertainties in PV and load powers and compares optimization algorithms such as Particle Swarm Optimization (PSO) and Genetic Algorithm (GA) to demonstrate the effectiveness of the proposed methodology on the systems. In recent years, many papers based on evolutionary algorithms have been presented. The ability of evolutionary algorithms to solve nonlinear problems has been the main reason for all researchers to solve this problem with these algorithms [19]. An improved differential evolution algorithm is used in which discrete and continuous variables are considered with the aim of reducing losses [20]. Reactive power control programming is performed in distribution networks and includes wind generation uncertainties. Other references such as genetic algorithm [21], particle aggregation algorithm [19,22], evolutionary programming [23], differential evolution [24-26], metal annealing [27], search engine optimization algorithm [28, 29], propeller algorithm [30] The Gray Wolf Algorithm [31], the Teaching and Learning Algorithm [32] and the Combined Particle Swarm Algorithm [33], have solved the problem that none of the mentioned articles have examined the effect of uncertainties. However, recent studies have explored the application of various algorithms to address the issue of loss reduction in distribution networks, including the use of Cuckoo and Cultural Algorithms [37], the combination of Improved Taguchi Method and Dandelion Algorithm [38], and the correlation of Taguchi Method and Genetic Algorithm [39].

In this paper, the ORPD problem and voltage control using GA are done in a situation where the effect of uncertainty caused by WTs is considered. Obviously, conventional unloading methods can no longer be used when uncertainty arises. Therefore, to solve this problem, the probabilistic optimal power flow (POPF) method is used.

The significant advantages of this paper are summarized as blow:

1) Solving ORPD problem considering uncertainties of DG units and Time-varying load.

2) Applying the Taguchi method for modeling load, solar irradiance, and wind speed uncertainties.

3) Comparing the result of the Taguchi method with the POPF method such as: Scenario-Based, LHS, and 2PEM for answering the problem.

2. Expression of the ORPD

The objective function is expressed in Equation (1) [34].

$$\min P_L = \sum_{l=1}^{nl} P_{Loss,l} \tag{1}$$

Where P_L is the total network loss. This optimization problem has some constraints. Equations (2) and (3) show equal limits in the network. Equations (4) and (5) express unequal constraints.

$$V_i \sum_{i=1}^{N} V_j \left(G_{ij} \cos \delta_{ij} + B_{ij} \sin \delta_{ij}\right) + P_{Di} - P_{Gi} - P_{wi} = 0 \tag{2}$$

$$V_i \sum_{i=1}^{N} V_j \left(G_{ij} \sin \delta_{ij} + B_{ij} \cos \delta_{ij}\right) + Q_{Di} - Q_{Gi} - Q_{ci} = 0 \tag{3}$$

$$V_i^{min} \leq V_i \leq V_i^{max} \tag{4}$$

$$|T_i| \leq T_i^{max} \tag{5}$$

2.1. Load demand uncertainty Modeling

Generally, the uncertainty or in other words (random variable) RVs of load demand can be modelled using the normal or Gaussian probability density functions (PDFs) Equations (6):

$$PDF_L(S_L) = \frac{1}{\sqrt{2\pi}\sigma_L} \exp\left(-\frac{(S_L - \mu_L)^2}{2\sigma_L^2}\right) \tag{6}$$

2.2. Wind energy uncertainty modelling

The Weibull PDF is usually to define speed distribution by Equations (7) that is shown in Figure 1:

$$PDF_V(v) = \frac{\beta}{\alpha}\left(\frac{v}{\alpha}\right)^{\beta-1} \exp\left(-\left(\frac{v}{\alpha}\right)^{\beta}\right) \tag{7}$$

Further, the output power from a wind power plant is expressed by Equations (8):

$$P_W(V) = \begin{cases} 0 & V \leq V_i \text{ and } V_o \leq V \\ \left(\dfrac{V^3 - {V_i}^3}{{V_r}^3 - {V_i}^3}\right) P_r & V_i \leq V \leq V_r \\ P_r & V_r \leq V \leq V_o \end{cases} \tag{8}$$

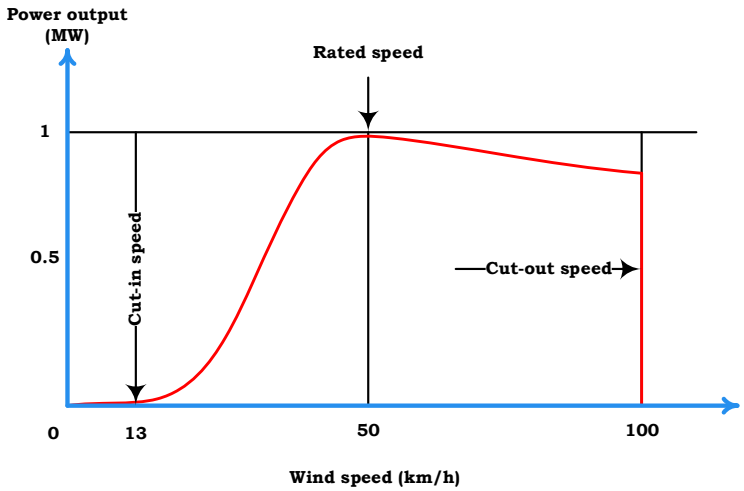

Figure 1. Wind turbine production capacity [28].

3. Orthogonal Arrays

An orthogonal array (OA) is a type of fractional factorial matrix in which the rows reflect the levels of random variables (RVs) in each experiment, while the columns indicate specific factors. Historically, the concept of OA was referred to as magic squares. The term "orthogonal" is used to describe OAs due to the independent examination of each column. The orthogonal array (OA) is comprised of a matrix, as depicted in Table 1, whereby numerical values are organized systematically in both horizontal rows and vertical columns. Each row within the matrix represents an individual experiment, while each column corresponds to a random variable (RV). Therefore, the dimensions of the matrix may be expressed as "("N" _"exp" * N)" multiplied by N. The symbol "L" represents the level assigned to the i^th variable in the "j" ^"th" experiment [26, 36].

4. POPF with TM

In POPF, the relationship between input and output RVs is according to Equation (9):

$$Y_{in} = f\ (X_{out}) \quad (9)$$

The input and output RVs vectors are Y_{in} and X_{out}, respectively, and f is a nonlinear function. In POPF, the factors are called as RVs. In the POPF the whole details of Taguchi method are shown in Figure2 and explained in [39].

5. Simulation Results

The utilization of the 57-bus IEEE standard network is used to attain the efficacy of the Taguchi method. The system under consideration is equipped with a total of seven generators and eighty transmission lines, out of which seventeen lines are equipped with a tap changer. Additionally, three pieces of reactive power compensating equipment have been placed at bases 15, 25, and 53 for the purpose of compensation. The network experiences an initial loss of 33 MW in the absence of wind turbines. The performance range of the variables is shown in Table 1, while additional network information may be found in reference [19].

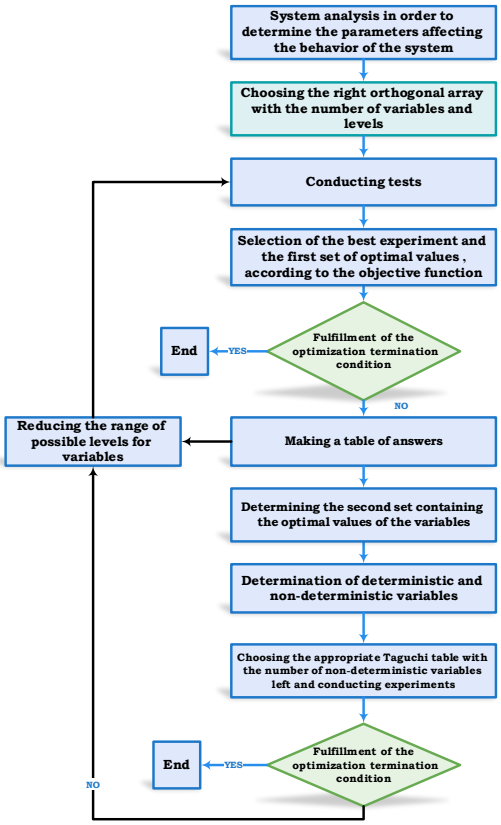

Figure 2. Taguchi and POPF flowchart [39].

Table 1. Orthogonal array $OA_{N_{exp}}\ (N_L)^N$.

Experiment number	Level of each variable			
	RV1	**RV2**	**...**	**RVN**
1	L_{11}	L_{12}	...	L_{1N}
2	L_{21}	L_{22}	...	L_{2N}
....	....	....	...	....
N_{exp}	$LN_{exp}1$	$LN_{exp}2$	...	$LN_{exp}N$

The methodology is executed using the MATLAB and MINITAB software platforms. The present scenario entails the existence of a wind farm located in bus 38, possessing a nominal capacity of 100 MW. In order to replicate the operations of this wind farm, wind velocity data obtained from the North Dakota site and the Watford area have been employed [25]. The mean wind velocity within this region is recorded as 8.5 meters per second, with a corresponding standard deviation of 5.55. Figure 2 displays the distribution of wind speeds over a one-year period, revealing a noticeable right skewness in the data. Table 2 presents the outcomes according to the control variables. The findings presented in Table 3 indicate that the observed values for the variables fall within the acceptable range. Figures 2 to 9 provide diagrams illustrating the changes in several factors, such as generator voltage, tap position, and control equipment production. These diagrams offer improved control over the condition of the variables. The findings indicate the allowable range of values for all variables throughout the 500 iterations of the algorithm. It is evident that initially, there is significant variability among all variables.

However, as the number of repetitions increases, there is a progressive attainment of relative convergence among all variables. Additionally, Figure 9 presents the output voltage of all the buses, illustrating the permissible range of values for their output voltage. Table 4 presents several approaches for predicting postoperative pancreatic fistula (POPF), including point estimate, Taguchi, Scenario-based, and Latin hypercube sampling, along with their respective outcomes.

Table 2. Limitations of control variables.

Variable	Max[p.u.]	Min [p.u.]	Step
VG	1.06	0.94	---
V	1.06	0.94	---
T	1.1	0.9	0.01
QC_{18}	1.0	0	---
QC_{25}	0.059	0	---
QC_{53}	0.063	0	---

Table 3. Results for system variables.

VG_9	VG_8	VG_6	VG_3	VG_2	VG_1
1.037	1.055	1.035	1.044	1.058	1.06
T_{34-32}	T_{7-29}	T_{24-26}	T_{24-25}	T_{24-25}	T_{21-20}
4	8	12	8	5	12
T_{14-46}	T_{15-45}	T_{11-41}	T_{4-18}	T_{4-18}	VG_{12}
7	8	1	1.058	1.06	1.033
T_{9-55}	T_{39-57}	T_{40-56}	T_{11-43}	T_{13-49}	T_{10-51}
4	8	12	8	5	12
-	-	-	QC_{53}	QC_{25}	QC_{18}
-	-	-	7	8	1

Table 4. Values of μ and σ using other alternative techniques approaches.

Entire losses	TM	Scenario	LHS	2PEM
μ [MW]	27.5	40.8	48.36	36.1
σ	9.10	19.17	28.42	13.2

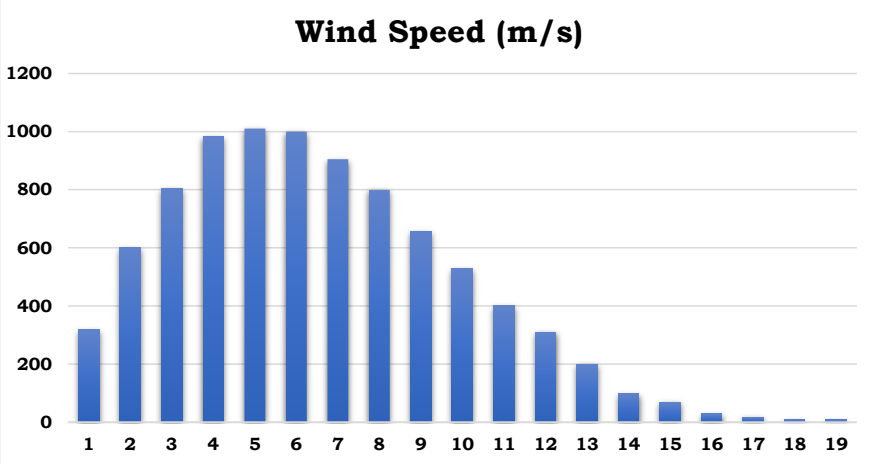

Figure 3. Wind speed frequency diagram [40].

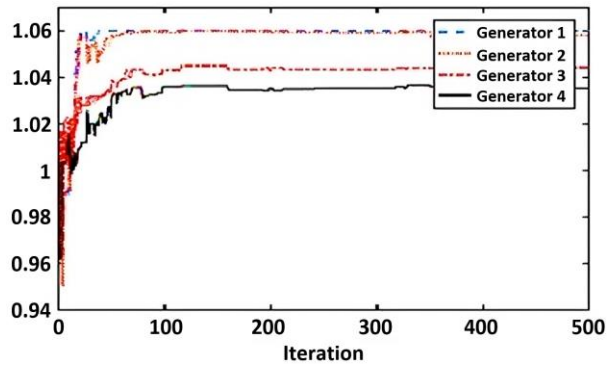

Figure 4. Trend of voltage changes of generators 1 to 4

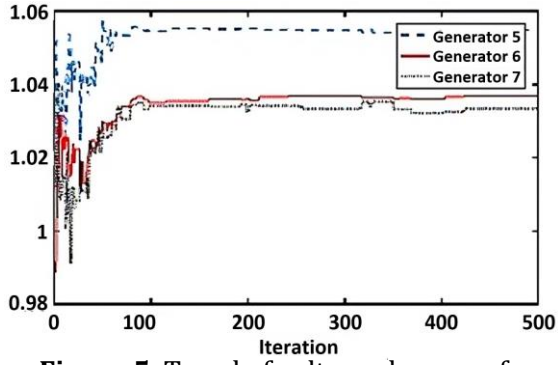

Figure 5. Trend of voltage changes of generators 5 to 7.

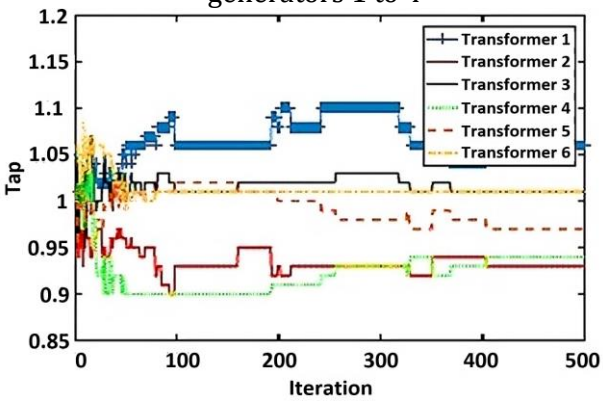

Figure 6. Trend of transformers 1 to 6 transformers.

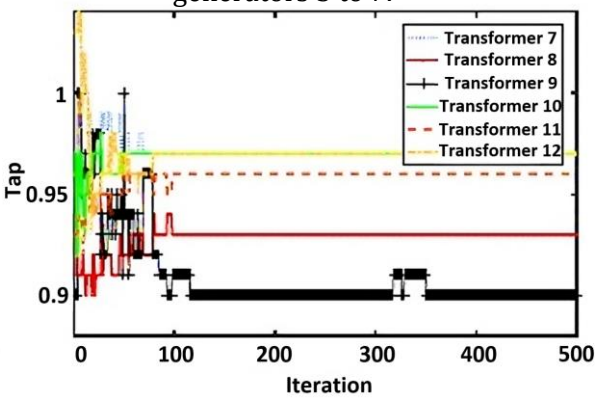

Figure 7. Trend of transformers 7 to 12 transformers.

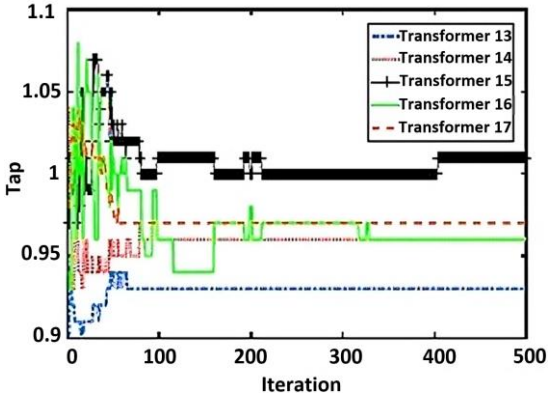

Figure 8. The process of changing the Taps of transformers 13 to 17.

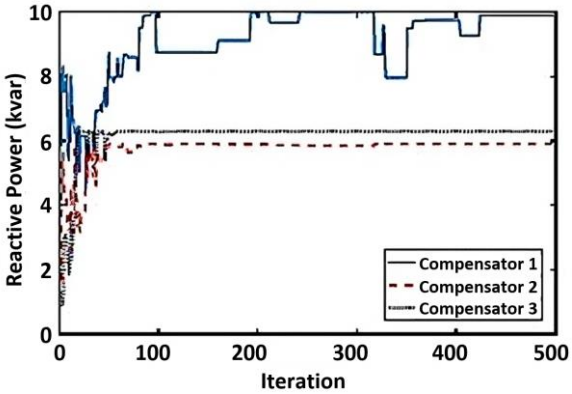

Figure 9. Trend of compensating equipment changes.

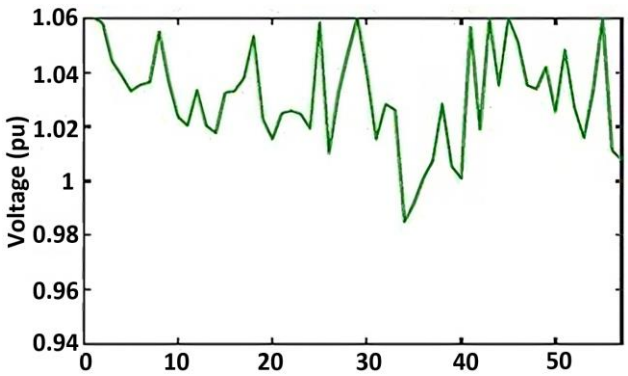

Figure 10. Voltage profile of all buses.

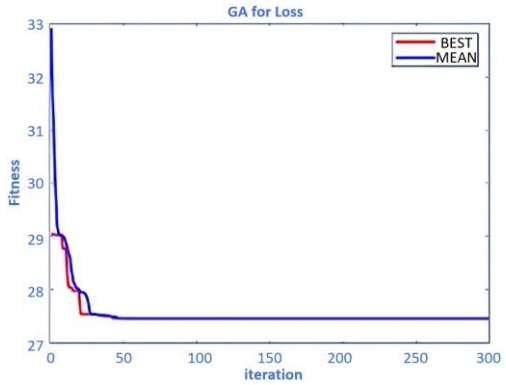

Figure 11. Convergence of loss optimization by GA.

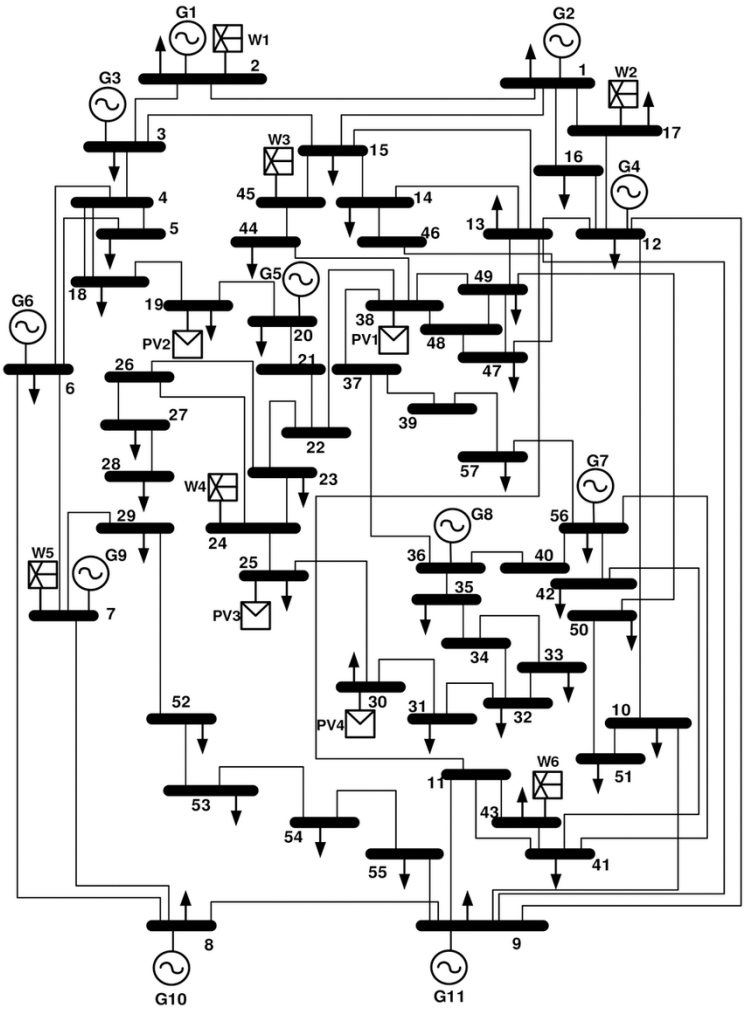

Figure 12: IEEE Standard 57-bus Network.

6. Conclusion

This article discusses the issues of reactive power distribution and voltage management in the presence of distributed generator units using an evolutionary genetic algorithm and statistical quality based on orthogonal arrays. It has been shown that this approach can solve the OPRD problem when used to the IEEE 57-bus standard network. The findings indicate that when DG unit output capacity is uncertain, there is a reduction in overall network losses as opposed to when it is not. In addition, all control variables remain inside their permitted range both during the issue solving process and at the conclusion of the method. The value of the system losses from the test, 27.5 MW, is the optimal load flow that can be acquired from the Taguchi method test using the genetic algorithm. The levels set by the TM are also obtained; however, the answer obtained for losses of the same system from the normal OPF by the Newton-Raphson load flow method is 33 MW. This suggests that the TM modifies the POPF of factor levels so that the system experiences the fewest losses possible and minimizes the difference between 33 and 27.5, which is equal to 5.5 MW, a noteworthy amount.

References

[1] A. A. A. Mohamed, Y. S. Mohamed, A. A. El-Gaafary, and A. M. Hemeida, "Optimal Power Flow using Moth Swarm Algorithm," *Electric Power Systems Research*, vol. 142, pp. 190-206, 2017.

[2] I. Rahman, and J. Mohamad-Saleh, "Hybrid Bio-Inspired Computational Intelligence Techniques for Solving Power System Optimization Problems: A Comprehensive Survey," *Applied Soft Computing*, vol. 69, pp. 72-130, 2018.

[3] H. R. Nikzad, and H. Abdi, "A Robust Unit Commitment Based on GA-PL Strategy by Applying TOAT and Considering Emission Costs and Energy Storage Systems," *Electric Power Systems Research*, vol. 180, 106154, 2020.

[4] L. Chinmoy, S. Iniyan, and R. Goic, "Modeling Wind Power Investments, Policies and Social Benefits for Deregulated Electricity Market–A Review," *Applied energy*, vol. 242, pp. 364-377, 2019.

[5] W. Zhang, Y. Xu, Z. Y. Dong, Y. Wang, and R. Zhang, "An Efficient Approach for Robust SCOPF Considering Load and Renewable Power Uncertainties," *2016 Power Systems Computation Conference (PSCC)*, pp. 1-7, 2016.

[6] M. Ebeed, A. Alhejji, S. Kamel, and F. Jurado, "Solving the Optimal Reactive Power Dispatch using Marine Predators Algorithm Considering the Uncertainties in Load and Wind-Solar Generation Systems," *Energies*, vol. 13, no. 17, p. 4316, 2020.

[7] F. Gami, Z. A. Alrowaili, et al., "Stochastic Optimal Reactive Power Dispatch at Varying Time of Load Demand and Renewable Energy Resources using an Efficient Modified Jellyfish Optimizer," *Neural Computing and Applications*, vol. 34, no. 22, pp. 20395-20410, 2022.

[8] M. H. Ali, A. M. A. Soliman, et al., "A Novel Stochastic Optimizer Solving Optimal Reactive Power Dispatch Problem Considering Renewable Energy Resources," *Energies*, vol. 16, no. 4, p. 1562, 2023.

[9] R. Jamal, J. Zhang, et al., "Solution to the deterministic and stochastic Optimal Reactive Power Dispatch by integration of solar, wind-hydro powers using Modified Artificial Hummingbird Algorithm," *Energy Reports*, vol. 9, pp. 4157-4173, 2023.

[10] S. Karimi, S. Hosseini-Hemati, and A. Rastgou, "Stochastic Multi-Objective ORPD for Active Distribution Networks," *Sustainable Energy Technologies and Assessments*, vol. 57, 103235, 2023.

[11] M. Yan, M. Shahidehpour, et al., "A Convex Three-Stage SCOPF Approach to Power System Flexibility with Unified Power Flow Controllers," *IEEE Transactions on Power Systems*, vol. 36, no. 3, pp. 1947-1960, 2020.

[12] N. Mezhoud, and M. Amarouayache, "Multi-Objective Optimal Power Flow Based Combined Non-Convex Economic Dispatch with Valve-Point Effects and Emission Using Gravitation Search Algorithm," *Journal of Applied Research in Electrical Engineering*, vol. 2, no. 1, pp. 26-36, 2023.

[13] M. Gholami, and M. J. Sanjari, "Optimal Operation of Multi-Microgrid System Considering Uncertainty of Electric Vehicles," *International Journal of Engineering*, vol. 36, no. 8, pp. 1398-1408, 2023.

[14] B. Y. Qu, Y. S. Zhu, et al., "A Survey on Multi-Objective Evolutionary Algorithms for the Solution of the Environmental/Economic Dispatch Problems," *Swarm and Evolutionary Computation*, vol. 38, pp. 1-11, 2018.

[15] S. Li, W. Gong, L. Wang, X. Yan, and C. Hu, "Optimal Power Flow by Means of Improved Adaptive Differential Evolution," *Energy*, vol. 198, 117314, 2020.

[16] K. Mardanimajd, S. Karimi, and A. Anvari Moghaddam, "Voltage Stability Improvement in Distribution Networks by Using Soft Open Points," *International Journal of Electrical Power & Energy Systems*, vol. 155, 109582, 2024.

[17] R. Leng, Z. Li, and Y. Xu, "Two-stage Stochastic Programming for Coordinated Operation of Distributed Energy Resources in Unbalanced Active Distribution Networks with Diverse Correlated Uncertainties," *Journal of Modern Power Systems and Clean Energy*, vol. 11, no. 1, pp. 120-131, 2023.

[18] R. Elazab, M. Ser-Alkhatm, M. A. A. Adma, and K. M. Abdel-Latif, "A Two-Stage Stochastic Programming Approach for Planning of Svcs in PV Microgrids under Load and PV Uncertainty Considering PV Inverters Reactive Power using Honey Badger Algorithm," *Electric Power Systems Research*, vol. 228, 109970, 2024.

[19] B. R. Prusty, and D. Jena, "A Critical Review on Probabilistic Load Flow Studies in Uncertainty Constrained Power Systems with Photovoltaic Generation and a New Approach," *Renewable and Sustainable Energy Reviews*, vol. 69, pp. 1286-1302, 2017.

[20] H. Nosratabadi, M. Mohammadi, and A. Kargarian, "Nonparametric Probabilistic Unbalanced Power Flow with Adaptive Kernel Density Estimator," *IEEE Transactions on Smart Grid*, vol. 10, no. 3, pp. 3292-3300, 2018.

[21] F. J. Ruiz-Rodriguez, J. C. Hernandez, and F. Jurado, "Iterative Harmonic Load Flow by using the Point-Estimate Method and Complex Affine Arithmetic for Radial Distribution Systems with Photovoltaic Uncertainties," *International Journal of Electrical Power & Energy Systems*, vol. 118, 105765, 2020.

[22] J. C. Hernandez, F. J. Ruiz-Rodriguez, F. Jurado, and F. Sanchez-Sutil, "Tracing Harmonic Distortion and Voltage Unbalance in Secondary Radial Distribution Networks with Photovoltaic Uncertainties by an Iterative Multiphase Harmonic Load Flow," *Electric Power Systems Research*, vol. 185, 106342, 2020.

[23] Y. Pan, L. Zhang, Z. Li, and L. Ding, "Improved Fuzzy Bayesian Network-Based Risk Analysis with Interval-Valued Fuzzy Sets and D–S Evidence Theory," *IEEE Transactions on Fuzzy Systems*, vol. 28, no. 9, pp. 2063-2077, 2019.

[24] C. Zhang, H. Chen, et al., "An Interval Power Flow Analysis Through Optimizing-Scenarios Method," *IEEE Transactions on Smart Grid*, vol. 9, no. 5, pp. 5217-5226, 2017.

[25] E. Acar, G. Bayrak, et al., "Modeling, Analysis, and Optimization under Uncertainties: A Review," *Structural and Multidisciplinary Optimization*, vol. 64, no. 5, pp. 2909-2945, 2021.

[26] M. Farhat, S. Kamel, A. M. Atallah, and B. Khan, "Optimal Power Flow Solution Based on Jellyfish Search Optimization Considering Uncertainty of Renewable Energy Sources," *IEEE Access*, vol. 9, pp. 100911-100933, 2021.

[27] A. Faramarzi, M. Heidarinejad, B. Stephens, and S. Mirjalili, "Equilibrium Optimizer: A Novel Optimization Algorithm," *Knowledge-Based Systems*, vol. 191, 105190, 2020.

[28] D. K. Panda, and S. Das, "Smart Grid Architecture Model for Control, Optimization and Data Analytics of Future Power Networks with More Renewable Energy," *Journal of Cleaner Production*, vol. 301, 126877, 2021.

[29] H. Heidari, and M. Tarafdar Hagh, "Optimal Reconfiguration of Solar Photovoltaic Arrays using a Fast Parallelized Particle Swarm Optimization in Confront of Partial Shading," *International Journal of Engineering*, vol. 32, no. 8, pp. 1177-1185, 2019.

[30] M. Papadimitrakis, N. Giamarelos, et al., "Metaheuristic Search in Smart Grid: A Review with Emphasis on Planning, Scheduling and Power Flow Optimization Applications," *Renewable and Sustainable Energy Reviews*, vol. 145, 111072, 2021.

[31] W. Peng, A. Maleki, M. A. Rosen, and P. Azarikhah, "Optimization of a Hybrid System for Solar-Wind-Based Water Desalination by Reverse Osmosis: Comparison of Approaches," *Desalination*, vol. 442, pp. 16-31, 2018.

[32] D. Wang, D. Tan, and L. Liu, "Particle Swarm Optimization Algorithm: an Overview," *Soft computing*, vol. 22, no. 2, pp. 387-408, 2018.

[33] M. E. Meral, and D. Çelík, "A Comprehensive Survey on Control Strategies of Distributed Generation Power Systems under Normal and Abnormal Conditions," *Annual Reviews in control*, vol. 47, pp. 112-132, 2019.

[34] P. Rajesh, C. Naveen, A. K. Venkatesan, and F. H. Shajin, "An Optimization Technique for Battery Energy Storage with Wind Turbine Generator Integration in Unbalanced Radial Distribution Network," *Journal of Energy Storage*, vol. 43, 103160, 2021.

[35] H. Yu, and W. D. Rosehart, "An Optimal Power Flow Algorithm to Achieve Robust Operation Considering Load and Renewable Generation Uncertainties," *IEEE Transactions on Power Systems*, vol. 27, no. 4, pp. 1808-1817, 2012.

[36] K. M. D. Puspitasari, J. Raharjo, A. S. Sastrosubroto, and B. Rahmat, "Generator Scheduling Optimization Involving Emission to Determine Emission Reduction Costs," *International Journal of Engineering*, vol. 35, no. 8, pp. 1468-1478, 2022.

[37] M. Najjarpour, and B. Tousi, "Loss Reduction of Distribution Network by Optimal Reconfiguration and Capacitor Placement using Cuckoo and Cultural Algorithms," *8th International Conference on Technology and Energy Management (ICTEM)*, pp. 1-5, 2023.

[38] M. Najjarpour, and B. Tousi, "Probabilistic Reactive Power Flow Optimization of The Distribution System in The Presence of Distributed Units Uncertainty Using the Combination of Improved Taguchi Method and Dandelion Algorithm," *International Journal of Engineering*, vol. 37, no. 1, pp. 37-47, 2024.

[39] M. Najjarpour, B. Tousi, and S. Jamali, "Loss Reduction in Distribution Networks with DG Units by Correlating Taguchi Method and Genetic Algorithm," *Iranian Journal of Electrical & Electronic Engineering*, vol. 18, no. 4, 2022.

[40] B. Gasbaoui, and B. Allaoua, "Ant Colony Optimization Applied on Combinatorial Problem for Optimal Power Flow Solution," *Leonardo Journal of Sciences*, vol. 14, pp. 1-17, 2009.

Declaration of Competing Interest

The authors declare that they have no known competing financial interests or personal relationships that could have appeared to influence the work reported in this paper. The ethical issues, including plagiarism, informed consent, misconduct, data fabrication and/or falsification, double publication and/or submission, redundancy, have been completely observed by the authors.

Credit Authorship Contribution Statement

Majid Najjarpour: Conceptualization, Data curation, Formal analysis, Investigation, Methodology, Software, Roles/Writing - original draft. **Behrouz Tousi:** Supervision. **Amirhossein Karamali:** Writing-review & editing.

Bibliography

Majid Najjarpour was born in 1997 in Urmia, West Azerbaijan, Iran. He received his Diploma and Pre-university degrees from Ferdowsi High School Tabriz in Tabriz in 2014 and 2015, respectively all in Mathematics and Physics fields. Winning the title of the first person of the Mathematical Olympiad in East Azerbaijan Province, Iran in 2011 and Member of Tabriz and Mathematics House and B.Sc. and M.Sc. degrees from Urmia University in Urmia in 2019 and 2021, respectively all in Electrical Engineering. He is currently working towards a Ph.D. degree in the Department of Electrical Engineering at Iran University of Science and Technology (IUST) in Tehran, Iran since Sep.2021 he was ranked first in M.Sc. and was accepted without exams by using the quota of talented students in M.Sc. and Ph.D. His field of interest includes Power System Protection, Distribution Systems Protection, and Automation.

Behrouz Tousi received the B.Sc. degree in Electronic Engineering from University of Tabriz, Tabriz, Iran. He received the M.Sc. and Ph.D. degrees both in Electric Power Engineering from Amirkabir University of Technology, Tehran, Iran, in 1995 and 2001, respectively. He is now a Professor at Faculty of Electrical and Computer Engineering, Urmia University, Urmia, Iran. His research interests include analysis and applications of power electronics and electric power system studies.

Amirhossein Karamali was born in 2000 in Mahallat city, Iran. He completed his bachelor's degree in Electrical Engineering in 2022 and is currently pursuing a master's degree in Power Electronics and Electric Machines at Iran University of Science and Technology (IUST). His research focuses on the application of power electronic converters in power systems, with the goal of advancing renewable energy technologies for a sustainable future.

Journal of Green Energy Research and Innovation

Optimal Site Selection of Solar Power Plant Stations Using GIS-ANP and Genetic Optimization Algorithm in Markazi Province, Iran

Fatemeh Masteri Farahani, Azadeh Kazemi, Amir Hedayati Aghmashadi

Highlight

- The use of renewable resources for electricity production is unavoidable.
- Creating solar power plants can help reduce the environmental effects of fossil fuel consumption.
- Site selection of solar power plants using modern methods is important.
- Among the methods, the ANP method has not been used so far.
- It is better to use the genetic algorithm method to verify the location.

Graphical Abstract

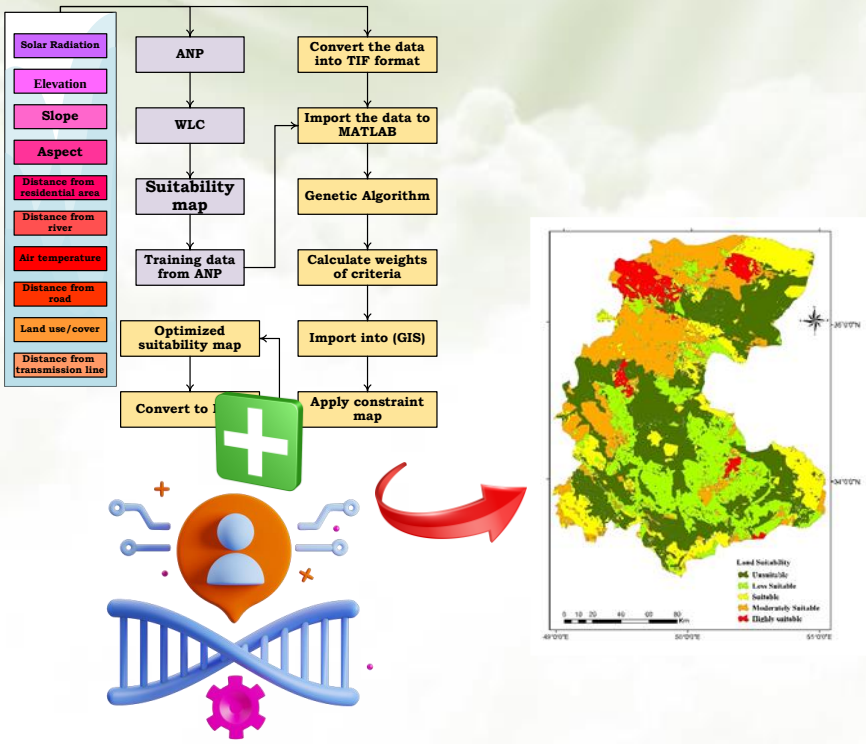

Use your device to scan and read the article online

Citation

F. Masteri Farahani, A. Kazemi, and A. Hedayati Aghmashadi, "Optimal Site Selection of Solar Power Plant Stations Using GIS-ANP and Genetic Optimization Algorithm in Markazi Province, Iran," *Journal of Green Energy Research and Innovation*, vol. 1, no. 4, pp. 47-63, 2024.

https://doi.org/10.61186/jgeri.1.4.47

JGERI Journal of Green Energy Research and Innovation

Online ISSN: 3041-9018

Journal of Green Energy Research and Innovation

Journal Homepage: www.jgeri.araku.ac.ir

Optimal Site Selection of Solar Power Plant Stations Using GIS-ANP and Genetic Optimization Algorithm in Markazi Province, Iran

Fatemeh Masteri Farahani [1], Azadeh Kazemi[1]*, Amir Hedayati Aghmashadi [2]

[1] *Department of Environmental Science and Engineering, Faculty of Agriculture and Environment, Arak University, 38156879 Arak, Iran.*

[2] *Department of Sustainable Landscape Development, Institute of Geosciences and Geography, Martin Luther University Halle-Wittenberg, 06120 Halle, Germany.*

* ***Corresponding Author:*** *a-kazemi@araku.ac.ir*

ARTICLE INFO

Keywords:
Solar power plant stations;
Genetic algorithm;
Optimal site selection;
Analytic network process (anp).

Article history:
Received: 14 April 2024;
Revised: 27 April 2024;
Accepted: 30 April 2024;

Article type:
Research Article

ABSTRACT

The demand for non-renewable energy sources in power generation is crucial for residential and commercial uses, significantly impacting national development. However, with the depletion of fossil fuels, there is a shift towards renewable energy sources such as solar, water, and wind, which have seen a surge in use over recent decades. In Iran, despite abundant fossil fuel resources, solar energy is vital due to the country's favorable geographic conditions for solar exploitation. This study applies the analytic network process (ANP) and Genetic algorithm (GA) to identify optimal locations for Solar Power Plant Stations in Markazi province, Iran. Key morphological factors considered include slope, elevation, and solar radiation. The research identified the northwest and northern parts of Markazi province as the most suitable for solar photovoltaic systems, primarily due to their simpler topography. Using a genetic algorithm, which outperformed the ANP, it was found that about 24,000 km^2 in these areas are apt for solar power facilities, categorized into highly suitable (2,429.312 km^2), moderately suitable (16,818.49 km^2), and suitable (5,029.007 km^2). Saveh showed the highest potential, while Ashtian, Khondab, and Shazand had the least. These findings provide crucial insights for stakeholders looking to develop solar energy projects in Markazi province.

1. Introduction

Throughout history, renewable energy has been utilized and is currently acknowledged as essential in light of the finite nature of fossil fuels and growing environmental apprehensions [1,2]. Burning fossil fuels leads to pollution and an increase in CO_2 emissions, but this can be mitigated by shifting towards renewable energy sources [3]. The demand for energy holds significant importance on both national and international levels. Presently, the primary sources of energy in Iran, as well as in many other countries, are fossil fuels like oil, natural gas, and coal. Given their lengthy natural formation process and limited availability, these nonrenewable resources are expected to become increasingly expensive as their reserves diminish. In light of these factors, there is a growing need for an energy transition towards renewable sources [4]. The increasing utilization of solar energy in urban environments has become a common practice,

emphasizing the significance of accurate tools and methods for assessing land potential for solar power generation at the local level [5].

Numerous studies have focused on analyzing solar power plants and selecting optimal sites using different methods. However, not much attention has been given to the Markazi province in Iran. Selecting optimal locations for building a solar power plant is a critical decision as it can result in higher energy output, improved efficiency, as well as better economic advantages.

Al Garni et al. [6] studied several applications of the geographical information systems (GIS) and an analytical hierarchy process (AHP) technique to assess the factors and calculate a land suitability index (LSI) for analyzing potential locations in Saudi Arabia. Merrouni et al. [7] evaluated the appropriateness of the Eastern area of Morocco for accommodating extensive Concentrating Solar Power facilities through a merger of GIS and AHP. Habib et al. [8] identified the optimal sites for setting up photovoltaic plants in Egypt through a combination of GIS, Remote Sensing (RS), and Multi-Criteria Decision Making (MCDM). Hassaan et al. [9] developed a GIS model for conducting a multi-criteria suitability analysis to identify the best locations for photovoltaic plants in Kuwait. Mirzaei et al. [10] attempted to identify the most suitable site for establishing a solar power plant using six distinct criteria among five cities in southern Turkey. This was done through three widely recognized MCDM approaches, namely ANP, AHP, and PROMETHEE.

A nation's prosperity is linked to its ability to achieve energy self-sufficiency, thus reducing reliance on foreign energy supplies. The socioeconomic soundness and stability of a country are closely connected to its energy independence and efforts to diversify domestic energy sources. Even if a country possesses abundant primary energy resources, efficient conversion of these resources into secondary energy requires advanced technology and expertise. Cost-effective utilization of readily available domestic natural resources such as hydropower is achievable through less sophisticated technologies at minimal costs. It is essential to prioritize sustainability and minimize greenhouse gas emissions in this process [11]. Markazi province, situated in Iran, is recognized as a significant industrial hub. The third largest fossil fuel power plant in Iran with significant greenhouse gas emissions is located in this province. Given its considerable potential for solar power plant construction, a comprehensive assessment of suitable locations for such facilities is crucial. This study introduces a new method for evaluating the viability of renewable energy sources in Markazi province. By integrating ANP with a genetic optimization algorithm, the research identified the most suitable sites with high potential for establishing PV systems in the study area. The study explored the suitability of ANP and genetic algorithms (GA) in site selection for solar power through a qualitative method rather than using predefined metrics. The effectiveness and accuracy of GA were compared and evaluated against ANP for each region individually.

2. Data and methodology

2.1. Study area

Markazi province is located in the center of Iran, with an area of 29530 km^2, covering latitudes 33°23’–35°33’ N and longitudes 48°56’–51°3’ E. It is made up of 12 counties, 35

cities, and 13,941 villages. Markazi covers 1.82% of Iran's expanse, with a population of 1,429,475, which is 1.6% of Iran's total population. It has a complex geomorphology, with elevations of 950 m in the north and 3,388 m in the southwest. Markazi's climate is semi-arid continental, and its summers are sunny and warm and its winters are generally rainy and cool.

Notable distinctions in the region are influenced by its characteristics and elevation, with the northern section exhibiting a semi-desert climate, the eastern section exhibiting altitude-driven coldness, and the southern section being home to freezing highlands [12]. As an industrial hub, this province is perfect for constructing solar farms for several reasons, including strategic location, ample solar radiation year-round, numerous expansive plains, diverse geographical features enabling the use of various modern panel mounting structures, and a growing population that requires more electricity. Solar farms can benefit the region by reducing power imports, creating a self-sufficient province, improving its energy-based sustainability, combating air pollution, and boosting public health. Presently, energy imports cannot meet the province's demand, which shows the urgency of establishing such plants. Figure 1 demonstrates the location of the study area.

2.2. The GIS Database

The research data was gathered from a variety of sources, each of which is comprehensively described.

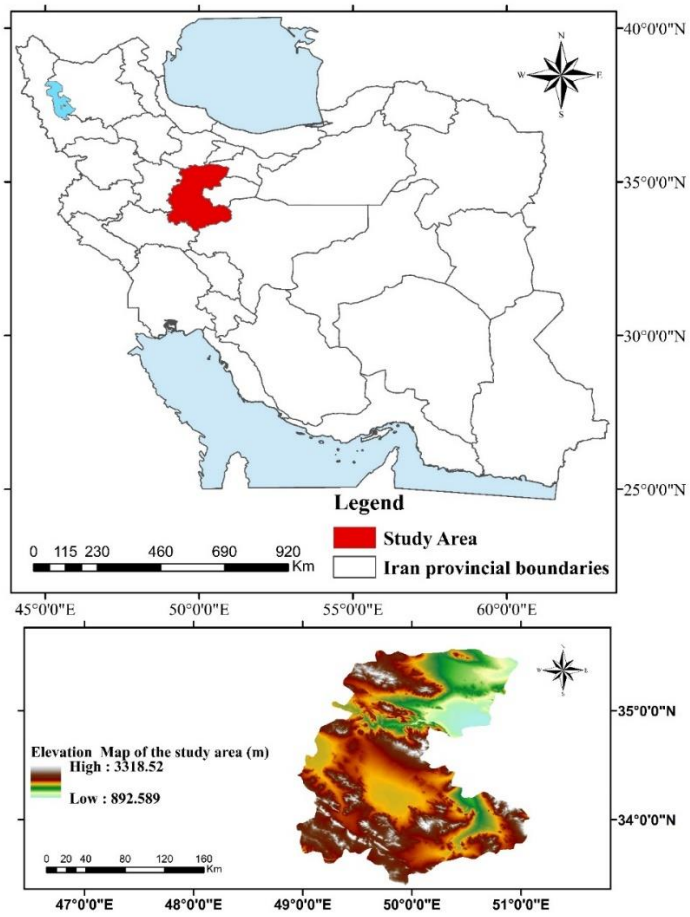

Figure 1. (a) Map and geographical coordinates of Iran, (b) elevation map of the study area.

2.2.1. Solar radiation

Optimal locations for photovoltaic power generation were primarily identified based on solar irradiance levels [13]. Solar radiation data for Markazi was derived from Shuttle Radar Topography Mission data at a 30 × 30 m resolution. The analysis revealed an average annual solar radiation of 1,574 kWh/m^2, indicating the province's potential for establishing solar farms. Surface solar radiation values were computed for 1000 random points across the study area using ArcGIS 10.8 and later interpolated with Kriging Interpolation. The resulting data showed that in Markazi province, the annual minimum solar radiation was 1,374 kWh/m^2, and the maximum value was 1,776 kWh/m^2, making it suitable for installing solar panels. Figure 2 illustrates a raster classification dividing suitability into five classes, while Table 1 shows the classified solar radiation values across the research area.

2.2.2. Digital Elevation Model (DEM)

The elevation of a region can have a significant effect on its industrial sites. The height above sea level has an inverse correlation with atmospheric density [14]. Greater elevations lead to increased expenses and challenges in transporting infrastructure and labor. DEM enables analysis of the fundamental topographic features (such as elevation, aspect, slope, and sky view). In complex terrains, solar radiation distribution undergoes significant changes. A digital elevation model and a geometric approach that depends on DEM resolution accuracy can be used to assess topographic effects. DEM provides an artificial horizon and the sun's relative position for each point. The Shuttle Radar Topography Mission's DEM provides data on elevation, solar radiation, slope, and aspect for the study area. Figure 2 illustrates the digital area elevations while Table 1 displays classified research-area elevations.

2.2.3. Slope

When choosing the best place for establishing solar power plants, it is important to analyze its slope [15]. How much sunlight an area gets can change based on how steep it is, which also influences where to put solar panels to collect energy from the sun. In this study, we made a map of the area's slope using ArcGIS 10.8 and data from SRTM with a detail level of 30 m DEM. We then split these slopes into five different categories shown in Figure 2 and Table 1.

2.2.4. Aspect

Aspect is very important for PV farms because the direction they face greatly affects how much sunlight they get [16]. The east, west, and south sides get more sunlight than the north. Areas that are flat or face south get the most sun throughout the year [16].

2.2.5. Distance from residential areas

Constructing solar power plants near residential areas can affect their environment and future developments. Locations within 30 km or more than 3 km are deemed most suitable. Areas with a distance of over 50 km but fewer than 3 km are considered least suitable [17].

2.2.6. Distance from rivers

The proximity to running water is another important feature. There is a river network in this region, which was derived from SRTM DEM to be used in generating a distance map via the Euclidean distance toolbox in ArcGIS.
As per existing literature, the raster data was categorized into five classes, with details available in Table 1. Figure 2 demonstrates the map of distance from rivers.

2.2.7. Distance from roads

The next important feature for site selection is roadways. These networks play a significant role in transporting equipment, providing site access, facilitating regular maintenance, and monitoring farm operations. An optimal site must be situated at specific distances from the roads. Figure 2 shows a map of the study area's road network. The distances were determined using the Euclidean distance toolbox. Table 3 presents information related to proximity to roads.

2.2.8. Air temperature

In this study, a Land Data Assimilation System product for 2020 is used to analyze air temperature with a resolution of 0.1 degrees. The resulting raster is resampled to match the resolution of other data at 30 m and divided into five categories. The air temperature map of the research region can be seen in Figure 2, and statistical information for this thematic layer is provided in Table 1.

2.2.9. Distance from transmission lines

The main transmission line passing through the main cities is provided in a grid file. The polylines were created and cropped to the study area using ArcGIS. Proximity calculations for these polylines were categorized into five classes, as shown in Figure 2, with statistical details provided in Table 1.

2.2.10. Land use

An optimal solar power plant site should have flat terrain, no shading, and be located in non-agricultural areas. In our study area, we created a land use and land cover (LU/LC) map through Sentinel-2 imagery with a high resolution in the Google Earth Engine (GEE). Support Vector Machine algorithm was used to classify different LU/LC classes in the study area. The LU/LC map shows four classes which are detailed in Table 1, and visually presented in Figure 2.

2.2.11. Methodology

The study used GA and the ANP to identify suitable locations for establishing PV systems. The genetic algorithms were fed with the ANP outputs. Hence, these outputs were used to train ANP for weighing the related criteria, effectively integrating ANP information to enhance its performance in site selection. Selecting locations for large-scale solar farms and turbine systems can be a complex problem whose solution calls for examining various variables [15]. Solar potential is not the only factor to consider, rather land suitability and disposal are also important [16]. The research data was obtained in different formats from various

sources. Spatial data modeling, coding, and image processing were performed using a range of applications. LU/LC were obtained from GEE, and satellite imagery was analyzed using JavaScript.

Table 1. Statistical data on the research criteria.

Criteria	Ranking Values	Classes	Area percentage (km²)	Suitability
Solar Radiation (kWh/m2)	1	1374–1470	30.6	Unsuitable
	2	1470–1662	18.5	Very less suitable
	3	1662–1686	26.5	Less suitable
	4	1686–1746	9.4	Moderately suitable
	5	1746–1776	15	Highly suitable
Elevation (m)	5	2500–3300	2.9	Unsuitable
	4	2000–2500	29.4	Very less suitable
	3	1500–2000	50.4	Less suitable
	2	1000–1500	15	Moderately suitable
	1	800–1000	2.3	Highly suitable
Slope (%)	5	25–49	2.8	Unsuitable
	4	20–25	2.4	Very less suitable
	3	15–20	4.7	Less suitable
	2	10–15	8.5	Moderately suitable
	1	0–10	81.6	Highly suitable
Aspect	1	North	12.7	Unsuitable
	5	Northwest, west	23.3	Very less suitable
	2	Northeast	13.7	Less suitable
	3	East	11.7	Moderately suitable
	4	South, Southeast, Southwest,	38.6	Highly suitable
Distance to the residential area (km)	1	0–5	7.8	Unsuitable
	5	30–50	1.9	Very less suitable
	4	20–30	10.1	Less suitable
	3	10–20	30.5	Moderately suitable
	2	5–10	49.7	Highly suitable
Distance to river (m)	1	0–500	23	Unsuitable
	5	3500–7000	14	Very less suitable
	4	2500–3500	11	Less suitable
	3	1500–2500	19	Moderately suitable
	2	500–1500	33	Highly suitable
Air temperature (c°)	1	1–5	50.4	Unsuitable
	2	6–10	9.2	Very less suitable
	3	11–16	11	Less suitable
	4	17–21	21.8	Moderately suitable
	5	22–27	7.6	Highly suitable
Distance to road (km)	1	0-5	51	Unsuitable
	5	30–40	1	Very less suitable
	3	30–20	2	Less suitable
	4	10–20	19	Moderately suitable
	2	5–10	27	Highly suitable
Land use/land cover	1	Vegetation	71	Unsuitable
	2	Barren lands	23	Highly suitable Unsuitable
	3	Urban	0.5	Unsuitable
	4	Snow	0.6	Unsuitable
	5	Water	4.9	
Distance to the transmission line (km)	1	>70	13.2	Unsuitable
	2	50–70	15.6	Very less suitable
	3	30–50	19.5	Less suitable
	4	15–30	21	Moderately suitable
	5	<15	30.7	Highly suitable

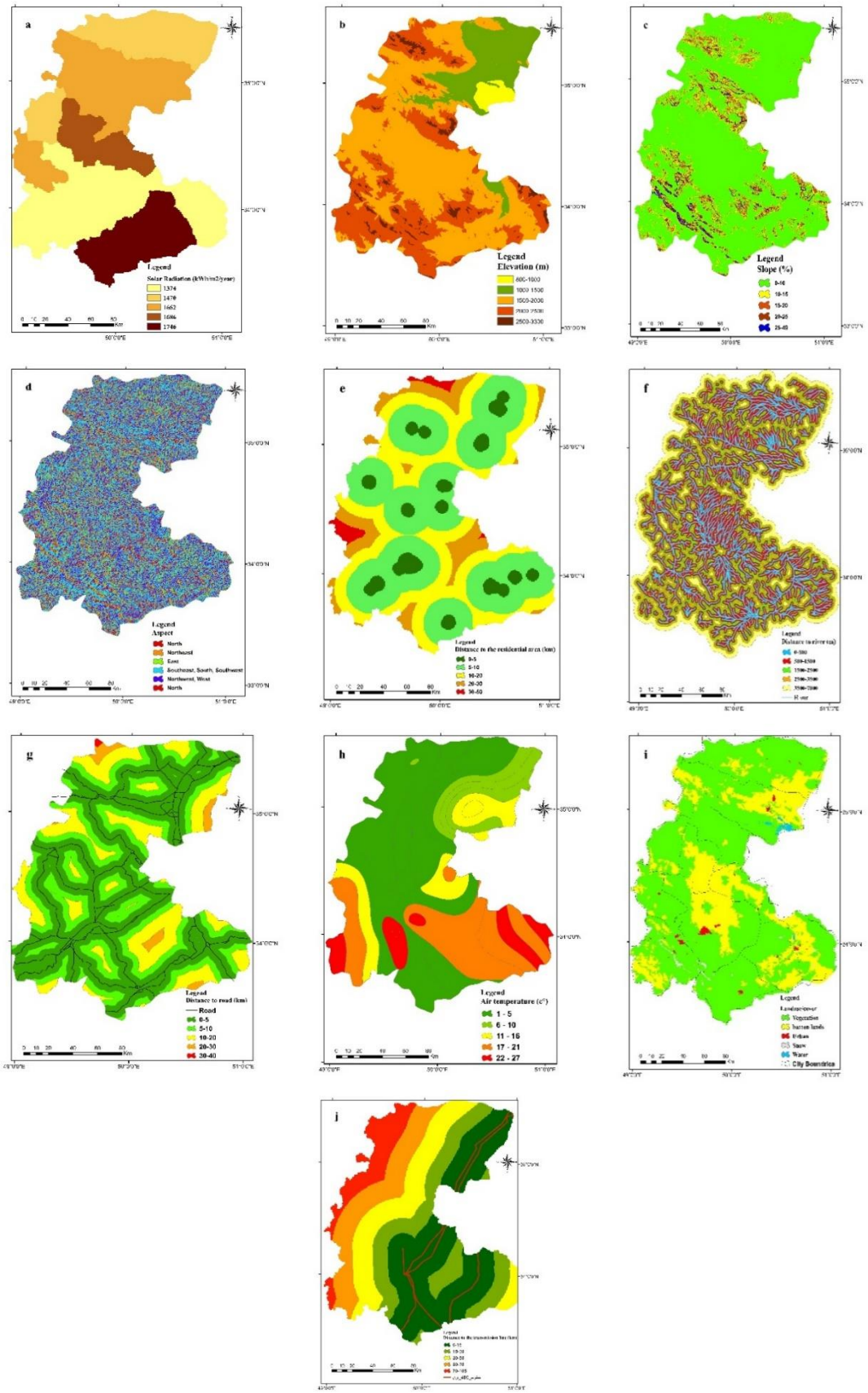

Figure 2. Criteria map used in this research; (a) solar radiation, (b) elevation, (c) slope, (d) aspect, (e), distance from residential area, (f) distance from river, (g) distance from road, (h) air temperature, (i) land use/land cover, (j) distance from transmission line.

ArcGIS (V10.8) was used for preparing the necessary input for site selection, modeling, and ultimate map outputs. Super Decision was employed to calculate criteria weights, while MATLAB's genetic algorithm optimized site selection. The research flowchart can be seen in Figure 3.

2.3.1. GIS-based multi-criteria analysis

For selecting sites in large-scale PV projects, various social, technological, economic, and environmental factors must be taken into account [18]. Researchers and policymakers use MCDM to effectively address this challenge. By using these techniques, decision-makers can identify and select appropriate locations. Figure 3 illustrates the connection between criteria, objectives, and options. GIS-based studies typically use MCDM methods for suitable site identification and selection based on their objectives. These methods include ANP, Analytic Hierarchy Process, Technique for Order of Preference by Similarity to Ideal Solution (TOPSIS), Simple Additive Weighting (SAW), Ordered Weighted Averaging (OWA), and Weighted Linear Combination (WLC). ANP is particularly popular since it is more flexible, simple, and transparent when it comes to site selection in GIS. On the whole, ANP proves an effective tool for GIS-based decision-making problems thanks to its ability to pinpoint optimal sites and, in the case of this study, boost solar energy production.

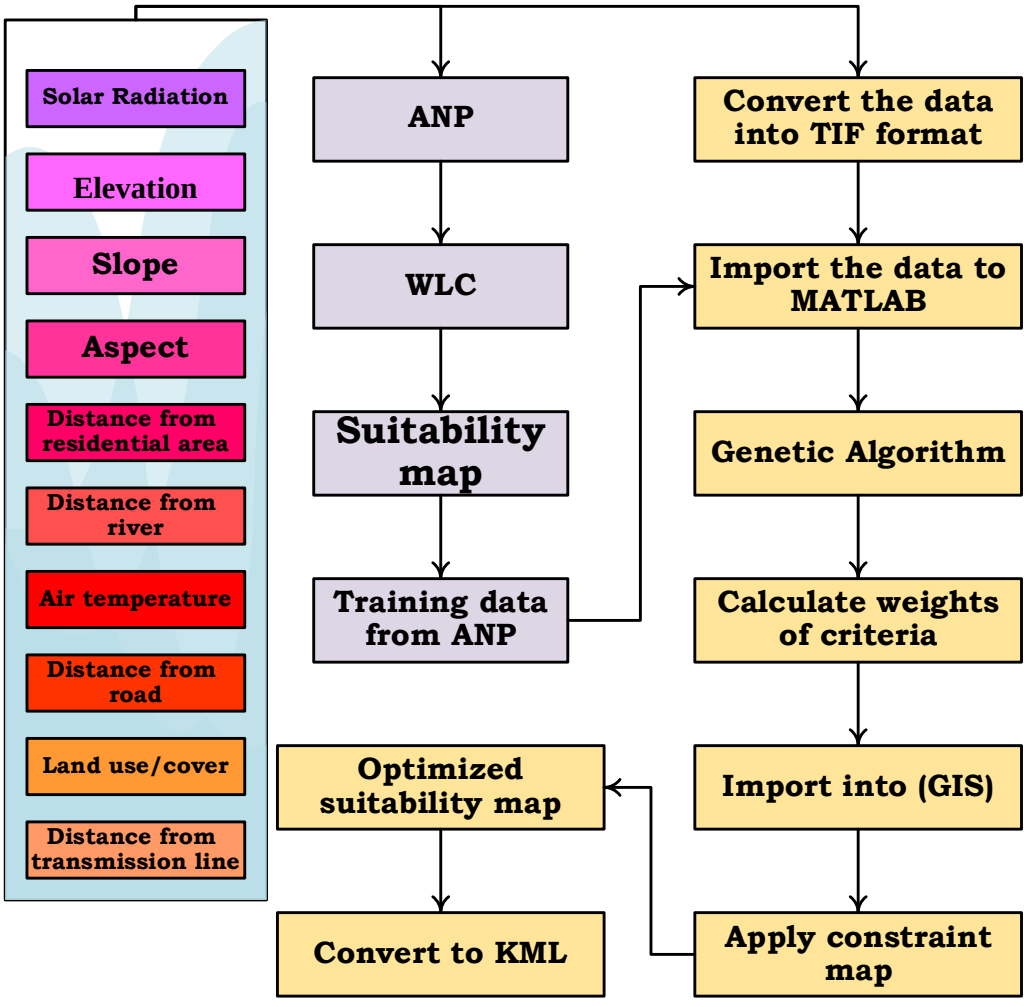

Figure 3. The methodology workflow.

2.3.2. Analytic Network Process (ANP)

Developed by Saaty in 1996, ANP is a method for multi-criteria decision-making [19]. It calculates priority scores based on relative assessments rather than absolute numbers. ANP is valuable for evaluating decision problems as it reveals the level of interdependence between criteria and alternatives [20].

The process of using ANP to make decisions is comparable to AHP, except for a few distinctions. AHP uses a source node (main goal) alongside a sink node (alternative goals), as well as a linear top-down structure without feedback from higher to lower levels. In contrast, in ANP no specific order is in place for arranging clusters, and the network can expand in every direction allowing influence to be extended within a cluster as well. ANP's alternative cluster can have feedback to other clusters or not [20].

2.3.3. Weighted Linear Combination (WLC)

WLC is a geographic information systems-based multicriteria assessment model commonly utilized to analyze whether or not different locations are suitable for the purpose under consideration. It can prioritize site selection and land use through value standardization, weighting, and overlaying [21].

GIS-based WLC can help clarify and consider criteria for selecting ideal locations for specific development activities [22]. WLC combines factors, sub-factors, and constraints to determine the overall land suitability. It uses weights to combine parameters affecting landslides. The main challenge of this method lies in assigning individual weights to each parameter separately [23]. The mathematical definition of weighted linear combination is represented as Equation (1).

$$WLC = \sum_{i=1}^{N} W_i \times K_i \quad (1)$$

Where
WLC is the Weighted Linear Combination
W_i is the Normalized weight of factor i
K_i is the criterion score of factor i
N is the number of factors.

2.4. Genetic algorithm

GA can model genetic selection and natural elimination in biological evolution [24]. Wu and Shan (2000) conducted significant research in this area, narrowing the search space to find optimal solutions [25]. Unlike conventional AI optimization algorithms, GA automatically collects information about the search space and controls the entire search process in a self-adaptive manner using random optimization techniques [26]. As a result, finding the best global solution becomes more likely without facing the overwhelming increase in possibilities caused by ignoring important information within the search space [27].

Genetic algorithms are known for their simplicity, robustness, and adaptability to parallel processing and numerous applications. They have been successfully employed to solve combinatorial optimization problems (COPs) as well as non-linear problems that have complicated constraints or an objective function that is not differentiable [28].

In GA, candidate solutions are ranked based on their quality, and any unqualified member is eliminated based on a specific fitness value. Acceptable solutions undergo genetic operations such as crossover, mutation, inversion, and translocation to generate new candidate solutions for the next generation. This process is iterated until reaching a specific convergent condition. The traditional knapsack problem serves as an illustration of this principle and its algorithm [25].

Sites are selected considering the specific purposes pursued, which should be aligned with the different considerations (economic, environmental, etc.) of the study area. The integration of MCDM and MODM with GA is employed to achieve practical and coherent outcomes. A fitness function is utilized to determine proper sites for establishing solar farms by taking into account multiple factors.

GA pursues two main objectives, namely to minimize or maximize factors. Factors to be minimized consist of distance from transmission lines, roads, and population centers, elevation, and slope. Meanwhile, factors to be maximized are LST, solar radiation, and air temperature. By incorporating these goals into the evaluation process through fitness scores given to potential solutions given their performance in fulfilling both criteria; feasibility is assessed by minimizing the determined factors while maximizing others. When using genetic algorithms to solve a problem, a fitness function is needed for each chromosome. This function returns a non-negative value indicating the merits or abilities of the chromosomes [29].

3. Results and discussion

3.1. ANP-based PV maps using WLC

The research data underwent processing and categorization to generate PV potential maps. ANP helped to determine the importance of different layers in the weighting process. These computed weights were then used to create PV potential suitability maps based on nine criteria, three of which were prioritized in the ANP process. The metrics for pairwise comparison and the obtained criteria weights can be seen in Tables 2 and 3.

3.2. Potential sites for solar power plants

ANP helped to identify the main areas with solar energy potential in the southern and eastern parts of Markazi province. The calculated weights of the layers significantly affected the results obtained by ANP.

According to ANP, higher weights were assigned to solar radiation, slope, and aspect, respectively, considering their suitability in receiving higher amounts of solar radiation in southern parts.

The northwestern and northern parts of the research area were not suitable due to higher topographic heterogeneity. The spatial distribution of the identified potential locations can be seen in Figures 4 and 5.

Table 2. Comparison matrix for solar power plant site selection.

Criteria	C1	C2	C3	C4	C5	C6	C7	C8	C9
Solar Radiation (C1)	1	3	1.3	3	5	3	5	3	5
Elevation (C2)		1	3	1.3	1.3	1.3	1.2	3	1.2
Slope (C3)			1	1	5	3	5	3	3
Aspect (C4)				1	3	3	3	3	3
Distance from residential area (C5)					1	1.3	1	1.3	1
Air temperature (C6)						1	3	1	3
Distance from road (C7)							1	1.3	1
Land use/cover (C8)								1	1.3
Distance from transmission line (C9)									1

Table 3. Obtained weights for solar power plant criteria.

Criteria	C1	C2	C3	C4	C5	C6	C7	C8	C9	Total
Weights	0.221	0.049	0.156	0.142	0.131	0.074	0.112	0.036	0.079	1

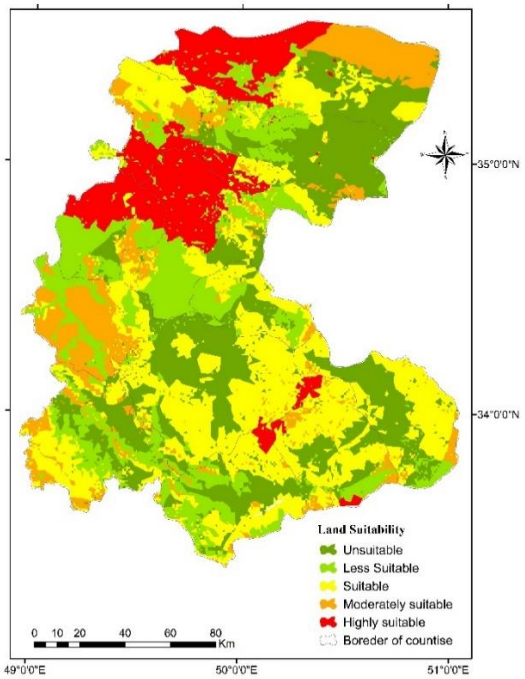

Figure 4. Land suitability map for solar energy potential based on ANP.

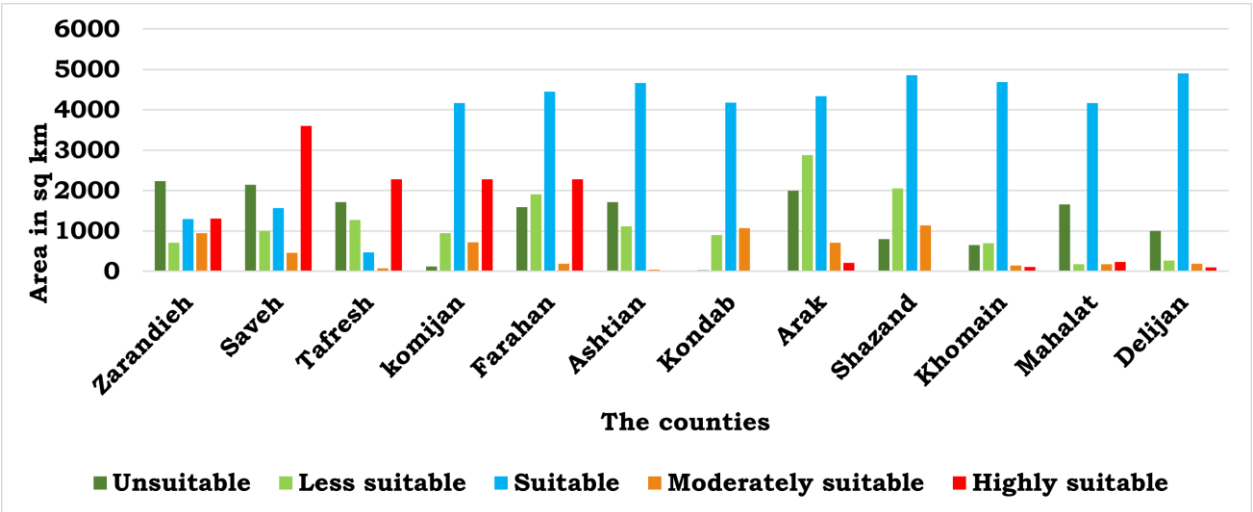

Figure 5. The area of lands with solar power potential in different counties based on ANP.

3.3. GA results

GA can be used for determining proper weights and ultimately selecting potential sites. In this study, the results of the GA method outperformed those of ANP. ANP outputs were used to train a genetic algorithm. Then, the values of nine effective factors (namely, land use, slope, elevation, aspect, air temperature, solar radiation, distance from transmission lines, distance from residential areas, and distance from roads) were extracted for 1000 random points across the study area. The suitability value of the ANP results was also determined. Two specific records were introduced to improve GA's performance in selecting optimal locations.

These included optimal values for each variable (highest suitability), and unfavorable values for lowest suitability. This data helped to identify the less favorable site selection criteria. By incorporating these outlier cases into the training dataset, our goal was to teach the GA optimization algorithm how to identify and give priority to the best locations. Therefore, the training data, which included these records, was imported into MATLAB to train the GA. As a result, the algorithm learned how to adjust itself and make better decisions in site selection. Table 4 displays the weights assigned to each layer.

3.4. GA-based potential sites for solar power plants

The genetic algorithm's findings indicated that morphological factors significantly influence the suitability of the area. Specifically, slope, elevation, and solar radiation had a strong impact on the GA results. A comprehensive investigation of the genetic algorithm output revealed that potential locations with lower topographic complexity are predominantly located in the northwestern and northern parts of the study area. Furthermore, the potential increased from east to west across the province. Figures 6 and 7 show the GA-based potential locations.

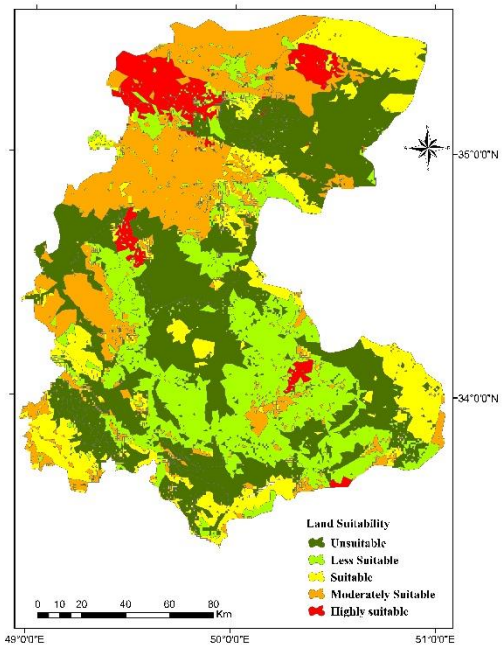

Figure 6. GA-based map of solar energy potential.

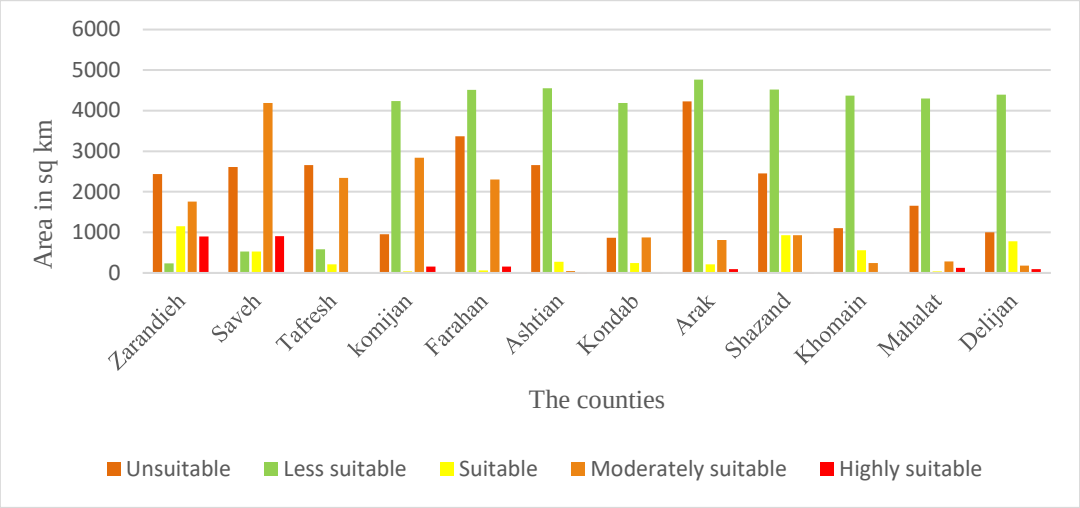

Figure 7. The area of lands with solar power potential in different counties based on GA.

Table 4. GA-based weights for the criteria.

Criteria	C1	C2	C3	C4	C5	C6	C7	C8	C9	Total
Weights	0.201	0.069	0.149	0.128	0.131	0.084	0.119	0.046	0.073	1

4. Discussion

The study's findings indicate that GA yielded more precise results compared to ANP. The GA-derived weights were utilized to pinpoint suitable locations for PV systems in the research area. GAs excel over ANP by encompassing a broader set of selection criteria. A comparison of the research results showed their alignment with those of other studies, including Mirzaei and Nowzari (2021) [10], Awasthi (2017) [6], and Merrouni et al. (2018) [7]; these studies assessed various approaches for a comparable issue through the use of GIS methods, MCDA, and optimization algorithms. The research revealed that morphological factors such as elevation, slope, and solar radiation had a substantial effect on site suitability. In the present study, areas with the highest potential for establishing solar power plants were located in the northwestern and northern regions of the Markazi province, which have less topographic complexity.

Noorollahi et al. [30], Van Hoesen and Letendre [31], and LEE [32] assessed the influence of topographic factors on solar power site suitability, yielding similar results to this research. These findings are important as they provide insights to policymakers and investors. They can serve as a guide for advancing large-scale solar projects in the province to expand renewable energy use while decreasing reliance on fossil fuels; however, it is worth noting that certain limitations such as overlooking socio-economic factors could hinder project development in these areas. Additionally, close attention must be paid to the expenses associated with building transmission lines to connect these sites to the national grid (Figure 8).

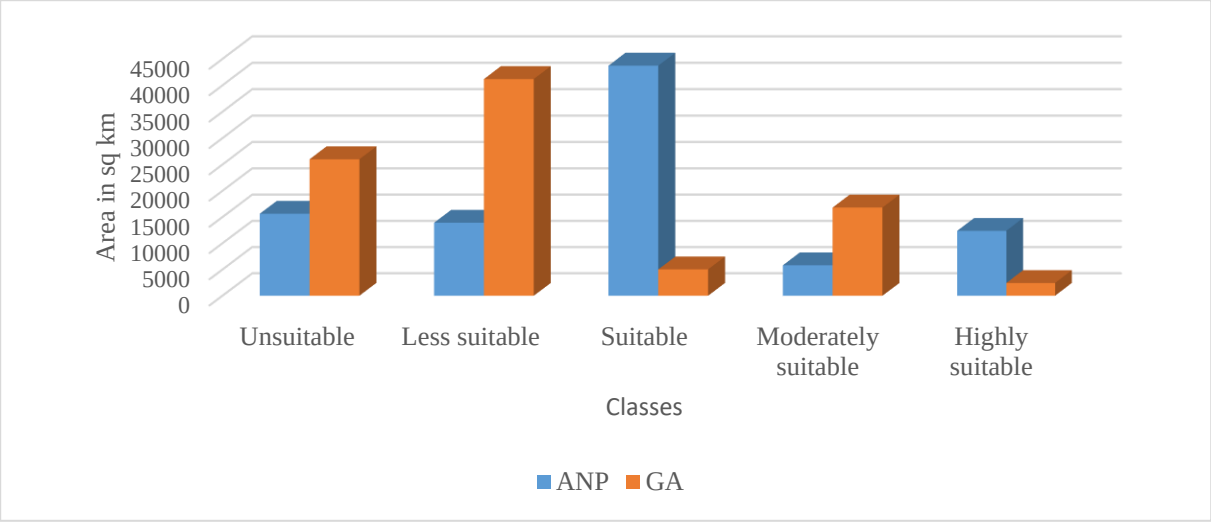

Figure 8. Comparison of GA and ANP outputs regarding potential areas for establishing solar power plants.

5. Conclusion

This study integrated GA with ANP in an attempt to identify and select optimal sites for establishing solar power plants. ANP played a vital for in training the genetic algorithm, enabling effective optimization using valuable information derived from the ANP. GA and ANP were compared to assess the accuracy of each region's selection without using particular factors.

The research findings indicate that the ANP approach identified specific areas in the Markazi province with high potential for solar power plant development. For instance, Saveh in the northwest and Zarandieh in the north of the province had the highest potential, respectively. According to ANP, Saveh had the most potential areas for PV systems, followed by Tafresh, Farahan, Komijan, and Zarandieh, whereas Khondab and Shazand had the least potential. According to the outputs of the genetic optimization algorithm, Saveh and Zarandieh had the highest potential. Both GA and ANP identified Saveh as a suitable area for establishing solar energy plants. Overall, GA favored northern sections as high-potential sites.

This research illustrated that the integration of ANP and evolutionary algorithms can enhance the precision and effectiveness of sites identified for renewable energy initiatives. The combination of these techniques enables the stakeholders and decision-makers to more effectively pinpoint and prioritize sites that are suitable for solar power installations. The results underscored the significance of a methodical approach in determining the best areas for developing green energy resources.

This research examined the potential for implementing renewable energy plants in the Markazi province and emphasized the advantages of utilizing solar power to address the country's energy demand. Due to substantial differences in the capacity of different areas for solar energy, policymakers should concentrate on promising regions and create the necessary infrastructure to support the development of solar farms in these areas.

References

[1] O. A. AL-Shahri, F. B. Ismail, et al., "Solar Photovoltaic Energy Optimization Methods, Challenges and Issues: A Comprehensive Review," *Journal of Cleaner Production*, vol. 284, 125465, 2021

[2] S. Zereshkian, and D. Mansoury, "A Study on The Feasibility of Using Solar Radiation Energy and Ocean Thermal Energy Conversion to Supply Electricity for Offshore Oil and Gas Fields in The Caspian Sea," *Renewable Energy,* vol. 163, pp. 66-77, 2021.

[3] S. Moonchai, and N. Chutsagulprom, "Short-term Forecasting of Renewable Energy Consumption: Augmentation of a Modified Grey Model with a Kalman Filter," *Applied Soft Computing*, vol. 87, 105994, 2020.

[4] A. Mollahosseini, S. A. Hosseini, M. Jabbari, A. Figoli, and A. Rahimpour, "Renewable Energy Management and Market in Iran: A Holistic Review on Current State and Future Demands," *Renewable and Sustainable Energy Reviews*, vol. 80, pp. 774-788, 2017.

[5] S. Zhang, and X. Li, "Future Projections of Offshore Wind Energy Resources in China using CMIP6 Simulations and a Deep Learning-based Downscaling Method," *Energy,* vol. 217, 119321, 2021.

[6] H. Z. Al Garni, A. Awasthi, "Solar PV Power Plant Site Selection using A GIS-AHP Based Approach with Application in Saudi Arabia," *Applied Energy*, vol. 206, pp. 1225-1240, 2017.

[7] A. A. Merrouni, F. E. Elalaouni, A. Ghenniouni, A. Mezrhab, and A. Mezrhab, "A GIS-AHP Combination for the Sites Assessment of Large-Scale CSP Plants with Dry and Wet Cooling Systems Case Study: Eastern Morocco," *Solar Energy*, vol. 166, pp. 2-12, 2018.

[8] S. M. Habib, A. E. R. E. Suliman, A. H. Al Nahry, and E. N. Abd El Rahman, "Spatial Modeling for the Optimum Site Selection of Solar Photovoltaics Power Plant in the Northwest Coast of Egypt," *Remote Sensing Applications: Society and Environment*, vol. 18, 100313, 2020.

[9] M. A. Hassaan, A. Hassan, and H. Al-Dashti, "GIS-Based Suitability Analysis for Siting Solar Power Plants in Kuwait," *The Egyptian Journal of Remote Sensing and Space Science*, vol. 24, no. 3, pp. 453-461. 2021.

[10] N. Mirzaei, and R. Nowzari, "Applying A Combination of AHP, ANP, and PROMETHEE Methods to Find the Optimal Location for Solar Power Plant," *Avrupa Bilim Ve Teknoloji Dergisi*, vol. 32, pp. 1076-1085, 2022.

[11] S. M. W. Sadat, and N. R. Sabory, "Afghanistan Renewable Energy Sector's Human Resources Estimation until 2032," *Repa Proceeding Series*, vol. 1, no. 1. pp. 96-101, 2020.

[12] H. Ataee, and R. Fanaee, "Studying the Climate Change of Markazi Province by Mann-Kendall Method," *Nivar*, vol. 36, no. 77-76, pp. 37-48, 2012.

[13] A. M. Patel, and S. K. Singal, "Optimal Component Selection of Integrated Renewable Energy System for Power Generation in Stand-Alone Applications," *Energy*, vol. 175, pp. 481-504, 2019.

[14] M. Zoghi, A.H. Ehsani, M. Sadat, M. J. Amiri, and S. Karimi, "Optimization Solar Site Selection by Fuzzy Logic Model and Weighted Linear Combination Method in Arid And Semi-Arid Region: A Case Study Isfahan-IRAN," *Renewable and Sustainable Energy Reviews*, vol. 68, pp.986-996, 2017.

[15] S. Türk, A. Koç, and G. Şahin, "Multicriteria of PV Solar Site Selection Problem using GIS-Intuitionistic Fuzzy Based Approach in Erzurum Province/Turkey," *Scientific Reports*, vol. 11, no. 1, p. 5034, 2021.

[16] U. Munkhbat, and Y. Choi, "GIS-based Site Suitability Analysis for Solar Power Systems in Mongolia, " *Applied Sciences*, vol. 11, no. 9, p. 3748, 2021.

[17] O. Soydan, "Solar Power Plants Site Selection for Sustainable Ecological Development in Nigde, Turkey," *SN Applied Sciences*, vol. 3, no. 1, p. 41, 2021.

[18] N. Kundakcı, "An Integrated Multicriteria Decision Making Approach for Tablet Computer Selection," *European Journal of Multidisciplinary Studies*, vol. 2, no. 5, pp. 31-43, 2017.

[19] T. L. Saaty, "Decision Making with Dependence and Feedback: The Analytic Network Process," *RWS Publications*, vol. 4922, no. 2, 1996.

[20] T. L. Saaty, "Fundamentals of The Analytic Network Process — Dependence and Feedback in Decision-Making with a Single Network," *Journal of Systems Science and Systems Engineering*, vol. 13, no. 2, pp. 129-157, 2004.

[21] E. L. Subandi, Widiatmaka, and M. Ardiansyah, "Use of WLC (Weighted Linear Combination) to Determine Land Priorities for Development of Paddy Fields in Gorontalo Regency, Indonesia," *International Journal of Engineering and Management Research*, vol. 9, no. 3, pp. 58-63, 2019.
[22] S. Yin, J. Li, et al., "Optimization of the Weighted Linear Combination Method for Agricultural Land Suitability Evaluation Considering Current Land use and Regional Differences," *Sustainability*, vol. 12, no. 23, pp. 1-26, 2020.
[23] J. J. Silva-Gallegos, C. A. Aguirre-Salado, et al., "Locating Potential Zones for Cultivating Stevia Rebaudiana in Mexico: Weighted Linear Combination Approach," *Sugar Tech*, vol. 19, pp. 206-218, 2017.
[24] F. Mehdipour, M. S. Mesgari, B. Golchin, and M. R. Akbari, "Facility Sitting Using GIS and Genetic Algorithms," *25th International Cartographic Conference*, vol. 1, pp. 1816-1823, 2011.
[25] S. Rahimi, M. Shadman Roodposhti, and R. Ali Abbaspour, "Using combined AHP-genetic algorithm in artificial groundwater recharge site selection of Gareh Bygone Plain, Iran," *Environmental Earth Sciences*, vol. 72, pp. 1979-1992, 2014.
[26] M. Kumar, D. M. Husain, N. Upreti, and D. Gupta, "Genetic Algorithm: Review and Application," *International Journal of Information Technology and Knowledge Management*, vol. 2, no. 2, pp. 451-454, 2010.
[27] F. Buontempo, "Genetic Algorithms and Machine Learning for Programmers," *The Pragmatic Bookshelf*, vol. 52, no. 1, pp. 123-230. 2019.
[28] S. Van Dijk, D. Thierens, and M. De Berg, "Using Genetic Algorithms for Solving Hard Problems in GIS," *GeoInformatica*, vol. 6, pp. 381-413, 2002.
[29] N. Nagkoulis, E. Loukogeorgaki, and M. Ghislanzoni, "Genetic Algorithms-Based Optimum PV Site Selection Minimizing Visual Disturbance," *Sustainability*, vol. 14, no.19, p.12602, 2022.
[30] E. Noorollahi, D. Fadai, M. A. Shirazi, and S. H. Ghodsipour, "Land Suitability Analysis for Solar Farms Exploitation Using GIS and Fuzzy Analytic Hierarchy Process (FAHP) - A Case Study of Iran," *Energies*, vol. 9, no. 8, p. 643, 2016.
[31] J. Van Hoesen, and S. Letendre, "Evaluating Potential Renewable Energy Resources in Poultney, Vermont: A GIS-Based Approach to Supporting Rural Community Energy Planning," *Renewable Energy*, vol. 35, no. 9, pp. 2114-2122, 2010.
[32] K. R. Lee, W. H. Lee, "Solar Power Plant Location Analysis Using GIS and Analytic Hierarchy Process," *Journal of the Korean Association of Geographic Information Studies*, vol. 18, no. 4, pp. 1-13, 2015.

Declaration of Competing Interest

The authors declare that they have no known competing financial interests or personal relationships that could have appeared to influence the work reported in this paper. The ethical issues, including plagiarism, informed consent, misconduct, data fabrication and/or falsification, double publication and/or submission, redundancy, have been completely observed by the authors.

Credit Authorship Contribution Statement

Fatemeh Masteri Farahani: Conceptualization, Data curation, Methodology, Resources, Software, Roles/Writing - original draft. **Azadeh Kazemi:** Formal analysis, Funding acquisition, Investigation, Project administration, Supervision, Validation, Visualization, Writing-review & editing. **Amir Hedayati Aghmashadi:** Conceptualization, Data curation, Formal analysis, Methodology, Supervision, Roles/Writing-original draft,

Bibliography

Fatemeh Masteri Farahani was born in 1998, in Arak, Iran. She received her B.Sc. and M.Sc. degrees in Environmental Science and Engineering and Environment (Assessment and Land Use Planning), respectively, from Arak University, in 2020 and 2023. Her fields of interest include The Environment and Wild Life.

Azadeh Kazemi is an assistant Professor with a PhD in environmental management and planning. She is currently a researcher at Arak University, Arak, Iran. She has more than 10 years of experience working with clients from different parties including indigenous peoples, private sections and governments to continuously improve their environmental performance. Her most important tasks, besides teaching and in the form of projects and assignments, are familiarizing himself with new environmental topics, carrying out environmental assessments, monitoring, planning and management, risk assessment and researching based on the remote sensing, environmental modelling and GIS.

Amir Hedayati Aghmashadi is a sustainability manager with a PhD in environmental planning. He is currently a researcher at Martin Luther University Halle-Wittenberg, Halle (Saale), Germany. He has more than 5 years of experience working with clients from different parties including indigenous peoples, private sections and governments to continuously improve their environmental performance. His most important tasks, besides teaching and in the form of projects and assignments, are familiarizing himself with new environmental topics, carrying out environmental assessments, monitoring, planning and management, risk assessment and complying with regulations based on the standards and criteria.

Journal of Green Energy Research and Innovation

A Survey on Renewable and New Sources of Energies for Electricity Power Production and Its Challenges

Mohammad Hossein Shakoor

Highlight

- Comprehensive study on renewable and new sources of energies to produce electricity power
- Advantages and disadvantages of new sources of energies are discussed
- Challenges of using and producing of renewable sources are discussed

Graphical Abstract

Use your device to scan and read the article online

Citation

M. H. Shakoor, "A Survey on Renewable and New Sources of Energies for Electricity Power Production and Its Challenges," *Journal of Green Energy Research and Innovation*, vol. 1, no. 4, pp. 64-85, 2024.

https://doi.org/10.61186/jgeri.1.4.64

JGERI Journal of Green Energy Research and Innovation

Online ISSN: 3041-9018

Journal of Green Energy Research and Innovation

Journal Homepage: www.jgeri.araku.ac.ir

A Survey on Renewable and New Sources of Energies for Electricity Power Production and Its Challenges

Mohammad Hossein shakoor *

Department of Computer Engineering, Faculty of Engineering, Arak University, Arak 38156-8-8349, Iran.

* ***Corresponding Author:*** *mh-shakoor@araku.ac.ir*

ARTICLE INFO

Keywords:
Electricity power,
Renewable energies,
New Source of energies.

Article history:
Received: 27 February 2024;
Revised: 18 April 2024;
Accepted: 23 April 2024;

Article type:
Research Article

ABSTRACT

Common sources of electricity production, such as fossil fuels, create a large amount of pollution; furthermore, these sources will run out in the future. Therefore, the use of new sources and renewable energies are very vital for electricity production. This paper provides a comprehensive study to explore and analyze new and renewable electrical energy sources for the production of electricity. The study assesses the awareness, perceptions, and preferences of individuals regarding innovative technologies and sources that have the potential to reshape the landscape of electrical power generation. In this research, various types of novel and renewable sources for electricity production are explained and the challenges, advantages, and disadvantages of each of these methods are discussed.

1. Introduction

Using new and renewable sources of energy instead of traditional fossil fuels is increasing every year in the world. In this paper, different types of these renewable sources of energy are discussed. Furthermore, some challenges and the solution to each challenge are explained.

The investigation of renewable energy sources for generating electricity is on the rise as a viable and environmentally friendly substitute for conventional fossil fuels. Wind power, solar system, and geothermal heat are examples of such sources, offering the benefit of emitting minimal CO2 into the air [1]. The use of renewable energy can help address the energy crisis and reduce traditional sources like oil, gas, and coal [2]. It also has a great effect on air pollution and many problems of using traditional fuels. The impact of renewable energy on carbon emissions and sustainability is complex. Factors such as per capita GDP, urbanization, and the percentage of total renewable energy reliance can influence the carbon intensity of electricity production [3]. Policymakers need to consider the time frame required for new energy policies to have a full impact on carbon emissions from electricity generation [4].

The diversity of renewable energy sources and individual country-level approaches in the world highlights the ongoing energy transition and the importance of supportive measures.

Renewable energy sources are being increasingly explored for electricity production as a sustainable solution to address the challenges of climate change and energy security. The depletion of conventional energy sources and the need for clean energy have led researchers to focus on alternative energy sources such as wind, solar, hydropower, and biomass. These sources offer advantages such as low-cost, high-energy efficiency, and fewer polluting gases [5,6]. Some studies have shown that renewable energy can contribute to reducing carbon emissions and achieving sustainable development [7].

However, the implementation of renewable energy projects still faces challenges such as logistics, conversion technologies, financing, regulation, and social acceptance. These challenges decrease the speed of development of new sources of energy especially in poor and advancing countries. The challenges are different in each area. The first challenge is logistics. Developing renewable energy projects often requires extensive logistical planning, especially for large-scale installations such as wind farms or solar parks [8]. This includes transportation of equipment, materials, and personnel to remote or difficult-to-access locations. The second problem is conversion technologies. While renewable energy sources like sunlight and wind are abundant, the technologies used to convert these sources into usable electricity are still evolving. Improvements in efficiency, reliability, and cost-effectiveness of conversion technologies are needed to make renewable energy more competitive with fossil fuels. Another challenge of renewable energy sources is related to financing issues [9]. The upfront costs of renewable energy projects can be significant, and securing financing can be challenging, particularly for smaller-scale projects or in regions with limited access to capital. Financial incentives, subsidies, and innovative financing mechanisms are often necessary to attract investment in renewable energy. Another problem of expanding renewable energy sources is called regulation: Regulatory frameworks play a crucial role in shaping the development and deployment of renewable energy projects. In some cases, outdated regulations or bureaucratic hurdles can impede progress, while in others, supportive policies such as feed-in tariffs or renewable energy mandates can drive investment and innovation [10]. Finally, each new technology such as new source of energy must be accepted by society and each nation.

In this paper, different new sources of energy are discussed. The challenges and the solutions to each challenge of these renewable sources of energy will be explained technically in another part of the paper. Addressing these challenges requires a multi-faceted approach involving collaboration between governments, industry stakeholders, financial institutions, and research institutions. By overcoming these obstacles, we can accelerate the transition to a more sustainable and environmentally friendly energy system powered by renewable sources.

Renewable sources of energy are progressing in the world every year. The European Union (EU) has set targets to increase the share of electricity from low-carbon sources, leading to significant changes in electricity production in EU countries [11]. Countries like India, the United States, China, and Germany have made significant progress in utilizing renewable energy for electricity generation, primarily from agricultural and forestry waste. Overall, the exploration of renewable energy sources for electricity production is crucial for achieving a sustainable and environmentally friendly energy system. The next parts of this paper provide an overview of the current state of electrical energy

production, highlighting the challenges associated with traditional sources and the need for exploring new alternatives. There are various types of new electrical energy sources that researchers are exploring to meet the increasing demand for sustainable and cleaner energy.

This paper is organized as follows: in section two, some traditional power energy sources are explained. Section three is the main part of the paper that presents renewable sources of energy. In section four the challenges of new sources of energy and the solution of each are discussed. Renewable energy sources in Iran are explained briefly in section five. Finally, the conclusion is reported in the last section.

2. Traditional energy sources

Crude oil, natural gas, and coal are some of the most popular and traditional sources to produce electrical power. Coal is the cheapest option for electricity production, while natural gas is more expensive but more efficient. However, almost it does not specifically mention crude oil as a popular source of power generation [12]. The main challenge of these sources of energy is related to air pollution. The air pollution caused by energy generation, including the burning of fossil fuels like crude oil, natural gas, and coal is a big problem in large cities. The pollutants have become a leading environmental hazard and cause many different illnesses [13]. Therefore, using new sources of energy and renewable sources of energy plays a great role in modern countries and it is one of priority of each advanced area.

3. New sources of electrical energy

3.1. Solar power

Advancements in solar cell technologies, such as perovskite solar cells, tandem solar cells, and flexible solar panels, have shown promise in improving efficiency and lowering costs. Tandem solar cells, which combine different types of sub-cells, have achieved high power conversion efficiencies, with recent studies reporting efficiencies of up to 32.5% [14]. Perovskite-based tandem solar cells have also demonstrated high efficiency, with one study achieving an efficiency of 29.8% [15]. Additionally, perovskite-based solar cells offer higher conversion efficiency at lower costs compared to standard market options [16]. Flexible solar panels, such as those based on perovskite materials, provide a lightweight and sustainable solution for photo voltaic [17]. These advancements in solar cell technologies have the potential to significantly improve the efficiency and cost-effectiveness of solar energy generation.

3.2. Wind power

Wind power is a form of renewable energy that has the potential to contribute significantly to the global energy mix. The uncertainty associated with wind power generation poses challenges for its effective utilization. Various methods have been developed to address this issue, including the use of generative models to accurately describe the uncertainty of wind power output [18]. Additionally, advancements in wind

turbine technology, such as shrouded wind turbines, have been made to improve the efficiency of wind power generation [19]. Furthermore, innovative power generation mechanisms, such as those utilizing planetary gear sets, have been proposed to enhance the conversion rate of wind energy into electric energy [20]. Forecasting methods have also been developed to optimize the management of wind power systems, with a focus on short-term forecasting to evaluate production possibilities [21]. Overall, these advancements and forecasting methods contribute to the efficient control and utilization of wind energy resources. To better provide this new source of electricity power it is necessary to increase turbine efficiency, advancements in offshore wind technology, and research on vertical-axis wind turbines are notable developments. Onshore wind turbines refer to placing them on land to harness wind energy. Furthermore, installed in bodies of water, typically in the ocean, they capture strong and consistent winds.

3.3. Hydropower

This type of energy is based on the energy potential of water. Focus on innovative turbine designs, such as fish-friendly turbines, and advancements in small-scale hydropower systems. Hydropower is one of the oldest power generation technologies and remains responsible for most of the renewable electricity generation globally. It has advantages such as providing sustainable energy and increasing production flexibility. However, its development has been accompanied by environmental and social challenges. Sustainable hydropower projects are possible with good planning and careful system design. The impact of power generation on existing hydropower varies from region to region, but globally it is expected to be small or slightly positive. Hydropower can contribute to a reduction in system electricity price and price volatility, especially at higher percentiles. It also has the potential to increase energy storage and play a significant role in mitigating power generation and changing water availability. However, it is important to address the environmental and social costs associated with hydropower [22].

Hydropower can be divided into some groups. Traditional hydropower utilizes the energy of flowing or falling water to generate electricity. Another form of this energy is based on tidal and wave energy that captures energy from the motion of tides or waves in oceans and seas[23].

The majority of hydropower dams in North America and Europe were constructed before 1975. However, in recent years, the focus of new dam construction has shifted towards Asia and South America. This trend has been particularly prominent over the last two decades. According to the World Resources Institute (WRI) database, out of the 7,155 hydropower dams listed, approximately 6,200 were built before 2001. Among these, around two-thirds are situated in North America (2,063) and Europe (1,922) [24].

Some researchers published a paper that is related to the potential impact of hydropower on local communities. This study presents a comprehensive assessment of the global effects of dam construction, utilizing various global spatial databases. Specifically, it offers valuable insights into the repercussions on the economy, population, and environmental quality resulting from the establishment of around 600 newly constructed hydropower dams, categorized by region and size. The findings reveal a significant decline in the local economy, population, and greenery within a 50-kilometer

radius of the dam sites, particularly in regions belonging to the Global South. These outcomes contradict the notion that dams enhance the well-being of individuals and ecosystem services. Consequently, this research underscores the necessity for policy interventions aimed at mitigating the impacts on populations and urban areas adjacent to small and medium-sized dams [25].

Hydropower dams play a crucial role in both the economy and population, despite covering a small portion of the total land area. This outcome is not entirely unexpected, given that humans have historically settled in areas with convenient access to water sources. Fang and Jawitz [26] conducted a study on the distance of human populations to water sources in the United States between 1790 and 2010, highlighting the increasing importance of water in determining settlement patterns after industrialization. Additionally, Kummu et al. [27] demonstrated that over half of the global population resides within a 3-km radius of a freshwater body, while only 10% live beyond a 10-km distance. It is worth noting the regional disparities, with North America and Europe leading in both economic output and population density in near of across nearly all dams, and South America significantly surpassing other regions in terms of economy and population in a circular boundary within 50 km of a dam for recently constructed dams.

3.4. Geothermal power

Geothermal energy is a reliable and sustainable source of renewable energy that has the potential to contribute significantly to the generation of electricity. It offers advantages such as low-carbon emissions, constant availability, and a lower cost of electricity. Geothermal reservoirs can serve as the base load demand for local grid systems, reducing dependence on fossil fuels [27]. Using enhanced geothermal systems (EGS) and the utilization of low-temperature geothermal resources for direct-use applications is one of the preparations for this source of energy. Another way of employing this source is related to geothermal heat pumps. They use the earth's consistent temperature beneath the surface to heat and cool buildings. The last technology is geothermal power plants that extract heat from the earth's interior to generate electricity.

3.5. Nuclear power

Nuclear power is considered a potential source of electricity generation, but it comes with various considerations and challenges. It has been used to meet power needs in many countries, but there are legal implications, high initial capital investment, and environmental consequences associated with its use. Nuclear energy is often seen as a backup alternative to renewable energy sources to reduce CO2 emissions and maintain energy stability [28]. However, the main problem with nuclear energy lies in the management of nuclear waste [29]. Additionally, implementing a nuclear power plant (NPP) in countries with small economies and electricity grids can be challenging due to financial constraints and the need for grid modifications. Despite these challenges, research has been conducted on developing new types of nuclear batteries that can serve as low-power sources. Overall, nuclear power has its advantages and disadvantages, and its suitability as a new source of electricity power depends on various factors and considerations.

For the better advance of this type of energy, some preparations can be made. Exploration of advanced reactor designs, including small modular reactors (SMRs) and Generation IV reactors, aiming for improved safety and efficiency. Furthermore, using advanced nuclear reactors that Include designs with enhanced safety features, increased efficiency, and reduced nuclear waste. Sometimes this type of power is referred to as fusion power [29]. Advanced reactor designs encompass a range of innovative approaches to nuclear energy production, addressing safety, efficiency, and sustainability concerns [30,31].

These designs include Generation IV reactors, small modular reactors, accident-tolerant fuels, and new research reactor concepts. Advanced modeling and simulation techniques play a crucial role in optimizing these designs, enabling the incorporation of more physics, higher fidelity models, and diverse computing hardware. The development of new reactor types like fast-neutron reactors, high-temperature gas-cooled reactors, molten salt reactors, and small modular reactors is reshaping the nuclear industry [32]. Additionally, the consideration of safeguards and security early in the design process is a key principle guiding the deployment of new and advanced reactors. As the industry transitions towards automation, remote operation, and fewer operators, human factors in reactor design are becoming increasingly important for the successful deployment and operation of these advanced systems.

Small Modular Reactors (SMRs) are gaining global attention due to their innovative design features and potential benefits. SMRs offer advantages such as modularity, passive safety systems, and suitability for cogeneration, making them competitive with large reactors (LRs) despite higher specific capital costs. SMRs are seen as a solution for limited grid capacities in developing countries and can address energy needs efficiently due to shorter build times and design simplification [33].

However, challenges like understanding nuclear fuel behavior, waste management, and ensuring safety through probabilistic risk assessment and nuclear safeguards need to be addressed for the successful deployment of SMRs [34]. Additionally, considering SMRs as sociotechnical systems is crucial to understanding their potential societal impacts and role in reshaping energy production and markets. Overall, SMRs represent a promising technology with the potential to enhance resilience and security in power supply system's [35].

Generation IV reactors represent a new generation of nuclear reactor designs with enhanced safety, sustainability, and efficiency features [36]. These reactors aim to address various energy needs, from electricity generation to process heat and waste minimization. The six main types of Generation IV reactors include Gas-Cooled Fast Reactors (GFR), Lead-Cooled Fast Reactors (LFR), Molten Salt Reactors (MSR), Sodium-Cooled Fast Reactors (SFR), Supercritical-Water-Cooled Reactors (SCWR), and Very-High-Temperature Reactors (VHTR). Research and development efforts are focused on advancing these reactor systems to be sustainable, safe, reliable, economically competitive, and proliferation-resistant. Power-cycle alternatives for Generation IV reactors, such as VHTRs and GFRs, are being explored to maximize their efficiency and performance [37,38].

Nuclear power can be divided into fission and fusion. Nuclear fission is a reaction in which the nucleus of an atom splits into two or more smaller nuclei. The fission process often

produces gamma photons and releases a very large amount of energy even by the energetic standards of radioactive decay. Fusion power or nuclear fusion is a process such as the sun's process that combines hydrogen atoms to release energy, offering a potentially limitless and clean energy source.

Fusion could generate four times more energy per kilogram of fuel than fission (used in nuclear power plants) and nearly four million times more energy than burning oil or coal. Fusion offers a potential long-term energy source that uses abundant fuel supplies and does not produce greenhouse gases or long-lived radioactive waste [39]. Fusion energy offers the potential for an inexhaustible source of energy that does not deplete natural resources or produce greenhouse gases. The EU-DEMO project aims to be the first demonstrative power plant based on nuclear fusion, with a focus on the feasibility and realization of the power electrical systems [40].

3.6. Biomass

Biomass is a significant source of renewable energy for electricity production. Advances in bioenergy technologies include the development of more efficient biofuel production methods and the utilization of waste materials for energy production. Bioenergy means converting organic materials such as wood, crop residues, and waste into electricity or heat. Furthermore, biogas refers to captures methane from organic waste for electricity generation. It includes various organic materials such as agricultural residues, forest residues, and municipal wastes [41].

Biomass can be converted into useful forms of energy through processes like Torre faction, pyrolysis, and gasification. These processes can produce charcoal, petroleum oil, natural gas, and liquid and gaseous biofuels from biomass.

The energy potential of biomass residues is substantial, with the ability to generate renewable electrical energy for small-scale electricity generation. Biomass power plants offer economic and environmental benefits, providing an eco-friendly alternative to fossil fuels [42]. The use of biomass for electricity production can reduce dependency on non-renewable energy sources and contribute to a better environment

Producing biomass creates a lot of air pollution that can impact human health. China and Brazil are two important countries that generate electricity from biomass. However, they have distinct patterns of fuel sources. China relies heavily on biomass residues from agriculture and waste-to-energy facilities that burn refuse. Figure 1 indicates some countries with the highest biomass energy production in 2022.

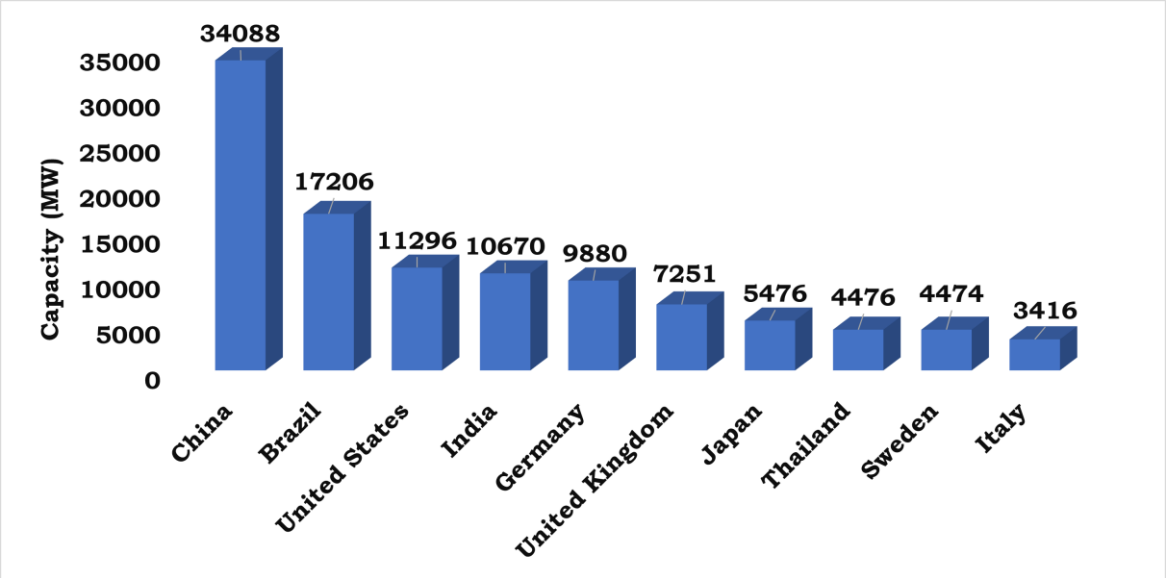

Figure 1. Countries with the highest bioenergy capacity in 2022.

3.7. Electrochemical cells

They are used to produce electricity by combining hydrogen and oxygen, with water as the byproduct. This process is a form of renewable energy for generating electricity. Water electrolysis is a technique that can be used to produce hydrogen without emitting any pollutants, and the hydrogen can then be used to generate electricity using a fuel cell [43]. Renewable sources of energy like solar and wind can be used to generate surplus electricity, which can then be used to produce hydrogen through water electrolysis. Hydrogen can be stored and used as fuel for generating electricity during times when renewable resources are not available or are less available [44]. This approach is part of the push to reduce carbon dioxide emissions and develop low-cost fuels from renewable sources to replace fossil fuels [45].

3.8. Flywheel energy storage

Flywheel energy storage systems use a spinning rotor to store and release energy. The rotor is a fast-rotating mass that stores energy in the form of mechanical energy [46]. These systems have various applications, including smoothing uneven torque in engines and machinery. More recently, flywheels have been developed to store electrical energy, enabled by directly mounted brushless electrical machines and power conversion electronics [47]. Flywheel energy storage systems have advantages such as high charge power, longer lifecycle, the ability to feed power back into the grid, and easy transportability [48]. They are also compared to other energy storage technologies, such as lithium-ion batteries, and are found to have great potential for rapid response, short duration, and high cycle applications. However, cost reduction is necessary for wider adoption, which can be achieved through the use of low-cost.

3.9. Battery storage

To save more energy in battery it is necessary to advance in battery technology for efficient energy storage and release. Also progress in battery technologies, including

lithium-ion batteries, solid-state batteries, and flow batteries. For saving a lot of energy they must use grid-scale energy storage solutions.

Battery energy storage systems (BESSs) are being used to store and release energy from renewable power sources such as wind and solar. These systems help to address the intermittent nature of renewables and ensure a steady and stable supply of electricity. BESSs can handle unexpected problems with renewable energy sources and play a crucial role in power generation by assisting other energy sources in meeting load requirements [49]. They can also reduce the negative effects of network congestion on the power system and decrease operational costs [50]. By integrating BESSs with renewable generation units, power fluctuations can be smoothed out, improving the stability, reliability, and power quality of power grids. Optimizing the planning and operation of BESSs is important to control their output power and improve profitability considering technical and lifetime constraints [51].

3.10. Smart grids

Smart grids enable the efficient integration of variable renewable energy sources into the power grid. It adjusts electricity usage in response to changes in supply and demand. Some papers such as [52] discuss the integration of renewable energy sources, such as wind and solar, into smart grids using wireless power transfer technology. Smart grid technology is crucial for the effective utilization of distributed energy resources and can help address the challenges of integrating renewable energy into the grid. Technologies such as dynamic compensation and dynamic line rating can improve grid management in areas with a high concentration of renewable energy sources [53].

Denizli in Turkey serves as a successful example of smart grid implementation, where an IoT-enabled smart grid application effectively utilizes electric vehicles as mobile storage to maintain energy consistency [54]. This particular case study demonstrated uptimes exceeding 100%, underscoring the significant potential of such innovative applications. Overcoming challenges related to integrating renewable energy sources, such as the variability and intermittency of solar and wind generation, requires comprehensive planning and evaluation studies to determine viable integration capacities [55]. Furthermore, the study underscores the significance of interdisciplinary research in smart grid technologies, emphasizing the necessity for heightened awareness and collaboration across diverse fields to expedite adoption and establish a sustainable and efficient energy landscape [56].

Another example of using the smart grid for renewable energy is Copenhagen, Denmark. It serves as an exemplary case study for successful smart grid implementation, aligning with sustainable energy goals. By integrating renewable sources like wind and solar power into its smart grid [57], Copenhagen has significantly reduced its carbon footprint and reliance on fossil fuels. The smart grid technology enables efficient electricity management and distribution, optimizing renewable energy utilization. Additionally, the city's smart grid system showcases benefits like improved energy efficiency, enhanced reliability, and effective integration of distributed energy resources [58]. This holistic approach not only ensures a cleaner and more sustainable energy supply but also

demonstrates the potential of smart grids in achieving environmental goals and enhancing overall energy sustainability.

The integration of renewable energy sources indeed comes with challenges that impact power grids. Challenges include the intermittency, variability, and uncertainty of solar and wind generation affecting operational economics [59]. As renewable energy sources replace conventional synchronous generators, grid strength decreases, posing stability challenges during integration. Converter-based sources, like wind and solar photovoltaic, are asynchronously connected to the grid, lacking ancillary services and affecting inertia and system strength, necessitating practical methodologies for evaluation [60]. To combat these challenges, planning, and evaluation studies are crucial to identify feasible integration capacities, analyze power system flexibility, and ensure stability through proper design considerations[61]. Countermeasures, such as battery energy storage systems, are utilized to cope with the variability and uncertainties of renewable energy sources albeit presenting technical challenges.

3.11. Piezoelectric and thermoelectric technologies

Piezoelectricity is a phenomenon where certain materials generate an electric charge in response to applied mechanical stress. This property is harnessed in various applications. Thermoelectric technology was mainly used to mitigate urban heat island effects and pavement rutting; piezoelectric technology can power low-power electronics such as wireless remote sensors for pavement disease and traffic condition monitoring; solar pavement has multiple functions based on its large power density. Future studies should focus on the durability, safety, and life cycle cost of energy generation technologies through a systemic approach [62].

3.12. Ocean thermal energy conversion (OTEC)

Ocean Thermal Energy Conversion (OTEC) refers to a process that uses temperature differences between warm surface water and cold deep water to generate power. Its plants pump large quantities of the deep cold sea or ocean water and warm surface them to run a power cycle and produce electricity. It is a new and clean energy source, environmentally sustainable, and capable of providing massive levels of energy. This new source of energy was first used in the 1880s and the first working power plant was built in Cuba. After that additional demonstration units were built periodically since 1930 [63]. In the case of OTEC, the need for a big temperature difference is balanced by the essentially infinite reservoirs of ocean water that can act as free fuel, so the low efficiency due to an average temperature difference of only 20°C is not as important. The Caribbean Islands are in the best location to be the test bed for scaling up OTEC. This technology can help support the system integration of high penetrations of variable renewable energy sources such as wind and solar [64].

This type of renewable energy has never become a mass-market technology to produce large amounts of electricity, because of the geographical limitations. However, there are countries in the Caribbean and elsewhere in the world that use this new source of energy to produce electricity power.

3.13. Kinetic energy harvesting

Kenotic energy harvesting refers to capturing energy from motion, such as vibrations or footsteps. It is the process of capturing and converting the energy generated by motion into usable electrical power. It involves the use of various mechanisms such as piezoelectric, electromagnetic, and electrostatic transduction to extract electrical power from vibrating or moving systems. Adaptive kinetic energy harvesting is a recent development that aims to increase the operating frequency range of kinetic energy harvesters by tuning the resonant frequency of the generator and widening its bandwidth [65]. Different devices and systems have been proposed for kinetic energy harvesting, including tubular-shaped magnet housings with wire coils and central magnets [66], rotating shells with fixing shafts and driving assemblies, and portable devices with magnets and movable wire coils [67]. These systems can generate alternating current, which can be converted into direct current using rectifiers and used to charge batteries or power portable electronic devices [68]. Additionally, advancements have been made in wearable kinetic energy harvesting, where energy is harvested from human motion to power autonomous wearable devices.

3.14. Other emerging technologies

The most traditional and new sources of electricity power have been mentioned before. However, some other types of new sources can be used for this purpose. RFID Energy Harvesting is one of them. It is a technology that extracts energy from radio frequency signals. This energy can be recycled and used to power low-energy devices in various applications. Despite all previous methods, this energy can be used in low scale consumption. Therefore, it cannot be mentioned as a new source of electricity sources. However, in this part of the paper, it is mentioned to complete the research of this paper [69].

Another type of new emerging technology is the Vertical Axis Wind Turbine (VAWT). It is an alternative design to the traditional horizontal axis of wind turbines. VAWTs have been proposed for use in generating electricity on highways, where the rapid movement of vehicles can drive the turbines and produce power for street lighting and toll plazas [70]. Although VAWTs have lower efficiency compared to Horizontal Axis Wind Turbines (HAWTs), they have the potential to play a significant role in future power production [71]. Small Scale Wind Turbine (SSWT) is another type of wind turbine. It is designed for decentralized energy generation. Small-scale wind turbines (SSWT) are designed to generate power in low wind speed regions. They face challenges such as low power coefficient and start-up difficulty. SSWTs can achieve a power coefficient of 43% at a wind speed of 3 m/s, but a wind speed of 5 m/s is needed to produce 600 W of power for household consumption [72]. Advanced solar technologies, such as emerging photo voltaic (EPVs) and ultrathin organic solar cells, offer flexible, lightweight, and conformable properties [73]. Life cycle assessments (LCAs) are necessary to evaluate the environmental sustainability of these technologies, considering the entire product life cycle. EPVs have the potential to penetrate various application areas, including portable devices, building-integrated power generation, and the transport industry [74].

Chalcopyrite and kieserite thin film solar cells have shown advancements in composition grading, surface passivation, and buffer enhancements. To increase the adoption of solar power, high-efficiency solar cells, and low-cost energy storage technologies are crucial. Multiple junction solar cells have demonstrated high efficiencies, with the theoretical potential to reach more than 70%. Overall, advanced solar technologies hold promise for achieving sustainable and efficient solar power generation [75].

Another type of new source of electric power is named as Concentrator Photo Voltaic (CPV). It uses lenses or mirrors to focus sunlight onto small, high-efficiency solar cells. Photovoltaic solar-energy conversion is one of the most promising technologies for generating renewable energy, and the conversion of concentrated sunlight can lead to reduced cost of solar electricity. Photovoltaic conversion of concentrated sunlight ensures an efficient and cost-effective sustainable power resource [76].

4. Challenges of renewable energy sources

The transition to new sources of renewable energy presents several challenges. Many renewable energy sources, such as solar and wind, are intermittent and variable in nature, meaning they depend on factors like weather conditions and time of day. Integrating large amounts of renewable energy into existing electricity grids can strain grid infrastructure and present technical challenges such as voltage and frequency regulation, grid stability, and grid congestion. Developing cost-effective and scalable energy storage technologies is crucial for enabling the reliable and efficient integration of renewable energy into the grid. Challenges include improving the energy density, cycle life, and cost-effectiveness of battery storage systems, as well as exploring alternative storage technologies such as pumped hydro, compressed air energy storage, and thermal energy storage [77].

Deploying large-scale renewable energy infrastructure, such as solar farms and wind turbines, requires significant land and resource utilization. Balancing the need for renewable energy deployment with land use considerations, environmental impacts, and competing land-use interests (e.g., agriculture, conservation) is a complex challenge. Inconsistent or inadequate policy and regulatory frameworks can hinder the deployment of renewable energy projects and investment in clean energy technologies. Establishing supportive policies, such as renewable energy targets, incentives for renewable energy deployment, and carbon pricing mechanisms, is essential for fostering a conducive environment for renewable energy development [78].

While the cost of renewable energy technologies has declined significantly in recent years, they may still face challenges competing with conventional fossil fuels in some regions, particularly where fossil fuel subsidies exist or where renewable energy resources are less abundant. Continued cost reduction through technological innovation, economies of scale, and supportive policies is necessary to enhance the cost competitiveness of renewable energy [79].

Infrastructure and Supply Chain are other challenges. Scaling up renewable energy deployment requires significant investments in infrastructure and supply chain development, including manufacturing facilities, transportation networks, and workforce

training. Building the necessary infrastructure and ensuring a resilient and diversified supply chain is critical for the sustainable growth of the renewable energy industry.

The most important problem is social acceptance and stakeholder engagement. Renewable energy projects can face opposition from local communities, environmental groups, and other stakeholders due to concerns related to visual impact, noise pollution, land use conflicts, and perceived health effects. Engaging with stakeholders, addressing community concerns, and ensuring transparency and participatory decision-making processes are important for fostering social acceptance and support for renewable energy projects [79]. Addressing these challenges requires a holistic and integrated approach involving policymakers, industry stakeholders, researchers, and communities. Collaboration, innovation, and sustained commitment to the transition to renewable energy are essential for achieving a sustainable and resilient energy future. Table 1 illustrates the challenges of each new method to produce electrical power. Table 1 indicates the challenges of each type of renewable energy source. However, the challenges can be reviewed independent of the type of energy source. In other words, all types of renewable energy sources have some main challenges that can be considered. Table 2 shows these main challenges and their solution [80-83].

Table 1. Challenges of using some renewable and new sources of energy.

Method	Challenges
Solar Power	Issues related to intermittent energy production and the need for effective energy storage solutions. Integration with the existing power grid also poses challenges. Energy reduction in winter and cloudy and rainy days
Wind Power	Concerns related to the impact on avian wildlife, intermittency, and the need for efficient energy storage solutions to handle variable wind conditions. Instability of energy production due to wind changes
Hydropower	Environmental concerns regarding river ecosystems, sedimentation, and the impact on fish migration patterns
Geothermal Power	Site-specific limitations and the need for improved drilling technologies to access deeper and hotter geothermal reservoirs
Nuclear Power	Public perception issues, concerns about nuclear accidents, and the management of nuclear waste remain significant challenges.
Biomass	Competition with food crops for land, concerns about deforestation, and the need for sustainable feedstock sources
Energy Storage	Cost, energy density, and environmental impacts of battery production and disposal
Piezoelectric	Finding suitable piezoelectric materials, sensitive to temperature, fatigue, and degradation over time, cost.
Thermoelectric generators	high temperatures, Thermal Stability and Reliability, durability and robustness of thermoelectric materials, integration into the traditional system
Smart Grids	Grid stability, cyber security concerns, and the need for updated infrastructure to accommodate decentralized energy sources.
Battery Storage	Cost, Batteries degrade over time, Safety concerns, Charging Time, Environmental Impact
Flywheel Energy Storage	lower energy density, mechanical stress, providing a vacuum or near-vacuum environment for Friction, Safety, Temperature, Cost
Ocean Thermal Energy Conversion	Technological Complexity, High Capital Costs, Environmental challenges, Transmission and Distribution, small scales
Kinetic Energy Harvesting	Low Power Density, Durability and Reliability, Environmental Impact, Variable and Unpredictable Sources

Table 2. Essential challenges and their solutions for using a renewable energy source.

Challenges	Comment	Solutions
Uncertainty [83]	Renewable energy sources such as solar and wind are intermittent, meaning their output fluctuates based on weather conditions. This poses challenges for maintaining a reliable energy supply.	**Energy Storage**: Developing cost-effective energy storage solutions such as batteries, pumped hydro storage, and thermal storage can store excess energy during periods of high production for use during low production periods. **Smart Grids**: Implementing advanced grid technologies to balance supply and demand in real-time, optimizing the use of renewable energy and traditional sources.
Grid Integration [84]	Integrating large amounts of renewable energy into existing grids can strain infrastructure and require significant upgrades.	**Grid Modernization**: Upgrading infrastructure to accommodate bidirectional power flows and decentralized generation from renewable sources. **Microgrids**: Establishing microgrids that can operate independently or connect to the main grid when necessary, enhancing resilience and flexibility.
Location Constraints [85]	The best renewable energy resources are often located in remote areas, far from population centers where energy demand is highest.	**Transmission Infrastructure**: Investing in transmission infrastructure to transport renewable energy from remote areas to urban centers efficiently. **Distributed Generation**: Promoting distributed generation closer to demand centers through rooftop solar, small wind turbines, and community-based renewable energy projects.
Cost and Financing [86]	While the cost of renewable energy has decreased significantly in recent years, upfront costs can still be a barrier to adoption.	**Incentives and Subsidies**: Providing financial incentives, tax credits, and subsidies to make renewable energy investments more attractive. **Power Purchase Agreements (PPAs):** Offering long-term contracts between renewable energy developers and consumers, guaranteeing a stable revenue stream for developers and predictable energy prices for consumers.
Resource Variability [83]	The availability of renewable energy resources varies geographically and seasonally.	**Hybrid Systems**: Combining multiple renewable energy sources (e.g., wind and solar) to mitigate variability and increase reliability. **Weather Forecasting**: Utilizing advanced weather forecasting technologies to anticipate renewable energy generation and optimize energy management.
Policy and Regulatory Challenges [84]	Inconsistent policies and regulations can create uncertainty for renewable energy developers and investors.	**Policy Stability**: Establishing long-term policies and regulatory frameworks that provide certainty and support for renewable energy development. **Carbon Pricing:** Implementing carbon pricing mechanisms to internalize the environmental costs of fossil fuel use and level the playing field for renewable energy.
Environmental Concerns [86]	While renewable energy sources are generally cleaner than fossil fuels, they can still have environmental impacts such as habitat disruption and land use.	**Siting and Planning:** Conducting thorough environmental assessments and engaging stakeholders in the siting and planning of renewable energy projects to minimize negative impacts. **Technological Innovation:** Investing in research and development of low-impact renewable energy technologies and practices.

Using these solutions requires collaboration among governments, businesses, communities, and academia to foster innovation, investment, and deployment of renewable energy technologies.

The challenges of producing and using new sources of energy are more complicated than those that are listed in Table 1. For example, for most of them, it is necessary to provide the necessary conditions and temperature levels. Most renewable energy technologies can supply heat at low and medium temperatures [84]. Among different renewable energies, solar energy has the highest potential to be incorporated into this sector. Nevertheless, using solar energy entails a larger area of land and adequate solar resources to produce the required heat [85].

The concentrated solar energy system can generate heat at a temperature of 550 Celsius at the industrial level. Studies on solar energy have reached temperatures at 1000 Celsius using advanced laboratory facilities [86]. Table 3 indicates the level of temperature for some groups of renewable energy sources [85].

Another challenge of the production of energy from renewable sources is related to complicated technology. Table 3 shows the technology type that is required for each kind of renewable energy source. Most renewable energy technologies currently deliver low- or medium-temperature process heat and are thus only applicable for some process requirements [85]. Concentrated solar power technology is showing promising results but requires larger land availability and sufficient solar resources. Currently, commercial applications of concentrated solar power can achieve process heat temperatures of up to 550 ◦ C.

5. Renewable energy sources in Iran

Renewable energy sources in Iran have been studied extensively in many researches [87,88]. They mentioned that Iran has a potential of 42000 MW for the use of renewable energies by 2020, but the capacity of renewable power stations constructed in Iran is only 800 MW [88].

Different regions of Iran have high wind, solar, and geothermal energy potential that has not been fully utilized to meet electricity needs. The country's energy matrix consists mostly of hydrocarbons, but there is a potential for a larger amount of renewable power, including bioenergy, to be incorporated [88].

The use of renewable energy in power generation in Iran has been prioritized using a multi-criterion decision-making approach, with solar PV identified as the most preferable technology for utility-scale power generation [89]. Overall, while Iran has the potential for significant renewable energy utilization, there is a need for further development and implementation of renewable power generation systems in the country. Table 4 shows the potential value of some types of renewable energy sources in Iran [90].

Table 3. Types of technologies and their temperature levels [85].

Category	Technology type	Temperature levels
Renewable source	Biomass, boiler	Low
	Biomass, high-temperature	Medium
	Biomass, combined-heat-and-power	High
	Biogas, anaerobic digestion	Low
	Solar PV	High
	Wind	High
	Heat pump	Low
	Geothermal direct use	Low
	Deep geothermal	Medium
Energy storage	Solar thermal	N/A
	Hydrogen	N/A
	Pump storage	N/A
	Battery storage	N/A

Table 4. Potential production values of some types of renewable energy sources in Iran [90].

Renewable Energy	Potential (MW)
Hydropower	26000
Solar energy	86198
Wind energy	18000
Biomass and biogas	19
Geothermal energy	187

6. Conclusion and future work

This paper provides a comprehensive study of new sources and renewable types of electricity power. Renewable energy sources, such as wind, solar, hydropower, etc. are crucial for meeting climate change targets, increasing energy security, and reducing reliance on fossil fuels. The development and utilization of these renewable sources have been growing rapidly, with 41.4% of energy generated from renewables in 2022 [91]. However, the intermittent and unpredictable nature of renewable energy poses challenges for the secure and stable operation of the electricity system. Attracting investors, integration into traditional power, and some other reasons such as time of acceptance and adaptation to society are other challenges of new technologies. To address this, new power systems based on renewable energy are being studied which can not only improve environmental sustainability but also save electricity costs and increase energy utilization. The investment in renewable power plants is encouraged due to their minimal running costs and potential economic benefits. The future of renewable energy lies in further advancements in wind power, hydropower, solar photovoltaic, etc. The environmental damages of some of these new energies are very small compared to fossil fuels and they are attractive in this sense.

References

[1] G. E. Halkos, and A. S. Tsirivis, "Electricity Production and Sustainable Development: The Role of Renewable Energy Sources and Specific Socioeconomic Factors," *Energies*, vol. 16, no. 2, pp. 721-721, 2023.

[2] K. A. Khan, S. M. M. Manir, et al., "Studies on Nonconventional Energy Sources for Electricity Generation," *International Journal of Advanced Research, Innovation and Ideas in Education*, vol. 4, no. 4, pp. 229-244, 2018.

[3] A. Matuszewska-Janica, D. Zebrowska-Suchodolska, U. A. Ala-Karvia, and M. Hozer-Kocmiel, "Changes in Electricity Production from Renewable Energy Sources in the European Union Countries in 2005-2019," *Energies*, vol. 14, no. 19, p. 6276, 2021.

[4] I. Pioro, R. B. Duffey, P. Kirillov, and R. Panchal, "Introduction: A Survey of the Status of Electricity Generation in the World," *Comprehensive Energy Systems*, vol. 1, no.1, pp. 1-34, 2018.

[5] P. Kumah, P. A. Sowah, A.-R. Adam, and A. J. Nyantakyi, "Emerging Energy Sources for Sustainable Power Generation: An Overview," *Engineering and Technology Journal*, vol. 8, no. 3, 2023.

[6] P. Singh, S. Shokeen, and S. Garg, "Generation of Power System Using Renewable Resources for Sustainable Development Leading Upcoming Technologies: An Analysis," *2022 OPJU International Technology Conference on Emerging Technologies for Sustainable Development (OTCON)*, Raigarh, Chhattisgarh, India, pp. 1-5, 2023.

[7] S. Bilgen, S. Keleş, A. Kaygusuz, A. Sarı, and K. Kaygusuz, "Global Warming and Renewable Energy Sources for Sustainable Development: A Case Study in Turkey," *Renewable and Sustainable Energy Reviews*, vol. 12, no. 2, pp. 372-396, 2008.

[8] G. Halkos, and A. S. Tsirivis, "Electricity Production and Sustainable Development: The Role of Renewable Energy Sources and Specific Socioeconomic Factors," *Energies*, vol. 16, no. 2, p. 721, 2023.

[9] V. da Silva Batista, J. V. S. Chagas, et al., "Sustainable Solutions for Clean Energy Production," *Seven Editora*, 2023.

[10] M. Pouresmaieli, M. Ataei, A. Nouri Qarahasanlou, and A. Barabadi, "Integration of Renewable Energy and Sustainable Development with Strategic Planning in the Mining Industry," *Results in Engineering*, vol. 20, 101412, 2023.

[11] S. S. Saran, and A. Ghosh, "Production of Electricity by Using Gravitational and Magnetic Energy," *presented at the 2018 IEEE International Conference on Current Development in Engineering and Technology (CCET)*, National Institute of Technology, Jamshedpur, India, 2018.

[12] A. Farnoosh, "Power Generation from Coal, Oil, Gas, and Biofuels," *The Palgrave Handbook of International Energy Economics*, 1st edition, pp. 111-130, 2022.

[13] R. M. Hannun, and A. H. Abdul Razzaq, "Air Pollution Resulted from Coal, Oil and Gas Firing in Thermal Power Plants and Treatment: A Review," *IOP Conference Series: Earth and Environmental Science*, vol. 1002, no. 1, p. 012008, 2022.

[14] S. Asmontas, and M. Mujahid, "Recent Progress in Perovskite Tandem Solar Cells," *Nanomaterials*, vol. 13, no. 12, p. 1886, 2023.

[15] H. Arbouz, "Towards Efficient Tandem Solar Cells Based on Lead-Free and Inorganic Perovskite Absorbers," *Thermal Science and Engineering*, vol. 6, no. 1, pp. 34-41, 2023.

[16] O. M. Saif, A. H. Zekry, M. Abouelatta, and A. Shaker, "A Comprehensive Review of Tandem Solar Cells Integrated on Silicon Substrate: III/V vs Perovskite," *Silicon*, vol. 15, pp. 6329-6347, 2023.

[17] N. E. I. Boukortt, C. Triolo, S. Santangelo, and S. Patanè, "All-Perovskite Tandem Solar Cells: From Certified 25% and Beyond," *Energies*, vol. 16, no. 8, p. 3519, 2023.

[18] L. Ma, C. Wu, et al., "Wind Power Scenario Generation Considering Wind Power Variations," *presented at the IEEE 5th International Electrical and Energy Conference (CIEEC)*, Beijing, China, 2022, pp. 2615-2620.

[19] M. H. Katooli, and Y. Noorollahi, "Shrouded Wind Turbines: A Critical Review on Research and Development," *International Journal of Ambient Energy*, vol. 43, no. 1, 2022.

[20] G. Mantriota, "Power Split Transmissions for Wind Energy Systems," *Mechanism and Machine Theory*, vol. 117, pp. 160-174, 2017.

[21] A. Augustyn, and J. Kamiński. "A Review of Methods Applied for Wind Power Generation Forecasting." Polityka Energetyczna, vol.21, no. 2, 139-150, 2018.
[22] M. Hafner, and G. Luciani, "The Palgrave Handbook of International Energy Economics", pp. 145-156, 2022.
[23] M. D. Shamout, K. A. Khamkar, A. Lal, P. Danaiah, A. Mukasheva, and N. Kaushik, "Hydropower Technology as a Renewable Energy Source of Power Generation and its Effect on Environment Sustainability," *International Interdisciplinary Humanitarian Conference for Sustainability (IIHC)*, pp. 1017-1020, 2022.
[24] E. F. Moran, M. C. Lopez, N. Moore, N. Müller, and D. W. Hyndman, "Sustainable Hydropower in the 21st Century," *Proceedings of the National Academy of Sciences of the United States of America*, vol. 115, pp. 11891-11898, 2018.
[25] M. S. Cho, and J. Qi, "Characterization of The Impacts of Hydro-Dams on Wetland Inundations in Southeast Asia," *Science of The Total Environment*, vol. 864, p. 160941, 2023.
[26] Y. Fang, and J. W. Jawitz, "The Evolution of Human Population Distance to Water in The Usa from 1790 To 2010," *Nature Communications*, vol. 10, p. 430, 2019.
[27] M. Kummu, H. de Moel, P. J. Ward, and O. Varis, "How Close Do We Live to Water? A Global Analysis of Population Distance to Freshwater Bodies," *PLOS ONE*, vol. 6, e20578, 2011.
[28] J. M. Pedraza, "The use of nuclear energy for electricity generation," pp. 327-414, 2022.
[29] J. Roano, C. Gomez et al., "Nuclear Energy as Backup to Renewable Energies," *Journal Renewable Energy*, vol. 6, no. 16, pp. 15-23, 2022.
[30] J. Shi, J. Liu, et al., "Editorial: Advanced modeling and simulation of nuclear reactors," *Frontiers in Energy Research*, vol. 11, 2023.
[31] B. B. Cipiti, S. Fitzwater, et al., "Advanced reactor safeguards: 2022 program roadmap," United States, 2022.
[32] R. Boring, "Human Factors for Advanced Reactors," in Human Factors in Software and Systems Engineering, *AHFE International Conference*, vol. 94, 2023.
[33] L. N. Ghimire, and E. A. Waller, "Small Modular Reactors: Opportunities and Challenges as Emerging Nuclear Technologies for Power Production," *Journal of Nuclear Engineering and Radiation Science*, pp. 1-47, 2023.
[34] I. N. Kessides, and V. V. Kuznetsov, "Small Modular Reactors for Enhancing Energy Security in Developing Countries," *Sustainability*, vol. 4, no. 8, pp. 1-27, 2012.
[35] A. Schindlauer, "The Contribution of Small Modular Reactors to the Resilience of Power Supply," *Journal of Nuclear Engineering*, vol. 3, no. 2, pp. 152-162, 2022.
[36] I. K. Damoah, "Stability and Bifurcation Analysis of Generation Iv Reactors Via Point Reactor Models with Temperature Reactivity Feedback," *Progress in Nuclear Energy*, vol. 160, 104674, 2023.
[37] J. R. Riznic, "Handbook of Generation IV nuclear reactors edition 2," *Journal of Nuclear Engineering and Radiation Science*, vol. 9, no. 3, 2023.
[38] I. L. Pioro, "Alternative power cycles for selected Generation-IV reactors," *Handbook of Generation IV Nuclear Reactors (Second Edition)*, pp. 759-775, 2023.
[39] R. Zadfathollah, A. Z. Paydar, S. K. Mousavi, and B. Zohuri, "Nuclear Fission or Fusion on Meeting Electricity Demand of Future Energy Source Economy and Policy," *Journal of Economics & Management Research*, vol. 4, no. 1, 2023.
[40] S. Minucci. S. Panella, S. Ciattaglia, M. C. Falvo, and A. Lampasi, "Electrical Loads and Power Systems for the DEMO Nuclear Fusion Project," *Energies*, vol. 13, no. 9, p. 2269, 2020.
[41] S. V. Stevanovic, and S. Stevanovic, "Biomass as A Renewable Energy Source," *Ekonomika Poljoprivrede*, vol. 69, no. 1, pp. 195-209, 2022.
[42] S. Mukherjee, C. Mazumder, et al., "Biomass Energy Resource – Future of Global Power Production, " *Journal of Scientific Research of the Banaras Hindu University*, vol. 66, no. 5, pp. 16-23, 2022.
[43] A. P. R. A. Ferreira, R. C. P. Oliveira, M. M. Mateus, and D. M. F. Santos, "A Review of the Use of Electrolytic Cells for Energy and Environmental Applications," *Energies*, vol. 16, no. 4, p. 1593, 2023.

[44] A. Atri, and A. Khosla, "A Review of Water Electrolysis, Fuel Cells and Its Use in Energy Storage," Renewable Energy Optimization, Planning and Control: *Proceedings of ICRTE*, pp. 275-288, 2023.
[45] L. A. Jolaoso, J. Asadi, C. Duan, and P. Kazempoor, "A Novel Hydrogen Economy Based on Electrochemical Cells Fully Integrated with Fossil Fuel Assets and Wastewater Resources," *Energy Sustainability*, vol. 85772, p. V001T10A001, 2022.
[46] P. N. Tiwari, A. K. Kurchania, et al., "Renewable Energy Sources Integration with Flywheel Energy Storage System based on Wind and Solar Energy," *IEEE International Conference on Current Development in Engineering and Technology (CCET)*, pp. 1-7, 2022.
[47] M. Skinner, and P. Mertiny, "Energy Storage Flywheel Rotors—Mechanical Design," *Encyclopedia*, vol. 2, no. 1, pp. 301-324, 2022.
[48] M. Ali, M. R. Sarker, M. H. M. Saad, and R. Mohamed, "Overview of Control System Topology of Flywheel Energy Storage System in Renewable Energy Application for Alternative Power Plant, *Przegląd Elektrotechniczny*, vol. 1, pp.147-155, 2022.
[49] Energy Storage, pp. 1-16, 2023
[50] K. M. Todakar, P. P. Gupta, and V. Kalkhambkar, "Battery Energy Storage Train Scheduling in Power System Considering Renewable Power Generation," *International Conference for Advancement in Technology (ICONAT)*, pp. 1-7, 2023.
[51] M. Javadi, X. Liang, Y. Gong, and C. Y. Chung, "Battery Energy Storage Technology in Renewable Energy Integration: a Review," *IEEE Canadian Conference on Electrical and Computer Engineering (CCECE)*, pp. 435-440, 2022.
[52] H. Allamehzadeh, and S. Shakya, "Renewable Energy Power Assimilation to the Smart Grid and Electric Vehicles via Wireless Power Transfer Technology," *IEEE Green Technologies Conference (GreenTech)*, pp. 275-279, 2023.
[53] T. A. Owunna, and E. I. Obeagu, "Overview of Smart Grid Technology as a Renewable Energy Source," *Journal of Energy Research and Reviews*, vol. 12, no. 3, pp. 6-15, 2022.
[54] N. Ugur, I. Bali, and S. Baydere, "A Simulated Case Study of Smart Grid's Impact on Enabling Renewable Energy," *Smart Networks Conference (SmartNets)*, pp. 1-6, 2022.
[55] S. Arunagirinathan, M. Chitra, and M. Subramanian, "Development of Large-Scale Green Energy Sources with Grid Integration: Practices and Challenges," *Journal of Electronics and Informatics*, vol. 5, no. 1, pp. 75-85, 2023.
[56] A. Samet, N. Hafize, Ş. Durmuş, and R. Bayindir, "Social Adoption of Smart Grids: The Research Agenda," *IEEE International Conference on Smart Grid*, pp. 1-5, 2023
[57] N. Malsa, T. Srivastave, et al., "SMART CITIES: P2P Energy Trading Using Blockchain," *Smart and Sustainable Intelligent Systems*, pp. 682-694, 2023.
[58] F. Mirshafiee, E. Shahbazi, M. Safi, and R. Rituraj, "Predicting Power and Hydrogen Generation of a Renewable Energy Converter Utilizing Data-Driven Methods: A Sustainable Smart Grid Case Study," *Energies*, vol. 16, no. 1, p. 502, 2023.
[59] S. Arunagirinathan, and M. Subramanian, "Development of Large-Scale Green Energy Sources with Grid Integration: Practices and Challenges," *Journal of Electronics and Informatics*, vol. 5, no. 1, pp. 75-85, 2023.
[60] S. El Wejhani, M. Elleuch, S. Tnani, K. Ben Kilani, and G. Ennine, "Renewable Energy Integration in Power System: Clarification on Stability Indices," *International Conference on Science and Technology of Emerging Materials (CISTEM)*, pp. 1-6, 2022.
[61] M. Saleem, S. Saha, U. Izhar, and L. M. Ang, "Integration Challenges of Inverter Based Renewable Energy Sources in Weak Grids," *IEEE Industry Applications Society Annual Meeting*, pp. 1-18, 2022
[62] J. Wang, F. Xiao, and H. Zhao, "Thermoelectric, Piezoelectric and Photovoltaic Harvesting Technologies for Pavement Engineering," *Renewable and Sustainable Energy Reviews*, vol. 151, 111522, 2021.
[63] A. Ghilardi, A. Baccioli, G. F. Frate, M. Volpe, and L. Ferrari, "Integration of Ocean Thermal Energy Conversion and Pumped Thermal Energy Storage: System Design, Off-Design and LCOS Evaluation," *Applied Thermal Engineering*, vol. 236, 121551, 2024.

[64] D. Colorado-Garrido, E. Mendoza-Bernal, L. M. Toledo-Paz, and B. A. Escobedo-Trujillo, "An Ocean Thermal Energy Conversion Power Plant: Advanced Energy Analysis and Experimental Validation," *Renewable Energy*, vol. 223, 120018, 2024.
[65] Y.-H. Shin, J. Choi, et al., "Automatic Resonance Tuning Mechanism for Ultra-Wide Bandwidth Mechanical Energy Harvesting," *Nano Energy*, vol. 77, pp. 104986, 2020.
[66] D. Zhu, and S. Beeby, "Kinetic Energy Harvesting," *Energy Harvesting Systems*, pp. 1-77, 2011.
[67] J. Song, L. Qi, Y. Wang, "A Dual-Function System Integrating Kinetic Energy Harvesting and Passenger Sensing for Urban Subway," *International Journal of Hydrogen Energy*, vol. 48, No. 100, pp. 40053-40070, 2023.
[68] M. Magno, L. Spadaro, J. Singh, and L. Benini, "Kinetic Energy Harvesting: Toward Autonomous Wearable Sensing for Internet of Things," *International Symposium on Power Electronics, Electrical Drives, Automation and Motion (SPEEDAM)*, pp. 248-254, 2016.
[69] R. Md. Ferdous, A. W. Reza, and M. F. Siddiqui, "Renewable Energy Harvesting for Wireless Sensors using Passive RFID Tag Technology: A Review," *Renewable and Sustainable Energy Reviews*, vol. 58, pp. 1114-1128, 2016.
[70] G. Lalagi, and D. Shrikantha, "Performance Study of a VAWT Based on Aspect Ratio and Aerodynamics of Rotor Blade," *Conference on Fluid Mechanics and Fluid Power*, vol. 1, pp. 397-402, 2021.
[71] T. A. Srinivas, M. J. S. Mohamed, S. A, P. Sukania, A. Pathani, and K. Sekar, "Smart Highway Technique using Wind Turbine with Vertical Axis (VAWT)," *International Conference on Power, Energy, Control and Transmission Systems (ICPECTS)*, pp. 1-5, 2022.
[72] M. A. Ibrahim, A. S. Alhfidh, and A. N. Hamoodi, "Performance Enhancement of Small-Scale Wind Turbine Based on Artificial Neural Network," *International Journal of Power Electronics and Drive Systems (IJPEDS)*, vol. 14, no. 3, pp. 1722-1730, 2023.
[73] M. Scharber, V. Rodin, et al., "Advanced Materials for Innovative Solar Cell Technologies - Part 1 (NanoTrust-Dossier No. 056en)," 2021.
[74] G. Siddharth, B. S. Sengar, and SH. Mukherjee, "Progress in Thin Film Solar Cell and Advanced Technologies for Performance Improvement," *Encyclopedia of Smart Materials,* vol. 2, pp. 661-680, 2022.
[75] R. Y. Lin, "Advanced Solar Power Technology-Multiple Junction Photovoltaics," *Innovations in Sustainable Energy and Cleaner Environment*, pp. 505-527, 2020.
[76] L. Zhang, Y. Hu, et al., "Performance Investigation on a Concentrating Photovoltaic Thermal System Integrated with Spectral Splitter and Absorption Heat Pump," *Applied Thermal Engineering*, vol. 237, 121772, 2024.
[77] R. K. Srivastava, "Technical Challenges and Prospects of Renewable Fuel Generation and Utilization at a Global Scale," *Biorefinery Production of Fuels and Platform Chemicals*, pp. 31-57, 2023.
[78] H. Shah, J. Chakravorty, and N. G. Chothani, "Protection Challenges and Mitigation Techniques of Power Grid Integrated to Renewable Energy Sources: A Review," *Energy Sources Part A-recovery Utilization and Environmental Effects*, vol. 45, np. 2, pp. 4195-4210, 2023.
[79] N. H. Riedel, and M. Spacek, "Challenges of Renewable Energy Sourcing in the Process Industries: The Example of the German Chemical Industry," *Sustainability*, vol. 14, no. 20, p. 13520, 2022.
[80] M. Davoudi, and H. Zarei, "An Overview on Optimal Control of Renewable Resources, Methods and Challenges," *Journal of Renewable Energy*, vol. 10, no. 1, pp. 153-165, 2023.
[81] E. Mahidin, H. Husin, N. Nasaruddin, and M. Zaki, "A Critical Review of the Integration of Renewable Energy Sources with Various Technologies," *Protection and Control of Modern Power Systems*, vol. 6, no. 1, pp. 1-18, 2021.
[82] A. Barik, G. Srinivasulu, and P. Balakrishna, "An Effective Method of Optimal DG Location, Type and Size to Deal with Power System Constraints," *International Conference on Smart Energy Systems and Technologies (ICSETS)*, 2019.
[83] P. E. Donohoo, M. Webster, and I. J. Pérez-Arriaga, "Algorithmic Investment Screening for Wide-Area Transmission Network Expansion Planning," *IEEE Power and Energy Society General Meeting (PESGM)*, pp. 1-5, 2013.

[84] S. J. Ericson, J. Engel-Cox, and D. J. Arent, "Approaches for Integrating Renewable Energy Technologies in Oil and Gas Operations," *National Renewable Energy Lab. (NREL)*, Golden, CO, USA, 2019.

[85] T. Igogo, K. Awuah-Offei, A. Newman, T. Lowder, and J. Engel-Cox, "Integrating Renewable Energy into Mining Operations: Opportunities, Challenges, and Enabling Approaches," *Applied Energy*, vol. 300, 117375, 2021.

[86] R. Jacob, M. Belusko, M. Liu, W. Saman, and F. Bruno, "Using Renewables Coupled with Thermal Energy Storage to Reduce Natural Gas Consumption in Higher Temperature Commercial/Industrial Applications, Renew," *Energy*, vol. 131, pp. 1035-1046, 2019.

[87] M. Khazaee, R. Zahedi, R. Faryadras, and A. Ahmadi, "Potential Assessment of Renewable Energy Resources and Their Power Plant Capacities in Iran," *Global Journal of Ecology*, vol. 7, no. 2, pp. 060-071, 2022.

[88] A. Ahmadi, "Potential Assessment of Renewable Energy Resources and their Power Plant Capacities in Iran," *New Energy Exploitation and Application*, vol. 1, no. 2, 2022.

[89] M. Mahdavi, K. Schmitt, R. A. V. Ramos, and H. H. Alhelou, "Role of Hydrocarbons and Renewable Energies in Iran's Energy Matrix Focusing on Bioenergy: Review," *IET Renewable Power Generation*, vol. 16, no. 15, pp. 3384-3405, 2022.

[90] S. Solaymani, "A Review on Energy and Renewable Energy Policies in Iran," *Sustainability*, vol. 13, no. 13, p. 7328, 2021.

[91] S. S. Das, J. Kumar, S. Dawn, and F. Salata, "Existing Stature and Possible Outlook of Renewable Power in Comprehensive Electricity Market," *Processes*, vol. 11, no. 6, p. 1849, 2023.

Declaration of Competing Interest

The author declare that they have no known competing financial interests or personal relationships that could have appeared to influence the work reported in this paper. The ethical issues, including plagiarism, informed consent, misconduct, data fabrication and/or falsification, double publication and/or submission, redundancy, have been completely observed by the authors.

Credit Authorship Contribution Statement

Mohammad Hossein Shakoor: Conceptualization, Formal analysis, Project administration, Supervision, Validation, Investigation, Methodology, Resources, Roles/Writing - original draft.

Bibliography

Mohammad Hossein Shakoor received the B.Sc. degree in Computer Engineering from Shiraz University, Shiraz, Iran, in 1998 and M.S. degree in computer architecture from Isfahan university, Isfahan, Iran, in 2003. He received Ph.D. in Artificial Intelligent of Computer engineering from Shiraz University, Shiraz, Iran in 2016. His research interests include Texture Classification, Pattern Recognition and Computer Vision.

Journal of Green Energy Research and Innovation

A New Method for DFIG Control under Unbalanced Grid Voltage Conditions

Mohammad Naser Hashemnia, Ali Dehghan Nayeri

Highlight

- Conducting a thorough examination of DFIG performance in the presence of unbalanced grid voltage conditions
- Presenting two strategies aimed at mitigating active and reactive power oscillations
- Introducing a high selectivity filter (HSF) to separate the fundamental component of stator phase currents from the harmonic components
- Demonstrating the effectiveness of the proposed method compared to traditional DPC controllers through extensive simulations

Graphical Abstract

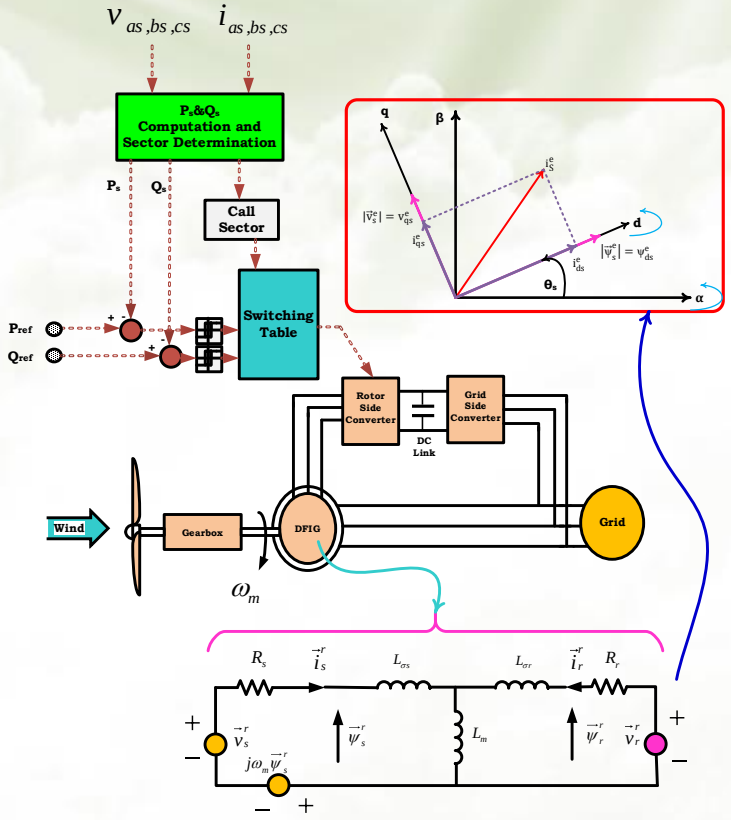

Use your device to scan and read the article online

Citation

M. N. Hashemnia, and A. Dehghan Nayeri, "A New Method for DFIG Control under Unbalanced Grid Voltage Conditions," *Journal of Green Energy Research and Innovation*, vol. 1, no. 4, pp. 86-116, 2024.

https://doi.org/10.61186/jgeri.1.4.86

Online ISSN: 3041-9018

Journal of Green Energy Research and Innovation

Journal Homepage: www.jgeri.araku.ac.ir

A New Method for DFIG Control under Unbalanced Grid Voltage Conditions

Mohammad Naser Hashemnia*, Ali Dehghan Nayeri

Department of Electrical Engineering, Mashhad Branch, Islamic Azad University, Mashhad, Iran.

* ***Corresponding Author:*** *hashemnia@mshdiau.ac.ir*

ARTICLE INFO

Keywords:
Direct power control,
Doubly-fed induction generator,
High selectivity filter,
PI regulator;
Stator flux.

Article history:
Received: 01 February 2024;
Revised: 28 April 2024;
Accepted: 04 May 2024;

Article type:
Research Article

ABSTRACT

This research presents a comprehensive analysis of the performance of direct power control (DPC) for doubly-fed induction generator (DFIG) under both balanced and unbalanced network voltages. Voltage unbalance in three-phase systems results in the presence of positive and negative sequences in both voltages and currents. This unbalance leads to many issues, including active power ripple, reactive power ripple, and an increase in the Total Harmonic Distortion (THD) of the stator current. Therefore, it is crucial to have efficient control of the system to reduce power fluctuations. This research presents two solutions that aim to mitigate the fluctuations in both active and reactive power. The first strategy employs PI regulators within the controller system. A high selectivity filter (HSF) is employed to separate the fundamental component of stator phase currents from the harmonic components. The second option utilizes DPC (Direct Power Control) based on stator flux. The suggested method computes the active and reactive powers that correspond to positive sequence variables. Since grid unbalance has a smaller impact on stator flux compared to stator voltage, it can be demonstrated that the second suggested controller exhibits superior performance to the conventional DPC controller in unbalanced situations. To evaluate the effectiveness of the suggested techniques, a simulation is conducted on a 2MW Doubly-Fed Induction Generator (DFIG) system using the MATLAB/Simulink environment. The results demonstrate that both of the suggested DPC control approaches outperform the conventional DPC controller in terms of control system performance, even under unbalanced situations. Furthermore, these improvements are achieved without significantly increasing the complexity of the control system.

1. Introduction

In recent years, the capacity of installed wind power plants has increased rapidly. Wind energy conversion systems can be classified into two main categories: fixed-speed turbines and variable-speed turbines. Variable-speed turbines operate at or near the point of maximum aerodynamic efficiency. Among the main features of variable speed wind turbines are increased annual energy production due to adaptation of turbine speed to wind speed leading to maximum turbine output power, reduced mechanical stress on

turbine, smooth power injection to network under fault conditions, reduced noise, and higher power quality [1]. Despite the significant benefits of a variable-speed wind turbine, its performance incurs additional expenses. Furthermore, a power electronic converter increases the complexity between the network and the generator. Nevertheless, its utilization is increasing due to its advantageous features. For variable-speed wind turbines, a power electronic converter is used between the wind generator and the grid. Doubly-Fed Induction Generators (DFIGs), permanent magnet synchronous generators, and wound rotor synchronous generators are the most commonly used types of machines in variable speed wind systems. DFIG has numerous advantages over other generators [2] due to its variable speed operation capability and low-cost partial scale converter, among others. Figure 1 shows a DFIG connected to the network. The rotor side converter controls the active and reactive powers of the stator while the grid side converter controls the DC link voltage and the reactive power exchanged.

Despite DFIG's numerous advantages, its primary drawback is that grid disturbances affect the machine due to the stator's direct connection to the grid. If no measures are taken, unbalanced network voltages may result in oscillations in active power, reactive power, and electromagnetic torque [2]. DFIG control methods can be classified into two categories: field-oriented control (FOC) and direct power control (DPC). A wide range of combinations, each with its specific advantages and disadvantages can be utilized [3-9]. Applying direct torque control (DTC) to DFIG in 2002 [9] was a solution to address control drawbacks and simplify PI controller tuning in the vector control method. The DTC control structure consists of an estimation block, hysteresis controllers, and a DTC switching table. The main control variables are the values of electromagnetic torque T_e^* and rotor flux ψ_r^* [9]. Just like the DTC, the DPC was developed over a decade ago primarily for controlling three-phase rectifiers [10]. In the DPC method, the main controlled variables are the stator active power P_s and stator reactive power Q_s [10]. Furthermore, DPC does not require estimation of the control variables as the stator's active and reactive powers may be computed using the stator's voltages and currents. Figure 2 shows the diagram of direct power control.

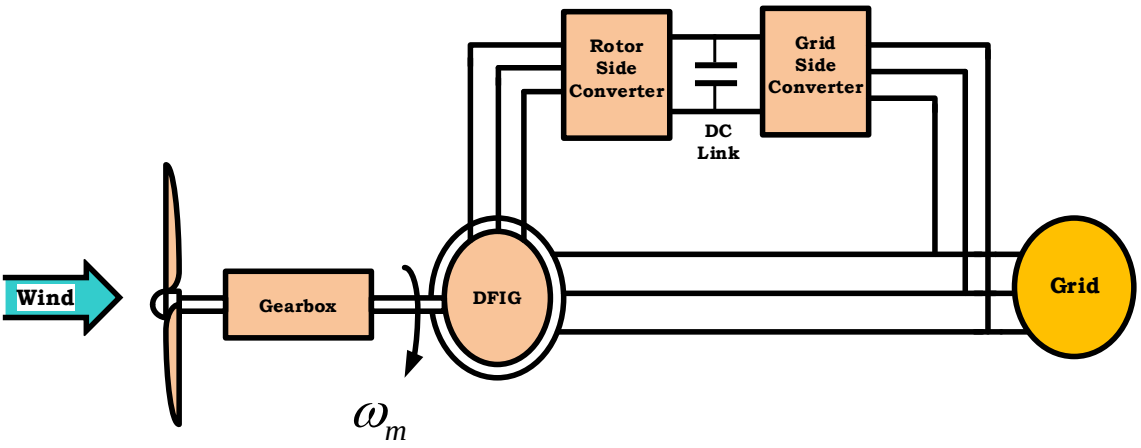

Figure 1. Schematic of a DFIG-based wind turbine connected to the grid.

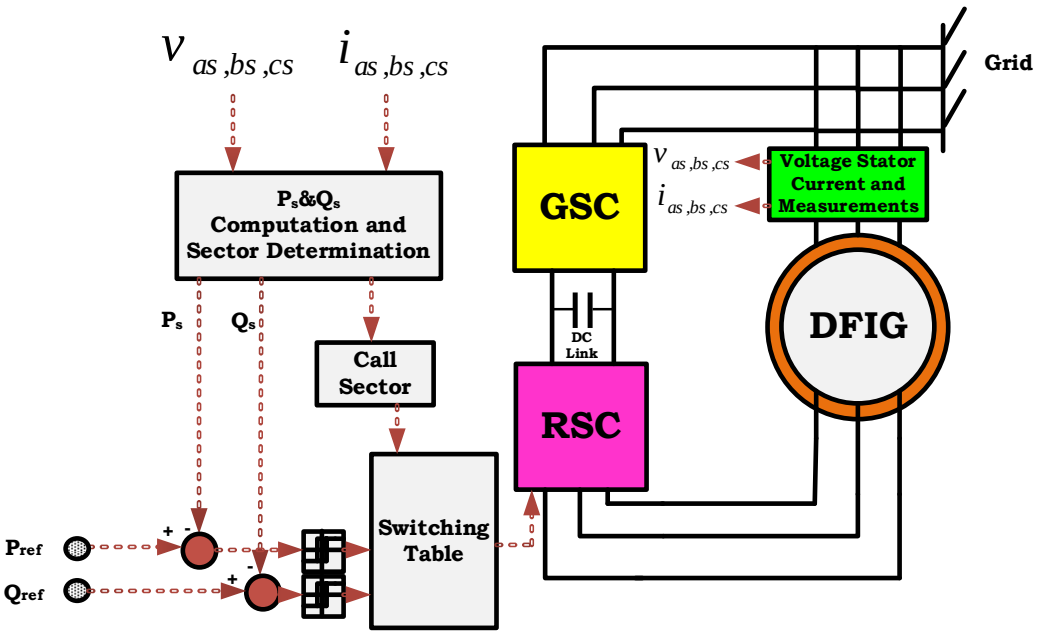

Figure 2. DPC controller structure.

Several researchers have been studying DPC and DTC for DFIG to minimize output ripple and maintain a constant switching frequency on the rotor side converter. These methods include space vector modulation (SVM) [11], discrete space vector modulation technique (DSVM), and predictive direct power control (PDPC) method [12]. All of these approaches have the potential to enhance the performance of DPC but at the cost of increased complexity. Although DPC has a fast response, its main limitation lies in the variable switching frequency. This issue can be resolved by replacing hysteresis controllers with PI controllers or implementing space vector modulation.

A model utilizing predictive control, a subset of space vector modulation, is employed in [12]. This model employs Predictive Direct Power Control (PDPC) to determine active and reactive power errors at the start of the sampling period. Following this phase and upon completion of the sampling time, the active and reactive power errors should be eliminated. Space vector modulation is utilized to generate the necessary switching pulses. The primary drawbacks of PDPC are the online computing issues of microprocessors and the complexity of control.

In [13], the required rotor voltage vectors over a constant period are applied using space vector modulation. Although this method leads to constant switching frequency, the calculation of duty ratios of each voltage vector increases the mathematical computation. Space vector modulation can be performed based on voltage and virtual flux. The DPC controller is characterized by the absence of current loops and the ability to directly control active and reactive powers. The power estimation block is comparable to that of conventional DPC. Direct power control with space vector modulation combines the benefits of direct power control, such as fast dynamic response, with the advantages of vector control, such as a reduced switching frequency. However, the control algorithm's complexity and slower dynamic response compared to direct power control are the main disadvantages of this method. The discrete SVM technique [14] utilizes three rotor voltage

vectors throughout the switching period. These vectors are chosen by the implementation of a modified lookup table and a 5-level hysteresis comparator.

A study is conducted in [15-17] on model predictive DPC (PDPC) control under unbalanced grid voltage conditions. In [15] a low-complexity model predictive control (LC-DPC) based on three voltage vectors is proposed. The results showed that LC-MPDPC can mitigate the current harmonics and reduce power and torque ripples. Reference [16] employs the principle outlined in reference [15]. This paper demonstrates the enhancement of the steady state and dynamic response of the machine by incorporating a second-order generalized integrator (SOGI). Reference [17] utilizes four voltage vectors instead of three, with one voltage vector being applied within a fixed sampling period. In this method, there is no requirement to estimate the rotor flux, and the selection of voltage vector sequences is determined by a straightforward algorithm. While the suggested control strategy exhibits a smoother response under both balanced and unbalanced voltage conditions, it is more complicated compared to previous (PDPC) techniques. A more advanced method for controlling the DFIG in the synchronous reference frame is proposed in [18]. This method is designed to work effectively under both balanced and unbalanced voltage conditions. The direct-resonant method employs a dual-frequency frequency to effectively eliminate negative sequence and harmonic components, resulting in the generation of sinusoidal currents.

The performance is enhanced in [19] through the integration of a disturbance observer and a proportional controller. PI controllers are employed to eliminate the second harmonic oscillatory component of power. Despite the improved power control demonstrated by the simulation results under unbalanced conditions, controller gains must still be adjusted due to the use of PI controllers. On the other hand, the control structure is highly complicated, which necessitates complicated computations and can be quite costly. A proposal was suggested in [20] to integrate vector control and direct torque control to optimize the performance of current, flux, and electromagnetic torque. This approach is preferred over using direct torque control or vector control alone. It ultimately improves the machine's performance in situations where the network is balanced. Compared to the DTC method, the power oscillations are reduced and a smoother response is observed. Compared to the vector control method, it demonstrates a faster dynamic response and reduced dependence on system parameters.

Despite demonstrating enhanced dynamic response and reduced torque and power fluctuations, it still encounters power fluctuations when exposed to unbalanced voltage conditions. In addition, the system utilizes hysteresis controllers leading to a variable switching frequency. Direct power control based on voltage and virtual flux is proposed in [21] for unbalanced voltage and distorted network conditions. By utilizing virtual flux rather than voltage to calculate power, the proposed method eliminates the effect of unbalanced voltage on instantaneous power and, consequently, oscillating active power. However, there are still fluctuations in reactive power.

Two four-switch three-phase converters (FSTPCs) have been implemented in place of two six-switch three-phase converters (SSTPCs) on the rotor and grid side converters

[22]. This method will generate four unbalanced voltage vectors. Three distinct targets are applied to compensate for active and reactive power, electromagnetic torque, and stator current to achieve balance among these four voltage vectors during unbalanced grid voltage conditions. While these objectives result in a reduction of active and reactive power fluctuations, the mitigation of electromagnetic torque variations, and the achievement of balanced stator currents, power oscillations remain. While using FSTPCs lowers costs and switching losses, there are drawbacks to this approach as well. For instance, the voltage gain is decreased for the same rated power, which results in an additional issue. A proposal is made in [23] to combine vector control and direct power control. The combination control method offers the advantages of both vector control and direct power control. The benefits of combining vector and direct power control over the conventional DPC method include a decrease in current THD, enhancement of both active and reactive powers, and fast dynamic response. However, this method exhibits higher THD and power oscillations compared to vector control. Additionally, its performance during voltage dips is deemed unsatisfactory. An investigation was conducted in [24] to study the control of electromagnetic torque and reactive power under unbalanced grid voltage conditions. The study focused on using a stator-flux-oriented reference frame and obtaining the stator flux through an observer. The controller produces sinusoidal currents that are injected into the grid. In the case of an unbalanced grid voltage, the authors of [25] suggest a Voltage Modulated (VM)-DPC approach for DFIGs that makes use of the extended power theory. The absence of sequence extractions causes fluctuations under unbalanced conditions, even though the combination of PI and VM-DPC strategy slightly improves control in normal situations.

A simplified DPC of DFIGs under both normal and unbalanced grid voltage conditions in a stationary reference frame is presented in [26]. This approach offers the advantages of eliminating the decomposition process, axes transformation, and compensation power terms. Stator active and reactive powers are controlled using Vector proportional-integral (VPI) controllers and the performance is compared with proportional-integral-resonant (PIR) controllers through simulations. In [27] a VM-DPC is designed to improve steady-state and transient performances under unbalanced grid voltage conditions. In conjunction with the VM-DPC, a parallel compensator regulates negative-sequence stator current, resulting in improved waveforms for stator current, stator active power, and stator reactive power. For the stator current and voltage, this technique necessitates the extraction of positive and negative sequences. To calculate positive and negative sequences, the authors of [28] devised a mixed integrator, which is a combination of second and third-order integrators. The hysteresis controllers of rotor currents and grid currents generate switching patterns for the rotor side converter and grid side converter, respectively. This method is claimed to possess superior capability in tracking reference currents when compared to the conventional DPC method. Additionally, it eliminates the requirement of tuning eight PI current regulators. A low-complexity model predictive direct power control method is proposed in [29]. This method aims to reduce power ripples and utilizes the extended reactive pq theory. This has decreased the computational

burden of the controller as it now only requires one prediction to determine the voltage vector for the next step. This approach offers several advantages, including the reduction of total harmonic distortion in grid current, fast dynamic response, and robustness to parameter variations.

When it comes to control methods, direct power control offers the fastest dynamic response at the lowest cost. Nevertheless, there are a few downsides to this approach, such as increased power ripples and variable switching frequency. Table 1 represents and compares the performance of the different control methods. Different aspects are considered in this comparison, such as dynamic response, power ripple, dependence on machine parameters, converter switching frequency, computational burden, and cost. Low power ripple and a constant switching frequency characterize the FOC method. In contrast to DPC, however, it has several drawbacks, including a sluggish dynamic response, a heavy dependence on machine parameters, and a greater computational burden. Although direct torque control offers fast dynamic response and minimal dependence on machine parameters, it is not without its limitations, including variable switching frequency and relatively higher power ripples. Both DTC and FOC require measurements of rotor current, which raises the cost of the control system.

High dynamic response and variable switching frequency are typical characteristics of controllers based on switching tables. DPC-SVM combines the advantages of DPC and FOC. DPC-SVM's key features are a constant switching frequency, straightforward implementation, a lower cost compared to alternative controllers, and a low power ripple. Predictive direct power control (P-DPC) has the potential to address the primary challenges associated with DPC. Nevertheless, its implementation is costlier due to the computational burden imposed by the control algorithm's complexity and the requirement for rotor current information. As an alternative to DTC, DPC eliminates the requirement to measure rotor currents, thereby decreasing the cost of control.

Table 1. Comparison of different control methods for DFIG.

Control method	Dynamic response	Power Ripple	Dependence on machine parameters	Switching frequency	Ease of implementation	Output current THD	Cost
FOC	Slow	Low	High	Constant	Complicated	Low	High
DTC	Fast	Very High	Low	Variable	Simple	Normal	High
DPC	Fast	High	Very Low	Variable	Simple	Normal	Low
SVM-DPC	Fast	Low	Low	Constant	Simple	Normal	Low
Predictive	Fast	Low	Very High	Constant	Complicated	Low	High

However, similar to DTC, higher power ripple and variable switching frequency are the primary drawbacks of DPC employing a switching table.

The key contributions of this paper are outlined below:

- Conducting a thorough examination of DFIG performance in the presence of unbalanced grid voltage conditions
- Presenting two strategies aimed at mitigating active and reactive power oscillations
- Introducing a high selectivity filter (HSF) to separate the fundamental component of stator phase currents from the harmonic components
- Demonstrating the effectiveness of the proposed method compared to traditional DPC controllers through extensive simulations

The structure of this paper is as follows: The second section examines the dynamic model of DFIG. Direct power control, various hysteresis band controllers, and switching tables are examined in the third section. The performance of DFIG in an unbalanced voltage condition was addressed in the fourth section. In the fifth section, proposed control approaches are outlined and compared to standard DPC. Finally, in sections six and seven, the simulation findings and conclusions are presented.

2. Structure and Dynamic Modeling of DFIG

Given the presence of feedback loops in the DFIG control system, it is important to take into account its dynamic behavior. DFIG control methods, such as DPC and FOC, are discussed using a two-axis model. The DFIG equivalent circuit can be defined in various reference frames, including the stator reference frame, rotor reference frame, and synchronous reference frame [30]. The rotor voltage equations are written in the rotor (natural) reference frame since the DFIG is controlled from the rotor side by the rotor side converter. The DFIG equivalent circuit in the rotor reference frame is depicted in Figure 3. It is important to mention that the model neglects saturation and core loss effects. Additionally, the grid is simplified as a pure voltage source, meaning the internal Thévenin impedance of the grid is not taken into account.

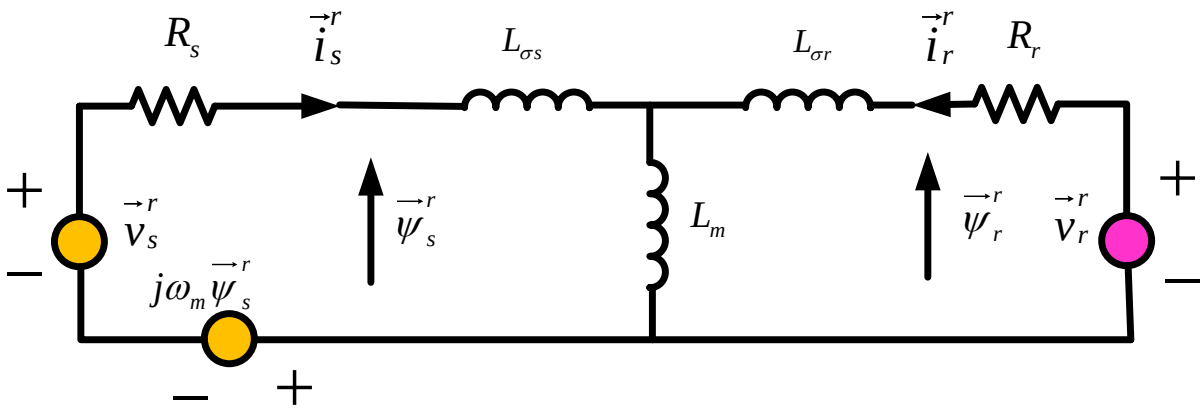

Figure 3. DFIG equivalent circuit in the rotor reference frame [30].

3. Conventional Direct Power Control Principles

Referring to Figure 3, the stator active and reactive power expressions can be derived in the rotor reference frame. Active power consumed and reactive power injected by the stator of the machine are taken to be positive [31]. Accordingly, the input active power of the stator from the network side, neglecting the stator resistance, is as follows:

$$P_s = \frac{3}{2}\mathrm{Re}\{(\dot{\vec{\psi}}_s^r + j\omega_m \vec{\psi}_s^r)\cdot \vec{i}_s^{r*}\} \tag{1}$$

Similarly, the output reactive power is calculated as follows:

$$Q_s = -\frac{3}{2}\mathrm{Im}\{(\dot{\vec{\psi}}_s^r + j\omega_m \vec{\psi}_s^r).\vec{i}_s^{r*}\} \tag{2}$$

The relative position of the stator and rotor flux space vectors in the rotor reference frame is shown in Figure 4, where θ_ψ is the spacial angle between the stator and rotor flux space vectors.

As shown in Appendix A, Equation (1) and (2), can be rewritten as follows:

$$P_s = -\frac{3}{2}\frac{L_m}{\sigma L_s L_r}\omega_s \left|\vec{\psi}_s^r\right|\left|\vec{\psi}_r^r\right|\sin\theta_\psi \tag{3}$$

$$Q_s = \frac{3}{2}\frac{\omega_s}{\sigma L_s}\left|\vec{\psi}_s^r\right|\left(\frac{L_m}{L_r}\left|\vec{\psi}_r^r\right|\cos\theta_\psi - \left|\vec{\psi}_s^r\right|\right) \tag{4}$$

Since there is a direct connection to the network, which is assumed to have a positive sequence only in this case, the magnitude of the stator flux space vector can be taken to be constant. The time derivatives of Eqauation (3) and (4) then yield:

$$\begin{aligned}\frac{dP_s}{dt} &= -\frac{3}{2}\frac{L_m}{\sigma L_s L_r}\omega_s \left|\vec{\psi}_s^r\right|\frac{d(\left|\vec{\psi}_r^r\right|\sin\theta_\psi)}{dt}\\ \frac{dQ_s}{dt} &= \frac{3}{2}\frac{L_m}{\sigma L_s L_r}\omega_s \left|\vec{\psi}_s^r\right|\frac{d(\left|\vec{\psi}_r^r\right|\cos\theta_\psi)}{dt}\end{aligned} \tag{5}$$

Therefore, fast changes in active and reactive powers are possible with corresponding changes in $\left|\vec{\psi}_r^r\right|\sin\theta_\psi$ and $\left|\vec{\psi}_r^r\right|\cos\theta_\psi$, respectively. In Figure 4, $\left|\vec{\psi}_r^r\right|\sin\theta_\psi$ and $\left|\vec{\psi}_r^r\right|\cos\theta_\psi$ represent, respectively, the components of the rotor flux perpendicular and in the direction of stator flux space vector.

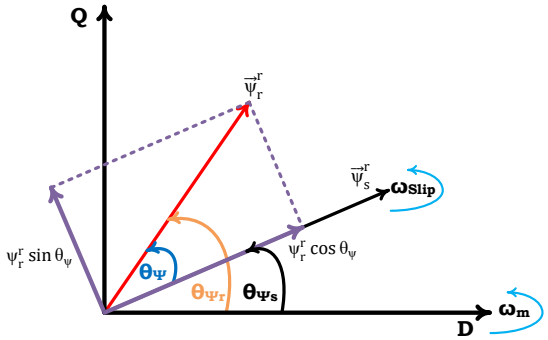

Figure 4. Stator and rotor flux space vectors in rotor reference frame [31].

Therefore, if the rotor flux changes in the direction of the stator flux space vector, then $\left|\vec{\psi}_r^r\right|\cos\theta_\psi$ and accordingly the stator reactive power Q_s changes; on the other hand, the change in rotor flux space vector is perpendicular to the stator flux, then $\left|\vec{\psi}_r^r\right|\sin\theta_\psi$ and stator active power P_s is modified.

The rotor side converter is a three-phase voltage source converter with two switches for each leg. In Figure 5, S_a, S_b and S_c represent the switching functions of every leg of the inverter. If the upper switches are connected, the positive DC voltage is applied, and if the lower switches are connected the applied voltage will be zero.

According to the combination of switching states, two null vectors (V_0,V_7) and six active vectors ($V_1 - V_6$) can be generated. By neglecting the voltage drop on the rotor resistance, the rotor voltage equation in its natural reference frame can be expressed as follows in Equation (6) [31]:

$$\vec{v}_r^r = R_r\vec{i}_r^r + \frac{d\vec{\psi}_r^r}{dt} \cong \frac{d\vec{\psi}_r^r}{dt} \tag{6}$$

The above expression shows that the rotor flux vector moves in the direction of the voltage vector applied to the rotor and its velocity is proportional to the magnitude of the applied voltage vector. It is thus possible to adjust the rotor flux velocity by choosing appropriate voltage vectors.

Figure 6 shows the stator flux and rotor flux space vectors in a rotating plane attached to the rotor with eight possible rotor voltage vectors. If the position of the stator flux is known, the effect of using $\left|\vec{\psi}_r^r\right|\sin\theta_\psi$ and $\left|\vec{\psi}_r^r\right|\cos\theta_\psi$ can be determined for each voltage vector. Figure 7 shows the initial position of rotor flux at moment t_1 and the final position of rotor flux at moment $t_1 + \Delta t$, assuming that the rotor flux is located in the first sector of the rotor reference frame. It may be noted that $\vec{\psi}_r^r$ is drawn ahead of $\vec{\psi}_s^r$ as the generating mode of operation has been considered.

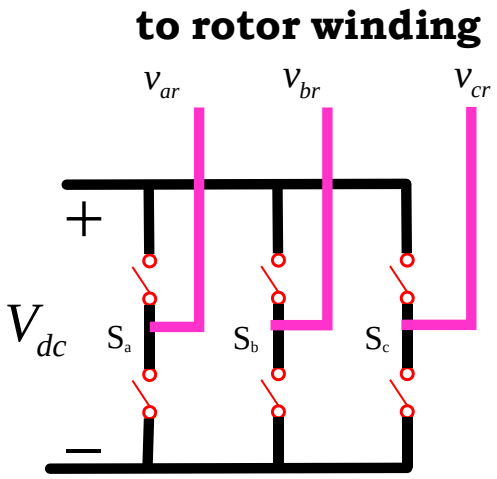

Figure 5. Schematic of a rotor-side VSI.

Using $\vec{v}_2$ and $\vec{v}_6$ leads to the increase of the final rotor flux and increases the stator-generated active power. Using $\vec{v}_1$ and $\vec{v}_5$ leads to the decrease of the final rotor flux and decreases the stator-generated active power. Using $\vec{v}_3$ and $\vec{v}_4$ does not affect the stator active power.

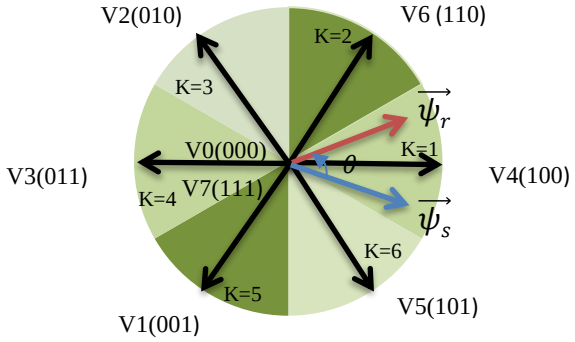

Figure 6. Voltage space vectors applied to the converter.

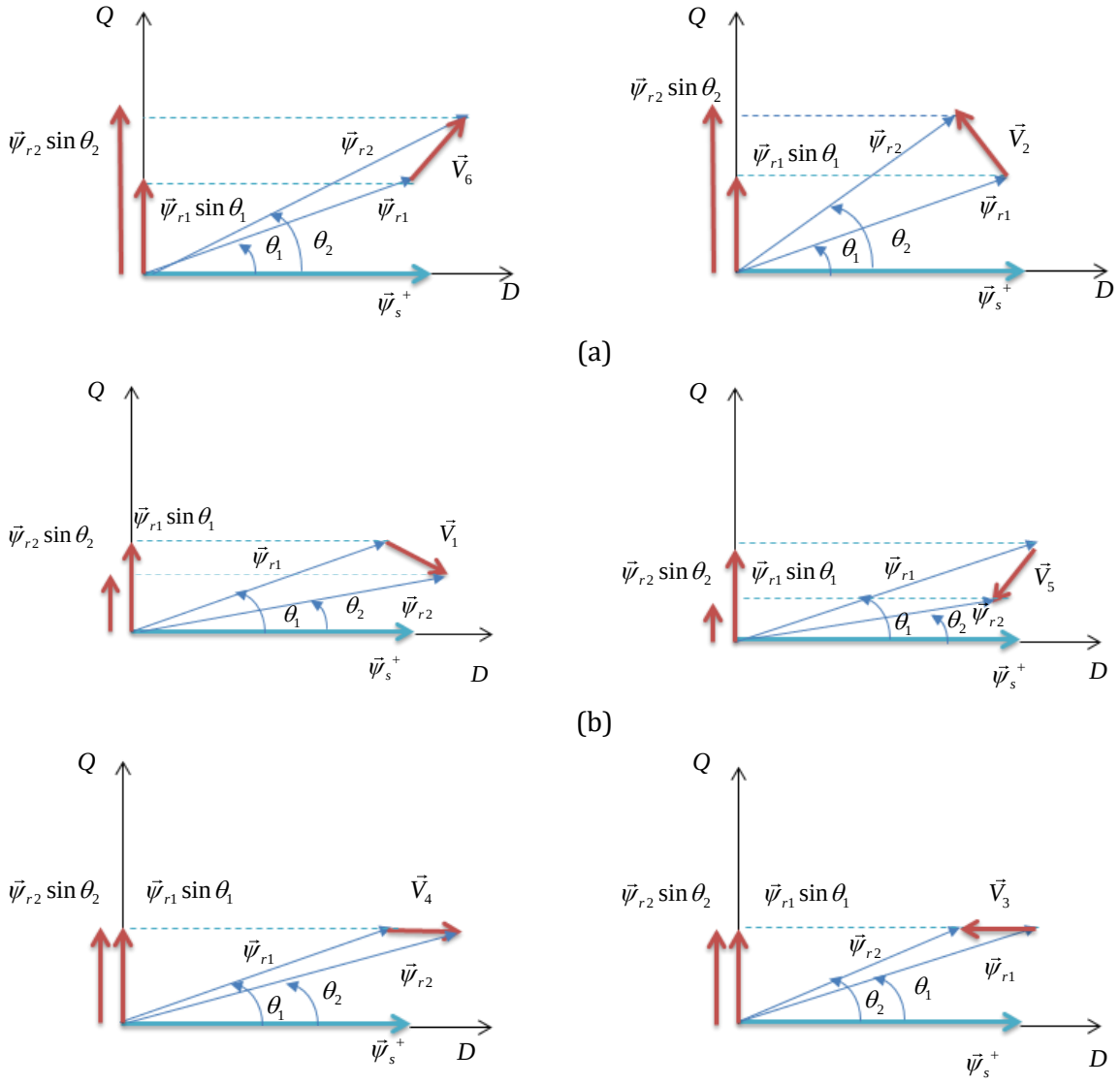

Figure 7. Effect of active vectors on active power, a: $\vec{v}_2$ and$\vec{v}_6$,b: $\vec{v}_1$ and $\vec{v}_5$, c: $\vec{v}_3$ and $\vec{v}_4$.

Table 2. Effect of voltage vectors on stator input active power and output reactive power.

K=1, 2, 3, .., 6	v_{k-2}	v_{k-1}	v_k	v_{k+1}	v_{k+2}	v_{k+3}
P_s	↑	↓	↑	↓	↓↑	↓↑
Q_s	↑	↑	↓	↓	↓	↑

Table 2 illustrates the effect of different voltage vectors on active and reactive powers. The angle between the stator flux and rotor flux may increase or decrease by applying a zero-vector depending on the operating mode of the machine. For sub-synchronous mode, the stator flux movement reduces the angle between the rotor flux and the stator flux ($\theta_2 < \theta_1$), which causes active power reduction and reactive power increment. In other cases, the stator flux movement increases the angle between the rotor and the stator flux ($\theta_2 > \theta_1$), which causes active power increment and reactive power reduction.

3.1. Flux estimation methods

Multiple techniques exist for determining the position of the rotor flow vector. The estimation of the rotor and stator flux is performed by incorporating the rotor angular position in [32]. One drawback of this technology is its dependence on rotor currents. Machine parameters are required to calculate flux, which reduces the speed of estimation and adds to the complexity of the control. This approach provides a more precise estimation of the angle of flux.

An alternative approach for determining the rotor flux angle involves utilizing the stator flux. The stator voltage is utilized in [31] to determine the stator flux angle. This approach assumes a small angle between the stator and rotor flux and considers the position of the rotor and stator flux inside the same sector. The stator flux is estimated in the stator reference frame by integrating the stator voltage while neglecting the stator resistance. This method can accurately estimate the stator flux due to the harmonic-free and constant frequency nature of the stator voltage. Integration is typically implemented by employing a low pass filter in practical applications.

In this work, the rotor flux angle is estimated using the stator flux. The voltage vector applied to the rotor windings is determined by the position of the rotor flux and the different active and reactive power states.

3.2. Direct Active and Reactive Power Control

In this section, the computed active and reactive powers are compared to their respective reference values, resulting in the generation of error signals, fed to two hysteresis comparators. Two-level, three-level, or four-level hysteresis controllers can be used which yield different switching tables for control of the rotor side converter. In [33],

a two-level hysteresis controller for active and reactive powers is used. In [34] a three-level controller is used for active power:

$$\begin{aligned} &P_{ref} \geq P + \Delta P \rightarrow dp = 1 \\ &P_{ref} \leq P - \Delta P \rightarrow dp = -1 \\ &P_{ref} \leq P - \Delta \mathrm{P} \quad or \quad P_{ref} \geq P + \Delta P \rightarrow dp = 0 \end{aligned} \tag{7}$$

and a two-level controller is used for reactive power, as:

$$\begin{aligned} &Q_{ref} \geq Q + \Delta Q \rightarrow dq = 1 \\ &Q_{ref} \leq Q - \Delta Q \rightarrow dq = -1 \end{aligned} \tag{8}$$

In Equation (7) and (8), ΔP and ΔQ represent the hysteresis bandwidth. The values 1/-1 indicate the need to increase/decrease stator active and reactive powers to approach the reference value.

A three-level hysteresis controller is employed in [31] to regulate both active and reactive powers. The three-level controller incorporates a greater number of switching states, resulting in improved accuracy of the control system for active and reactive power regulation.

A study was undertaken in [35,36] to investigate the impact of active and reactive power hysteresis bands on the performance of DPC drives. The study reveals that the hysteresis band has a significant influence on the THD of the stator current and the oscillations in the control system. The study conducted in [37] found that a narrower hysteresis band leads to an increase in switching frequency. Alternatively, when the hysteresis band is increased to 25% of rated power, the switching frequency decreases to 500 Hz. Therefore, by utilizing the output signals of hysteresis comparators (S_p and S_q) in conjunction with the angular information of the rotor flux space vector, an optimal switching table is created.

3.3. The effect of different switching tables

For a long time, switching table designs for DPC and DTC have been of interest. In [38-43], the differences between various switching tables are examined and reviewed. Since the majority of researchers have focused on analyzing DPC performance under balanced network voltage, the development of switching tables has primarily been done under this specific condition. The initial switching table developed by Noguchi is currently regarded as a standard for evaluating other tables [44]. This table exhibits significant fluctuations in both active and reactive power as a result of an incorrect choice of voltage vectors [38]. Later on, Malinowski introduced a new table for three-phase rectifiers [45]. Utilizing zero vectors in this table mitigates power fluctuations and enhances the performance of the control system. Researchers subsequently introduced novel switching tables. New tables significantly enhanced the dynamic and steady-state performance of the DPC in comparison to conventional tables by suppressing active and reactive power fluctuations more effectively [21]. One of the reasons that reactive power error in some tables was overlooked is due to the higher priority given to reducing ripple for active power [21]. In

general, the switching tables are classified according to their accuracy in power regulation, the amount of active power ripple, the current THD, the switching frequency, and the response time. In [40], a study is conducted on a switching table that utilizes active vectors. In this table, the elimination of zero vectors is based on their negligible impact on active and reactive powers. While this switching table has led to a faster response time, it has also caused an increase in power ripple, current THD, and switching frequency.

In this paper, a three-level hysteresis comparator is utilized for both active and reactive powers. A switching table of 54 different entries for voltage vectors is employed, as per the reference [31], which is presented in Table 3. Zero voltage vectors are utilized when there are no errors in both active and reactive power.

4. Performance Analysis under Unbalanced Voltage Conditions

Supplying DFIG with unbalanced grid voltage can have detrimental effects on its performance. These effects include increased losses, reduced efficiency and torque, and higher machine temperatures with uneven distribution [46]. The intensity of these effects is directly influenced by the severity of the unbalanced voltage in the machine terminals. For this reason, control system performance is crucial. Under unbalanced network conditions, three-phase quantities like voltage, current, and flux are separated into positive and negative sequence components by ignoring the zero sequence.

In [47], voltage, current, and flux in the stator reference frame have been separated into positive and negative sequence components as follows in Equation (9):

$$\vec{F}_{\alpha\beta}(t) = \vec{F}_{\alpha\beta+}(t) + \vec{F}_{\alpha\beta-}(t) = \left|\vec{F}_{\alpha\beta+}\right|.e^{j(\omega_s t+\varphi_+)} + \left|\vec{F}_{\alpha\beta-}\right|.e^{-j(\omega_s t+\varphi_-)} \quad (9)$$

where φ_+ and φ_- are phase shifts related to the positive and negative components. As shown in Figure 8, in the dq^+ reference frame, the d^+ axis is fixed to the positive voltage vector rotating at the speed of ω_s. For dq^- reference frame, the d^- axis rotates at the opposite direction at the speed of $-\omega_s$ and its phase angle related to the α axis is $-\theta_s$ [45].

Table 3. Switching Table for the DPC [31].

S_p	S_q	I	II	III	IV	V	VI
1	1	V_5	V_4	V_6	V_2	V_3	V_1
	0	V_4	V_6	V_2	V_3	V_1	V_5
	-1	V_6	V_2	V_3	V_1	V_5	V_4
0	1	V_1	V_5	V_4	V_6	V_2	V_3
	0	V_0, V_7	V_0, V_7	V_0, V_7	V_0, V_7	V_0, V_7	V_0, V_7
	-1	V_2	V_3	V_1	V_5	V_4	V_6
-1	1	V_1	V_5	V_4	V_6	V_2	V_3
	0	V_3	V_1	V_5	V_4	V_6	V_2
	-1	V_2	V_3	V_1	V_5	V_4	V_6

According to Figure 8, the transformation rules between $\alpha\beta$, dq^+ and dq^- reference frames are as follows in Equation (10):

$$\vec{F}_{dq}^{+} = \vec{F}_{\alpha\beta}.e^{-j\omega_s t},\ \vec{F}_{dq}^{-} = \vec{F}_{\alpha\beta}.e^{+j\omega_s t} \tag{10}$$

$$\vec{F}_{dq}^{+} = \vec{F}_{dq}^{-}.e^{-j2\omega_s t},\ \vec{F}_{dq}^{-} = \vec{F}_{dq}^{+}.e^{+j2\omega_s t} \tag{11}$$

F variables can be expressed as positive and negative sequence components [46]:

$$\vec{F}_{dq}^{+} = \vec{F}_{dq+}^{+} + \vec{F}_{dq-}^{+} + \vec{F}_{dq5-}^{+} + \vec{F}_{dq7+}^{+} \tag{12}$$

According to Equation (12), under unbalanced and distorted grid voltage, variable F consists of 5 and 7 harmonics, which rotate in the dq reference frame. In Equation (12), the superscripts "+" and "-" refer to the positive and negative reference frames, and the subscripts "+" and "-" refer to the positive and negative sequence components. Using Equation (11), Equation (12) can also be written as:

$$\vec{F}_{dq}^{+} = \vec{F}_{dq+}^{+} + \vec{F}_{dq-}^{-}e^{-2j\omega_s t} + \vec{F}_{dq5-}^{5-}e^{-6j\omega_s t} + \vec{F}_{dq7+}^{7+}e^{+6j\omega_s t} \tag{13}$$

As shown in Equation (13), in the dq^+ reference frame, F contains a dc term and oscillating components. As a result, Equation (13) can be represented as Equation (14):

$$\begin{aligned} \vec{F}_{d}^{+} &= \vec{F}_{d+}^{+} + \vec{F}_{d-}^{+} \\ \vec{F}_{q}^{+} &= \vec{F}_{q+}^{+} + \vec{F}_{q-}^{+} \end{aligned} \tag{14}$$

where:

$$\begin{aligned} \vec{F}_{d-}^{+} &= (\vec{F}_{d-}^{-}\cos 2\omega_s t + \vec{F}_{q-}^{-}\sin 2\omega_s t) + (\vec{F}_{d5-}^{5-}\cos 6\omega_s t + \vec{F}_{q5-}^{5-}\sin 6\omega_s t) + (\vec{F}_{d7}^{7}\cos 6\omega_s t - \vec{F}_{q7}^{7}\sin 6\omega_s t) \\ \vec{F}_{q-}^{+} &= (\vec{F}_{q-}^{-}\cos 2\omega_s t - \vec{F}_{d-}^{-}\sin 2\omega_s t) + (\vec{F}_{q5-}^{5-}\cos 6\omega_s t - \vec{F}_{d5-}^{5-}\sin 6\omega_s t) + (\vec{F}_{q7}^{7}\cos 6\omega_s t + \vec{F}_{d7}^{7}\sin 6\omega_s t) \end{aligned} \tag{15}$$

Therefore, stator voltage and current in the dq^+ reference frame, neglecting 5 and 7 harmonics, are as follows:

$$\begin{aligned} \vec{v}_{sdq}^{+} &= \vec{v}_{sdq+}^{+} + \vec{v}_{sdq-}^{-}e^{-2j\omega_s t} \\ \vec{i}_{sdq}^{+} &= \vec{i}_{sdq+}^{+} + \vec{i}_{sdq-}^{-}e^{-2j\omega_s t} \end{aligned} \tag{16}$$

Power relations are written as follows:

$$\begin{aligned} \begin{bmatrix} P \\ Q \end{bmatrix} = \begin{bmatrix} \overline{P} + \tilde{P} \\ \overline{Q} + \tilde{Q} \end{bmatrix} &= \frac{3}{2}\begin{bmatrix} \vec{v}_{d+}^{+}\vec{i}_{d+}^{+} + \vec{v}_{q+}^{+}\vec{i}_{q+}^{+} + \vec{v}_{d-}^{-}\vec{i}_{d-}^{-} + \vec{v}_{q-}^{-}\vec{i}_{q-}^{-} \\ \vec{v}_{q+}^{+}\vec{i}_{d+}^{+} - \vec{v}_{d+}^{+}\vec{i}_{q+}^{+} + \vec{v}_{q-}^{-}\vec{i}_{d-}^{-} - \vec{v}_{d-}^{-}\vec{i}_{q-}^{-} \end{bmatrix} \\ &+ \frac{3}{2}\begin{bmatrix} \vec{v}_{d-}^{+}\vec{i}_{d+}^{+} + \vec{v}_{q-}^{+}\vec{i}_{q+}^{+} + \vec{v}_{d+}^{+}\vec{i}_{d-}^{+} + \vec{v}_{q+}^{+}\vec{i}_{q-}^{+} \\ \vec{v}_{q-}^{+}\vec{i}_{d+}^{+} - \vec{v}_{d-}^{+}\vec{i}_{q+}^{+} + \vec{v}_{q+}^{+}\vec{i}_{d-}^{+} - \vec{v}_{d+}^{+}\vec{i}_{q-}^{+} \end{bmatrix} \end{aligned} \tag{17}$$

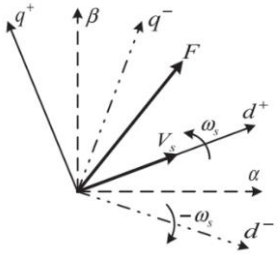

Figure 8. Relation between $\boldsymbol{dq^+}$ and $\boldsymbol{dq^-}$ reference frames [47].

The oscillating components of active and reactive power cause DC link voltage and electromagnetic torque ripples. To minimize these ripples, the oscillating terms of active and reactive powers in Equation (17) should be zero, as shown below in Equation (18):

$$\begin{bmatrix} \overline{P} \\ \overline{Q} \\ 0 \\ 0 \end{bmatrix} = \frac{3}{2} \begin{bmatrix} \vec{v}_{d+}^{+}\vec{i}_{d+}^{+} + \vec{v}_{q+}^{+}\vec{i}_{q+}^{+} + \vec{v}_{d-}^{-}\vec{i}_{d-}^{-} + \vec{v}_{q-}^{-}\vec{i}_{q-}^{-} \\ \vec{v}_{q+}^{+}\vec{i}_{d+}^{+} - \vec{v}_{d+}^{+}\vec{i}_{q+}^{+} + \vec{v}_{q-}^{-}\vec{i}_{d-}^{-} - \vec{v}_{d-}^{-}\vec{i}_{q-}^{-} \\ \vec{v}_{d\square}^{+}\vec{i}_{d+}^{+} + \vec{v}_{q\square}^{+}\vec{i}_{q+}^{+} + \vec{v}_{d+}^{+}\vec{i}_{d\square}^{+} + \vec{v}_{q+}^{+}\vec{i}_{q\square}^{+} \\ \vec{v}_{q\square}^{+}\vec{i}_{d+}^{+} - \vec{v}_{d\square}^{+}\vec{i}_{q+}^{+} + \vec{v}_{q-}^{-}\vec{i}_{d\square}^{-} - \vec{v}_{d-}^{-}\vec{i}_{q\square}^{-} \end{bmatrix} \tag{18}$$

Consequently, active and reactive powers can be written as follows in Equation (19):

$$P = \overline{P} + \tilde{P} \qquad Q = \overline{Q} + \tilde{Q} \tag{19}$$

As mentioned before, $\vec{v}_{dq+}^{+}$, $\vec{i}_{dq+}^{+}$, $\vec{v}_{dq-}^{-}$ and $\vec{i}_{dq-}^{-}$ are DC terms while $\vec{v}_{dq\sim}^{+}$ and $\vec{i}_{dq\sim}^{+}$ are oscillating terms with frequency of $2\omega_s$. Constant power terms ($\overline{P}$ and $\overline{Q}$) are due to the interaction between constant components of voltage and current in the synchronous frames. It should be noted that the 5th and 7th harmonics of the grid voltage have been neglected in this paper for the sake of simplicity.

5. Improving DFIG performance under unbalanced conditions

DFIG voltage and flux equations are written in the rotor reference frame concerning Figure 4 as follows:

$$\vec{v}_s^{\,r} = R_s\vec{i}_s^{\,r} + \frac{d\vec{\psi}_s^{\,r}}{dt} + j\omega_m\vec{\psi}_s^{\,r} \qquad \vec{v}_r^{\,r} = R_r\vec{i}_r^{\,r} + \frac{d\vec{\psi}_r^{\,r}}{dt} \tag{20}$$

$$\vec{\psi}_r^{\,r} = L_r\vec{i}_r^{\,r} + L_m\vec{i}_s^{\,r} \qquad \vec{\psi}_s^{\,r} = L_s\vec{i}_s^{\,r} + L_m\vec{i}_r^{\,r} \tag{21}$$

Since the stator side is connected to the grid and the stator voltage is unbalanced, Equation (20) and (21) also include the positive and negative sequence components. Therefore, stator active and reactive powers take the following form:

$$P_s = \overline{P_s} + \tilde{P}_s \qquad Q_s = \overline{Q_s} + \tilde{Q}_s \tag{22}$$

Equation (22) shows that the stator power under unbalanced conditions has DC and oscillating components. Our strategy in this paper is to reduce the oscillation of active and reactive powers of the rotor side converter under unbalanced voltage conditions. In this paper, two strategies are proposed to mitigate the effect of unbalanced voltage on active and reactive power ripples.

One method to detect and isolate harmonic components of current is the so-called instantaneous power p–q theory [47,48]. In this method, harmonics from the load currents are extracted by the computation of instantaneous power and using (HPF) and/or (LPF). This method is no longer used because of the complex computation of voltage and current. A more common method is described in [49]. In this method, only the currents are measured and the harmonic part is extracted. The main problem in this scheme is the lack of selective harmonic detection because of using (LPF) [50]. In [51] a

new time-domain harmonic detection method was proposed based on (HSF). This method requires current measurement and isolates a particular harmonic or separates the harmonic components from the fundamental component and current references can be calculated. In this paper, we propose (HSF) instead of conventional (LPF) to extract the fundamental component of stator current.

5.1. Direct power control with PI regulator

This section will address the implementation of direct power control with a PI regulator in the presence of unbalanced conditions. The simulation findings demonstrate that while the proposed method introduces complexity to the control system structure compared to the conventional DPC method, it effectively reduces power ripple in the presence of unbalanced voltage conditions. The controller structure is shown in Figure 9. In the first step, active and reactive powers are compared with their respective reference values, and calculated errors are passed to the PI controller. The output signals are considered as reference values for stator or rotor currents. To calculate rotor currents in the dq^+ reference frame, rotor currents should first be transformed to the synchronous reference frame. A PLL is used to calculate the reference frame angle. Instead of the rotor currents, stator currents can be used in the positive synchronous reference frame. In this case, only the angle of the positive sequence stator current (θ_s^+) is estimated using PLL. After comparison of the stator currents with their reference values, the outputs are given to hysteresis comparators. Similar to the conventional DPC method, the output signals from two hysteresis comparators are applied to the switching table to select the appropriate voltage vector. As mentioned before under unbalanced voltage conditions the stator current contains fundamental and harmonic components, that is:

$$\vec{i}_{sdq}^{+} = \vec{i}_{sdq+}^{+} + \vec{i}_{sdq-}^{-} e^{-2j\omega_s t} + \vec{i}_{sdq5-}^{5-} e^{-6j\omega_s t} + \vec{i}_{sdq7+}^{7+} e^{+6j\omega_s t} \quad (23)$$

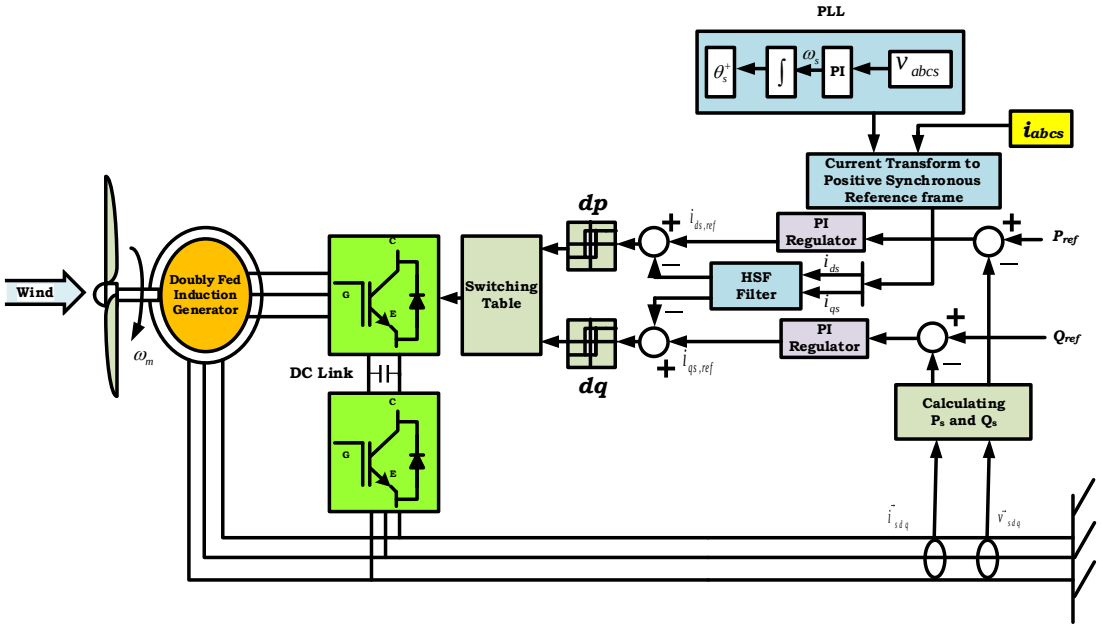

Figure 9. Structure of DPC with PI regulator under unbalanced grid voltage conditions.

In Equation (23) $\vec{i}^{+}_{sdq+}$, $\vec{i}^{-}_{sdq-}$, $\vec{i}^{5-}_{sdq5-}$ and $\vec{i}^{7+}_{sdq7+}$ are DC values. This means that the stator currents in the dq^{+} reference frame include DC and oscillating components. The HSF filter only passes the DC component in the positive synchronous frame ($\vec{i}^{+}_{sdq+}$); therefore, in this control method, the reference d and q stator currents are directly compared with corresponding DC components generated by the HSF filter. The details of the proposed filter are given in the following.

5.1.1. High selectivity filter (HSF)

A high selectivity filter (HSF) is used to separate the fundamental component of the signal instead of conventional (LPF) and (HPF) filters. Hong-sock Song in [52] shows that the integral in the synchronous reference frame is given as Equation (24):

$$V_{xy}(t) = e^{j\omega_s t}\int e^{-j\omega_s t}U_{xy}(t)dt \tag{24}$$

Where U_{xy} and V_{xy} are the instantaneous signals, before and after integration in the synchronous reference frame, respectively. Equation (24) can be expressed by the following transfer function after Laplace transformation:

$$H(s) = \frac{V_{xy}(s)}{U_{xy}(s)} = \frac{s + j\omega_s}{s^2 + \omega_s^2} \tag{25}$$

In Equation (25), constant K is introduced in the transfer function $H(s)$, to obtain an HSF with a cut-off frequency. So, the previous transfer function becomes:

$$H(s) = \frac{V_{xy}(s)}{U_{xy}(s)} = k\frac{(s+k) + j\omega c}{(s+k)^2 + \omega_c^2} \tag{26}$$

Replacing $V_{xy}(s)$ with X_{dq} and $U_{xy}(s)$ with $\hat{X}_{dq}$, Equation (26) is rewritten as Equation (27):

$$\begin{aligned}\hat{X}_d(s) &= \frac{k(s+k)}{(s+k)^2 + \omega_c^2}X_d(s) - \frac{k\omega_c}{(s+k)^2 + \omega_c^2}X_q(s)\\ \hat{X}_q(s) &= -\frac{k\omega_c}{(s+k)^2 + \omega_c^2}X_d(s) + \frac{k(s+k)}{(s+k)^2 + \omega_c^2}X_q(s)\end{aligned} \tag{27}$$

Where X can be current or voltage. Therefore, the above equation is written as Equation (28):

$$\begin{aligned}\hat{X}_d(s) &= \frac{k}{s}[X_d(s) - \hat{X}_d(s)] - \frac{\omega_c}{s}\hat{X}_q(s)\\ \hat{X}_q(s) &= \frac{k}{s}[X_q(s) - \hat{X}_q(s)] - \frac{\omega_c}{s}\hat{X}_d(s)\end{aligned} \tag{28}$$

The (HSF) block diagram for the separation of the fundamental component ($\hat{X}_{dq}$) from X_{dq} in the synchronous reference frame is shown in Figure 10. In this paper, we consider k=40 for good dynamic response.

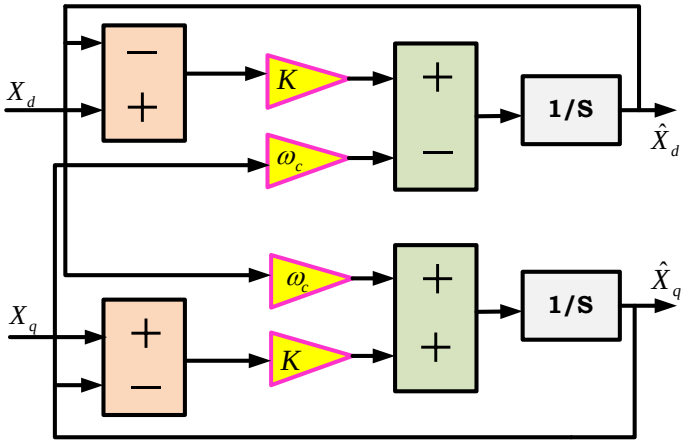

Figure 10. The block diagram of the HSF filter [52].

5.2. DPC using stator flux

In this section, the calculation of stator active and reactive powers in terms of stator flux is discussed. The relation between stator voltage and stator flux in the synchronous reference frame is shown in Figure 11 [53]. The stator apparent power can be expressed in terms of quantities in the stationary reference frame as follows:

$$S_s = \frac{3}{2}\vec{v}_s^{\,s}\vec{i}_s^{\,s^*} \tag{29}$$

According to the stator voltage equation in the stationary reference frame, if stator resistance losses are neglected, the flux and voltage can be related as follows:

$$\vec{v}_s^{\,s} = \frac{d}{dt}\vec{\psi}_s^{\,s} \tag{30}$$

$$\vec{\psi}_s^{\,s} = \vec{\psi}_s^{\,e} e^{j\omega_s t} \tag{31}$$

$$\frac{d}{dt}\vec{\psi}_s^{\,s} = j\omega_s \vec{\psi}_s^{\,e} e^{j\omega_s t} \tag{32}$$

Substitution of Equation (31) and Equation (32) in Equation (29), yields:

$$S_s = \frac{3}{2}\vec{v}_s^{\,s}\vec{i}_s^{\,s^*} = \frac{3}{2}\{(\dot{\vec{\psi}}_s^{\,s})\cdot\vec{i}_s^{\,s}\} = \frac{3}{2}\{(\dot{\vec{\psi}}_s^{\,e}e^{j\omega_s t})\cdot(\vec{i}_s^{\,e}e^{j\omega_s t})^*\} = \frac{3}{2}\{(\dot{\vec{\psi}}_s^{\,e}e^{j\omega_s t} + j\omega\vec{\psi}_s^{\,e}e^{j\omega_s t})\cdot(\vec{i}_s^{\,e}e^{j\omega_s t})^*\} \tag{33}$$

More manipulation of Equation (33) gives:

$$\begin{aligned} S_s &= \frac{3}{2}\{((\dot{\psi}_{ds} + j\dot{\psi}_{qs})e^{j\omega_s t} + j\omega_s(\psi_{ds} + j\psi_{qs}))e^{j\omega_s t})\cdot((i_{ds} + ji_{qs}))e^{j\omega_s t})^*\} \\ &= \frac{3}{2}\{e^{j\omega_s t}(\dot{\psi}_{ds} + j\dot{\psi}_{qs}) + j\omega_s\psi_{ds} - \omega_s\psi_{qs}))((i_{ds} - ji_{qs}))e^{-j\omega_s t})\} \end{aligned} \tag{34}$$

Further simplification yields:

$$S_s = \frac{3}{2}(\dot{\psi}_{ds}i_{ds} + \dot{\psi}_{qs}i_{qs} - \omega_s\psi_{qs}i_{ds} + \omega_s\psi_{ds}i_{qs} - j\dot{\psi}_{ds}i_{qs} + \dot{\psi}_{qs}i_{ds} + j\omega_s\psi_{qs}i_{qs} + j\omega_s\psi_{ds}i_{ds}) \tag{35}$$

In the above equation, terms containing derivatives are neglected because they are constant in the synchronous reference frame. Thus, Equation (35) is simplified as follows:

$$S_s = \frac{3}{2}\{-\omega_s\psi_{qs}i_{ds} + \omega_s\psi_{ds}i_{qs} + j(\omega_s\psi_{qs}i_{qs} + \omega_s\psi_{ds}i_{ds})\} \tag{36}$$

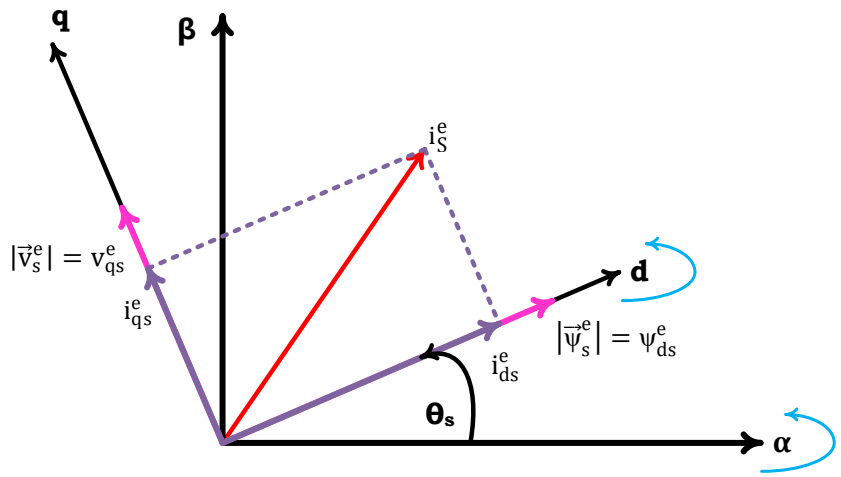

Figure 11. The relation between the flux and stator voltage space vectors [53].

Stator input active and reactive powers can be expressed in terms of the stator flux by separation of Equation (36) into its real and imaginary components, given in Equation (37) and Equation (38) [21, 32]:

$$P_s = \frac{3}{2}\omega_s(\psi_{ds}i_{qs} - \psi_{qs}i_{ds}) \tag{37}$$

$$Q_s = \frac{3}{2}\omega_s(\psi_{ds}i_{ds} + \psi_{qs}i_{qs}) \tag{38}$$

Equation (37) and (38) are derived assuming balanced grid voltage conditions. Under these conditions, the stator flux space vector in the positive synchronous reference frame will be a DC value, therefore it acts as a constant coefficient in the derivation as given in Equation (32).

As demonstrated in the preceding equations, active and reactive powers are less noisy and the output current is less distorted as a result of the reduced distortion in the stator flux compared to the case of voltage-based DPC implementation. This makes it possible to use a lower sampling frequency than what is used in DPC.

However, the required sampling frequency is still much higher than what is needed for FOC and SVM-DPC [54-57]. Equation (30) can be thought of as a first-order filtering of the stator voltage, yielding the stator flux linkage. Therefore, the unbalanced voltage effect on the stator flux is reduced [35].

The proposed stator flux-based DPC approach offers numerous advantages compared to conventional DPC. Several advantages include reduced noise in the output power, decreased current distortion, and lower sampling frequency. However, when compared to FOC, the proposed method suffers from variable switching frequency. Figure 12 depicts the block diagram for the stator flux-based DPC approach.

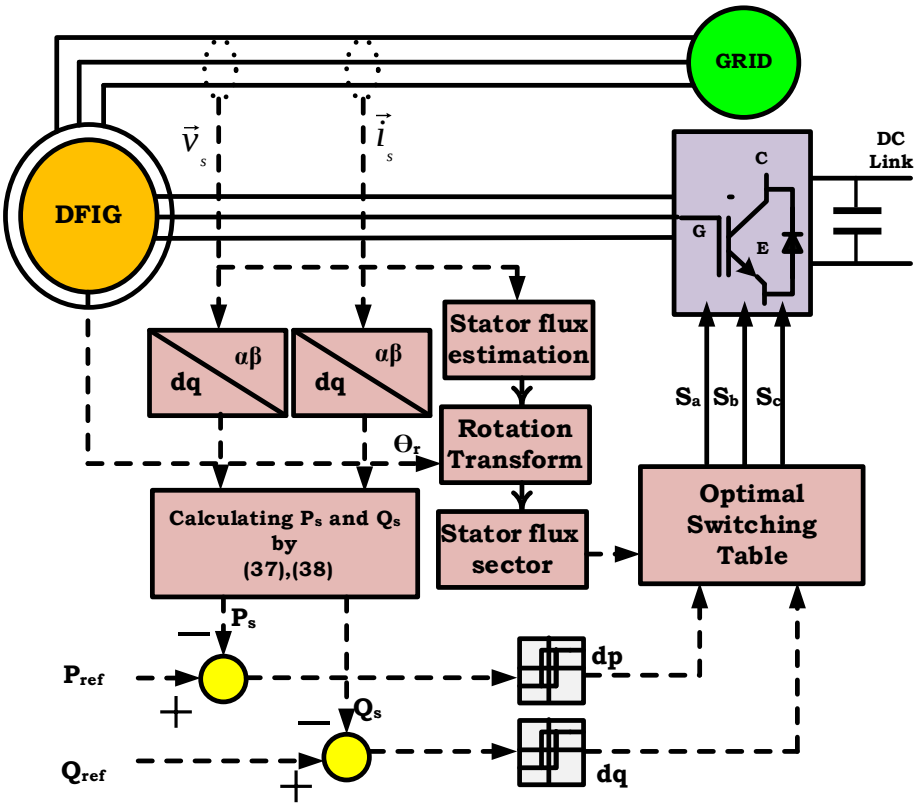

Figure 12. Block diagram of the proposed stator flux-based DPC method.

6. Computer simulation

This section will examine the performance of a grid-connected DFIG system using three controllers: the conventional DPC technique, as well as two DPC methods described in the article. The performance of the DFIG will be examined under both balanced and unbalanced grid voltages. The simulation is performed based on direct power control for the rotor side converter. For this purpose, MATLAB/ Simulink® software is used. The control of the grid-side converter is not addressed in this study. The DFIG parameters are presented in Table 4.

6.1. Direct power control under balanced conditions

In this case, the network voltage is considered balanced. For simplicity, a DC voltage source is used as the DC link in the simulations; in other words, the effect of the grid-side converter is neglected in this study. Figure 13 illustrates the tracking of stator active and reactive powers for a simulation time of four seconds. In the simulation, the stator active and reactive powers are set to -1200 KW and 0 KVAR, respectively. After two seconds, an active power step is applied with a value of 800 KW. Figure 13 demonstrates that the active and reactive powers reach their steady-state values within approximately 0.3 seconds. The rotor speed is taken to be constant throughout the simulation. This controller results in active and reactive powers that track their reference values with some fluctuations; nevertheless, the fluctuations are less than those caused by implementing a direct torque controller. The advantages of this controller include fast dynamic response and a simpler structure than other control algorithms. The following section will evaluate control performance under unbalanced voltage conditions.

Table 4. Simulation Parameters.

Line-to-line RMS voltage	300 V	**Magnetizing inductance**	84.7e-3 H
Stator resistance	0.531 Ω	**Grid frequency (Hz)**	60 Hz
Rotor resistance	0.408 Ω	**Moment of inertia**	0.02 Kg.m^2
Stator leakage inductance	2.5e-3 H	**Frictional coefficient**	0.01 $N.m.\text{sec}/rad$
Rotor leakage inductance	2.5e-3 H	**DC link voltage**	100 V

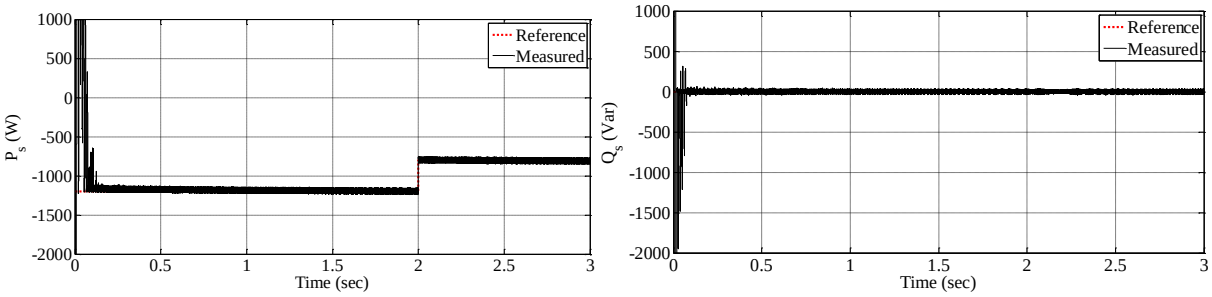

(a) (b)

Figure 13. measured and reference stator a) active power b) reactive power by conventional DPC controller (balanced conditions).

6.2. Direct power control under unbalanced conditions

This section investigates the performance of DFIGs using DPC controllers under unbalanced voltage conditions. Voltage unbalance can occur in the amplitude or phase angle of voltages. In this section, we will run simulations for both unbalances occurring simultaneously. Thus, as illustrated in Figure 14 unbalanced conditions occur within seconds 1-1.5 of simulation. Figures 14(a) and 14(b) show the three-phase stator voltage and current variations, respectively. It has been observed that unbalanced voltages cause harmonic components in stator current. Figure 14(c) depicts the rotor current of one phase. After one second of simulation, it is clear that unbalanced voltages caused deformation and harmonic components in the rotor current.

Figure 15(a) depicts the stator active power under unbalanced conditions, while Figure 15(b) depicts the stator reactive power under unbalanced conditions using conventional direct power control. Figure 15(a) and 15(b) show that a voltage dip (at second 1) caused severe active and reactive power oscillations, which could affect the rotor side converter, given that the converter's rated power is 25-30% of the generator power. After recovering from the voltage dip (at second 1.5), the controller achieves satisfactory performance in terms of tracking the reference powers. Figure 16 illustrates the performance of the proposed DPC method with a PI regulator. As previously stated, the stator current contains some harmonic content when the voltage is unbalanced. In this method, the stator current is first transformed into a positive-synchronous reference frame with the angle determined by the PLL. The proposed (HSF) filter separates the main component from the harmonic components. Only the positive sequence component of the stator current will be passed to the controller, resulting in less active and reactive power oscillations in Figure 16(a) and 16(b).

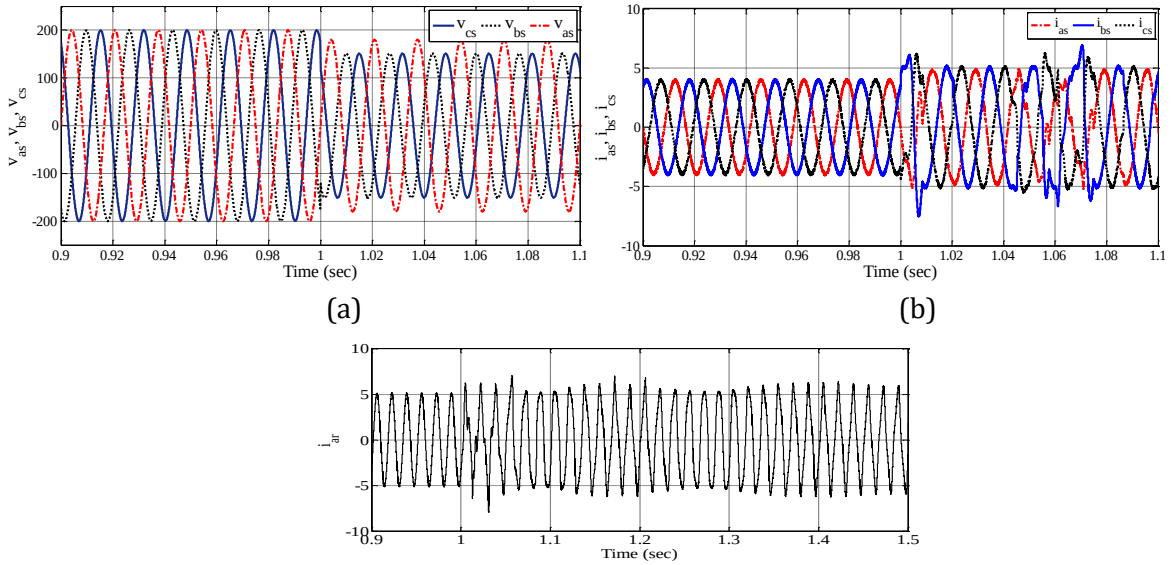

(a) (b)

(c)

Figure 14. a) v_{abcs} b) i_{abcs} c) i_{ar} : before and after voltage unbalance.

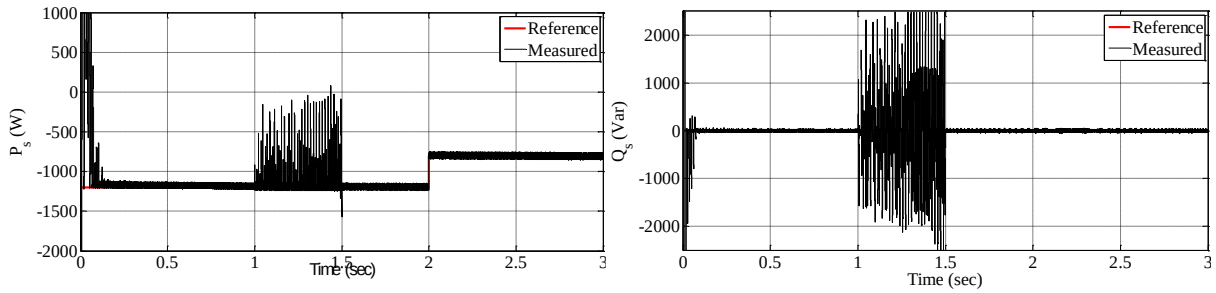

(a) (b)

Figure 15. Measured and reference stator a) active power b) reactive power using conventional DPC controller (unbalanced conditions).

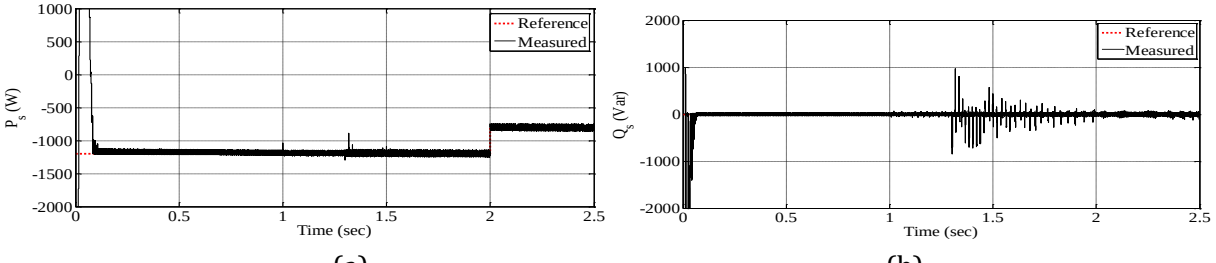

(a) (b)

Figure 16. Measured and reference stator a) active power b) reactive power using the proposed DPC method with PI regulator (unbalanced conditions).

The main advantages of this method are 1) accurate control with less stator harmonic current than conventional DPC, and 2) reduced stator power ripple. The main disadvantages of this method are increased implementation costs and a reduction in simulation speed due to the use of PI controllers. Figure 17 shows the positive, negative, and zero sequence components of the stator current. It is observed that the proposed control approach has resulted in stator currents with negligible negative and zero sequence components.

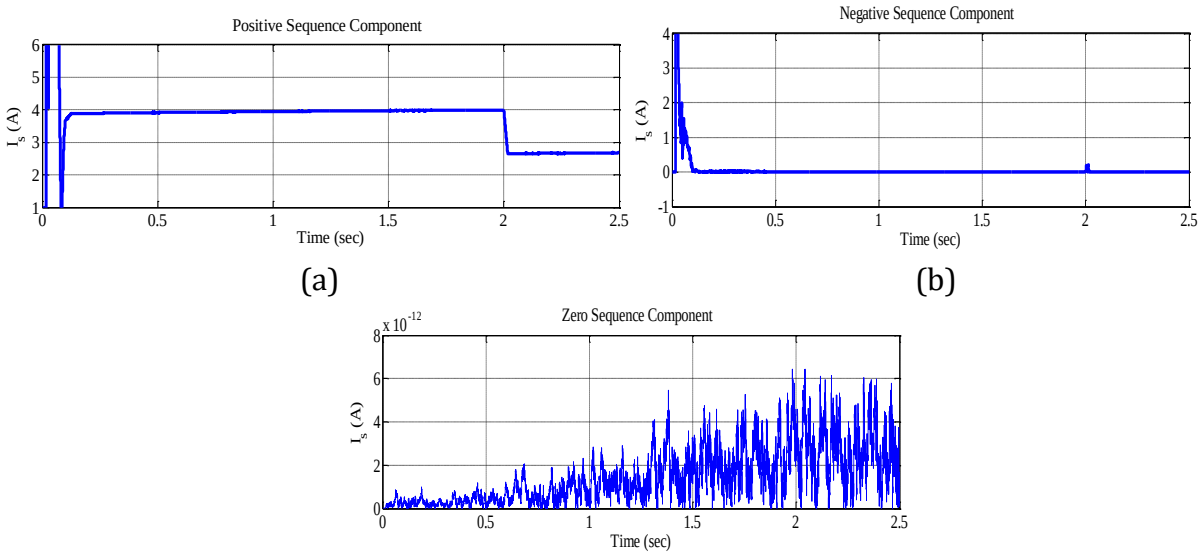

Figure 17. a) positive sequence, b) negative sequence, and c) zero sequence components of stator current.

Figure 18 depicts the stator and rotor currents for the proposed DPC method with a PI regulator under unbalanced voltage conditions. This method significantly reduces stator current distortion and produces sinusoidal currents. Figure 18(b) shows less rotor current deformation after 1 second compared to Figure 14(c), indicating superior control performance. Figure 19(a) and 19(b) illustrate the measured stator active and reactive powers using the proposed stator flux-based DPC method. As shown in the figures, the proposed control performs better with less oscillation than the conventional DPC.

The active and reactive power ripples have been significantly reduced, eliminating the need for positive and negative sequence separation. This controller can be used to stabilize the DC link voltage and regulate power exchange with the network and converter. The simulation results also show that the stator current has a lower THD. Unbalanced voltage has a smaller effect on stator flux than stator voltage, so power ripple is reduced. Figure 20 depicts a three-phase stator current and single-phase rotor current under unbalanced voltage conditions.

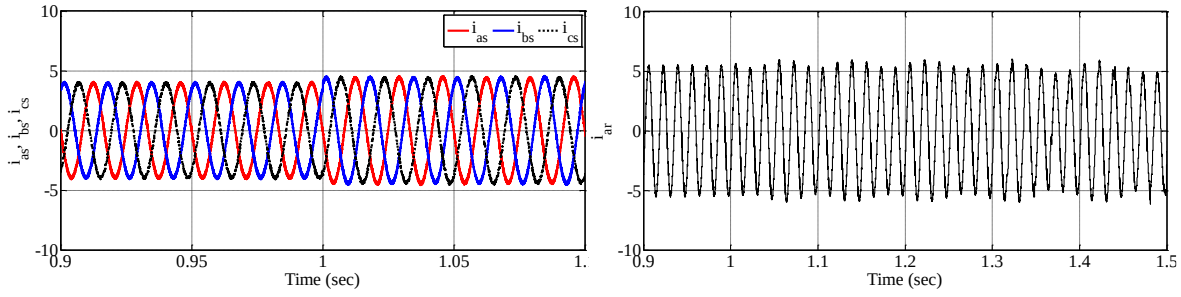

Figure 18. DFIG a) stator current b) rotor current using the proposed DPC with PI regulator under unbalanced conditions.

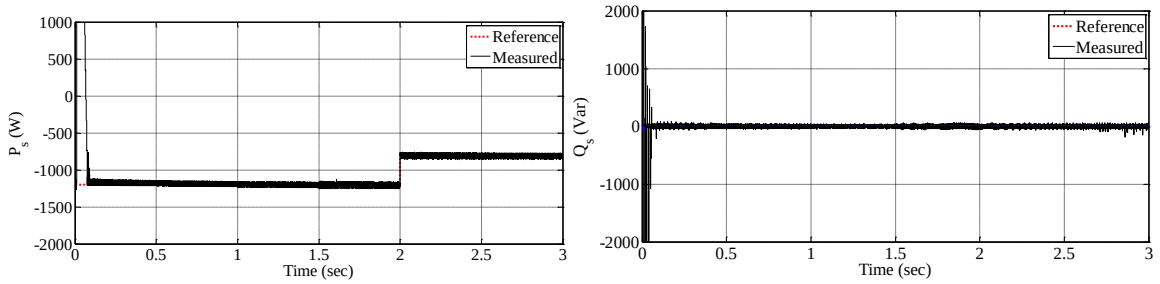

(a) (b)

Figure 19. Measured and reference stator a) active power b) reactive power using the proposed stator flux-based DPC controller under unbalanced conditions.

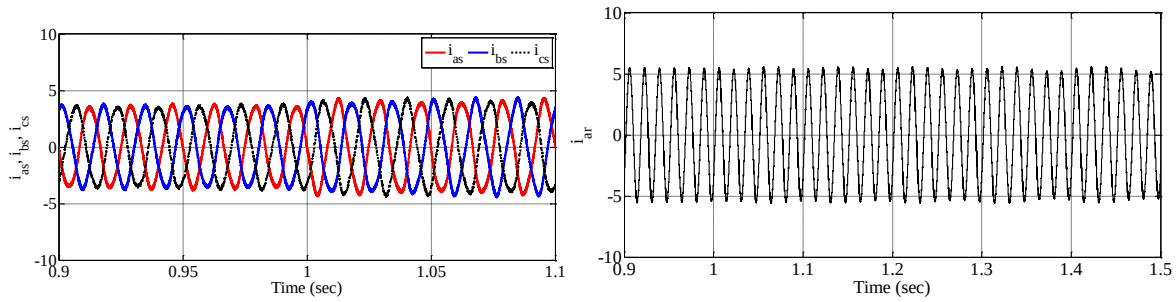

(a) (b)

Figure 20. DFIG a) stator current b) rotor current using the proposed stator flux-based DPC controller under unbalanced conditions**.**

The proposed method leads to less distortion of stator and rotor currents in comparison to Figure 14. Figure 21(a) and 21(b) show the stator current THD under unbalanced conditions for the conventional DPC method and the proposed DPC method with PI regulator, respectively. As shown in the figure, the stator current THD with the proposed DPC method with PI regulator is significantly lower than with the conventional DPC method. The main harmonics in DPC with PI regulator are the third, fifth, and seventh.

The main harmonics for the stator flux-based DPC method are the third and fifth harmonics, as Figure 21(c) illustrates. This figure shows that THD is significantly lower than with the conventional DPC method under unbalanced grid voltage conditions. While the conventional DPC method experiences power and torque fluctuations under unbalanced voltage conditions, the proposed methods provide a smoother, less fluctuating, and faster dynamic response in the event of voltage unbalanced or dip conditions.

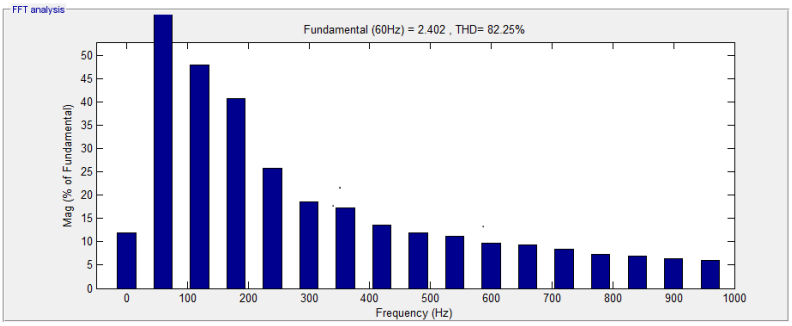

(a)

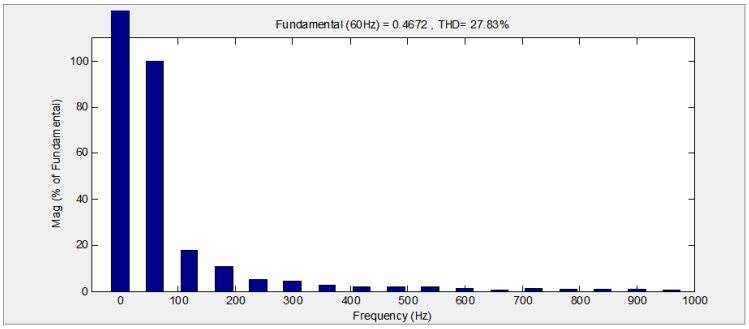

(b)

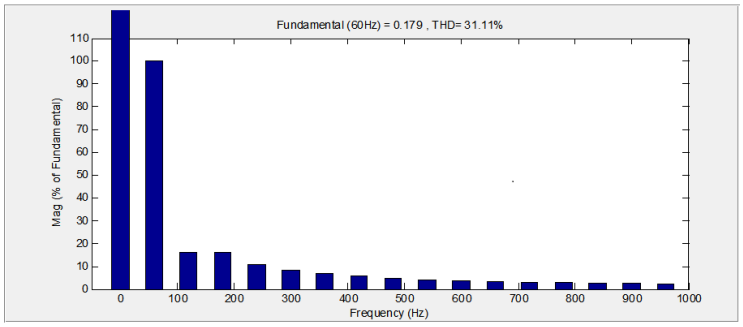

(c)

Figure 21. stator current THD under unbalanced conditions, a) Conventional DPC method, b) Proposed DPC method with PI regulator, c) Proposed stator flux-based DPC method**.**

In this paper, in the first proposed method, a novel HSF filter was proposed to extract the fundamental component of stator current and inject it into the controller during fault conditions; it was observed that the proposed controller can mitigate power and torque fluctuations while also reducing stator current THD. Using hysteresis comparators resulted in faster dynamic response and greater robustness than PWM techniques. The flux-based stator DPC method was the second alternative to the conventional DPC method. The simulation results demonstrate the efficacy of this method. Table 5 is provided for a comprehensive comparison of the approaches. The table differentiates between the structure and performance of the proposed PI-DPC method and the stator flux-based DPC method compared to the conventional DPC method.

Table 5. comparison of the proposed PI-DPC method and Stator flux-based DPC method with the conventional DPC method**.**

	PI-DPC	Stator flux-based DPC
Generator power ripple	Lower	Lower
Rotor speed ripple	Lower	Lower
RSC PWM	No	No
Number of PI controllers	Two	-
Controller bandwidth	Higher	Higher
Steady-state response	Smoother	Smoother
Transient response	slower with less overshoot and fluctuations	Faster with less overshoot and fluctuations
Complexity	More	Similar
Current THD	Lower	Lower

7. Conclusion

This paper described theoretical improvements in DFIG-based wind energy conversion systems under balanced and unbalanced grid voltage conditions. A dynamic model based on space vector relations in the rotor reference frame was examined. In the next step, the performance of DFIG under unbalanced voltage conditions was investigated. It was demonstrated that unbalanced voltages result in both positive and negative components in the current and voltage, which contribute to an increase in active and reactive power ripple as well as current THD. Methods for improving DFIG performance were briefly introduced. Direct power control with a PI regulator results in better performance and less power ripple due to the injection of positive sequence components of stator current into the controller under unbalanced voltage conditions. Stator flux-based DPC combines the advantages of DPC and FOC. These benefits include a low THD of the output currents and a straightforward implementation process (in comparison to predictive DPC). Additionally, this controller is more cost-effective than other options that were examined, and it also produces lower power ripples. Simulation results confirmed an improvement in control system performance compared to conventional DPC without requiring significant changes to the controller structure. The THD of stator current under unbalanced conditions was found to be approximately 82% for the conventional DPC method, while it was reduced to approximately 27% and 31% for the proposed DPC methods with PI regulator and stator flux-based method, respectively. The direct power control method is compared to other control methods, including predictive control, vector control, direct torque control, and DPC-SVM. Although it improves control and reduces oscillations in power and switching frequency, it also increases controller complexity and slows dynamic response. To enhance the reactive power capability and voltage stability of the wind turbine system, it is recommended to integrate a static compensator (STATCOM) at the connection point in future work.

APPENDIX A:

The moduli of stator flux ($\left|\vec{\psi}_s^r\right|$) are constant due to direct connection to the grid. The following expressions are used:

$$\vec{i}_s^r = \frac{\vec{\psi}_s^r}{\sigma L_s} - \frac{\vec{\psi}_r^r L_m}{\sigma L_s L_r} \qquad \text{(a1)}$$

$$\dot{\vec{\psi}}_s^r = \left|\vec{\psi}_s^r\right| j\dot{\theta}_s e^{j\omega_s t} = j(\omega_s - \omega_m)\vec{\psi}_s^r$$

Replacing $\vec{i}_s^r$ and $\dot{\vec{\psi}}_s^r$ in (1) gives:

$$P_s = \frac{3}{2}\mathrm{Re}\{(j(\omega_s - \omega_m)\vec{\psi}_s^r + j\omega_m\vec{\psi}_s^r)\cdot(\frac{\vec{\psi}_s^r}{\sigma L_s} - \frac{L_m\vec{\psi}_r^r}{\sigma L_s L_r})^*\} = \frac{3}{2}\mathrm{Re}\{(j(\omega_s\vec{\psi}_s^r)\cdot(\frac{\vec{\psi}_s^r}{\sigma L_s} - \frac{L_m\vec{\psi}_r^r}{\sigma L_s L_r})^*\}$$

Keeping in mind that:

$$\frac{3}{2}\mathrm{Re}\{(j(\omega_s\vec{\psi}_s^r)\cdot(\frac{\vec{\psi}_s^r}{\sigma L_s})^*\} = 0$$

The active power expression can be simplified as follows:

$$P_s = -\frac{3}{2}\frac{L_m}{\sigma L_s L_r}\omega_s \operatorname{Re}\{(j\vec{\psi}_s^r \vec{\psi}_r^{r*})\} \quad \text{(a2)}$$

This can also be written in terms of the moduli of stator flux, moduli of rotor flux, and the angle (θ_ψ) between them:

$$P_s = -\frac{3}{2}\frac{L_m}{\sigma L_s L_r}\omega_s \left|\vec{\psi}_s^r\right|\left|\vec{\psi}_r^r\right|\cos(90-\theta_\psi)$$
$$P_s = -\frac{3}{2}\frac{L_m}{\sigma L_s L_r}\omega_s \left|\vec{\psi}_s^r\right|\left|\vec{\psi}_r^r\right|\sin\theta_\psi \quad \text{(a3)}$$

Similarly, replacing (a1) in (2) gives:

$$Q_s = -\frac{3}{2}\operatorname{Im}\{(j(\omega_s-\omega_m)\vec{\psi}_s^r + j\omega_m\vec{\psi}_s^r).(\frac{\vec{\psi}_s^r}{\sigma L_s} - \frac{L_m\vec{\psi}_r^r}{\sigma L_s L_r})^*\} = -\frac{3}{2}\operatorname{Im}\{(j(\omega_s\vec{\psi}_s^r).(\frac{\vec{\psi}_s^r}{\sigma L_s} - \frac{L_m\vec{\psi}_r^r}{\sigma L_s L_r})^*\}$$

$$= -\frac{3}{2}\frac{\omega_s}{\sigma L_s}\operatorname{Im}\{j\vec{\psi}_s^r.\vec{\psi}_s^{r*} - j\vec{\psi}_s^r\frac{L_m}{L_r}\vec{\psi}_r^{r*}\} = -\frac{3}{2}\frac{\omega_s}{\sigma L_s}.\left|\vec{\psi}_s^r\right|^2 + \frac{3}{2}\frac{\omega_s}{\sigma L_s}\frac{L_m}{L_r}\operatorname{Im}\{j\vec{\psi}_s^r\vec{\psi}_r^{r*}\}$$

Using the identity

$$\operatorname{Im}\{j\vec{\psi}_s^r\vec{\psi}_r^{r*}\} = \operatorname{Re}\{\vec{\psi}_s^r\vec{\psi}_r^{r*}\}$$

Stator reactive power can be written as (a4):

$$Q_s = \frac{3}{2}\frac{\omega_s}{\sigma L_s}\left|\vec{\psi}_s^r\right|(\frac{L_m}{L_r}\left|\vec{\psi}_r^r\right|\cos\theta_\psi - \left|\vec{\psi}_s^r\right|) \quad \text{(a4)}$$

References

[1] S. E. Aimani, "Modeling and Control Structures for Variable Speed Wind Turbine." *International Conference on Multimedia Computing and Systems*, pp. 1-5, 2011.

[2] F. Iov, and F. Blaabjerg, "Power Electronics and Control for Wind Power Systems." *Power Electronics and Machines in Wind Applications proceedings of international conference in Lincoln, USA*, pp. 1-16. 2009.

[3] R. Cardenas, R. Peña, S. Alepuz, and G. Asher, "Overview of Control Systems for the Operation of DFIGs in Wind Energy Applications," *IEEE Transactions on Industrial Electronics*, vol. 60, no. 7, pp. 2776-2798, 2013.

[4] A. Bouafia, F. Krim, and J. P. Gaubert, "Design and Implementation of High Performance Direct Power Control of Three-Phase PWM Rectifier, via Fuzzy and PI Controller for Output Voltage Regulation," *Energy conversion and management*, vol. 50, no. 1, pp. 6-13, 2009.

[5] J. Hu, L. Shang, Y. He, and Z. Q. Zhu, "Direct Active and Reactive Power Regulation of Grid-Connected DC/AC Converters Using Sliding Mode Control Approach," *IEEE transactions on power electronics*, vol. 26, no. 1, pp. 210-222, 2010.

[6] P. Antoniewicz, and M. P. Kazmierkowski, "Virtual-Flux-Based Predictive Direct Power Control of AC/DC Converters with Online Inductance Estimation," *IEEE Transactions on Industrial Electronics*, vol. 55, no. 12, pp.4381-4390, 2008.

[7] S. Peresada, A. Tilli, and A. Tonielli, "Indirect Stator Flux-Oriented Output Feedback Control of a Doubly Fed Induction Machine," *IEEE Transactions on Control Systems Technology*, vol. 11, no. 6 pp. 875-888, 2003.

[8] A. Ramkumar, S. Durairaj, and K. Dhivya, "Behavior of DFIG With Direct Torque Controller at Unbalanced and Distorted Grid Voltage Conditions," *Applied Mechanics and Materials*, vol. 626, pp. 150-154, 2014.

[9] S. Arnalte, J. C. Burgos, and J. L. Rodriguez-Amenedo, "Direct Torque Control of A Doubly-Fed Induction Generator for Variable Speed Wind Turbines," *Electric power components and systems*, vol. 30, no. 2, pp. 199-216, 2002.
[10] Y. Djeriri, A. Meroufel, A. Massoum, and Z. Boudjema, "A Comparative Study Between Field Oriented Controlstrategy and Direct Power Control Strategy for DFIG," *Journal of Electric Engineering*, vol. 14, no. 2, pp. 9-9, 2014.
[11] M. Malinowski, M. Jasinski, and M. P. Kazmierkowski, "Simple Direct Power Control of Three-Phase PWM Rectifier using Space-Vector Modulation (DPC-SVM)," *IEEE Transactions on Industrial Electronics*, vol. 51, no. 2, pp. 447-454, 2004.
[12] S. A. Larrinaga, M. A. Rodriguez Vidal, E. Oyarbide, and J. R. Torrealday Apraiz, "Predictive Control Strategy for DC/AC Converters Based on Direct Power Control," *IEEE Transactions on Industrial Electronics*, vol. 54, no. 3, pp. 1261-1271, 2007.
[13] W. S. Kim, S. T. Jou, K. B. Lee, and S. Watkins, "Direct Power Control of a Doubly Fed Induction Generator with a Fixed Switching Frequency," *IEEE Industry Applications Society Annual Meeting*, pp. 1-9, 2008.
[14] D. Casadei, G. Serra, and A. Tani, "Improvement of Direct Torque Control Performance by using a Discrete SVM Technique," *29th Annual IEEE Power Electronics Specialists Conference (Cat. No. 98CH36196)*, vol. 2, pp. 997-1003, 1998.
[15] D. Sun, and X. Wang, "Low-Complexity Model Predictive Direct Power Control for DFIG Under Both Balanced and Unbalanced Grid Conditions," *IEEE Transactions on Industrial Electronics*, vol. 63, no. 8, pp. 5186-5196, 2016.
[16] Y. Zhang, J. Jiao, et al., "Model Predictive Direct Power Control of Doubly Fed Induction Generators Under Balanced and Unbalanced Network Conditions," *IEEE Transactions on Industry Applications*, vol. 56, no. 1, pp. 771-786, 2019.
[17] M. E. Zarei, C. Veganzones Nicolás, and J. Rodríguez Arribas, "Improved Predictive Direct Power Control of Doubly Fed Induction Generator During Unbalanced Grid Voltage Based on Four Vectors," *IEEE Journal of Emerging and Selected Topics in Power Electronics*, vol. 5, no. 2, pp. 695-707, 2016.
[18] L. Li, H. Nian, L. Ding, and B. Zhou, "Direct Power Control of DFIG System Without Phase-Locked Loop Under Unbalanced and Harmonically Distorted Voltage," *IEEE Transactions on Energy Conversion*, vol. 33, no. 1, pp. 395-405, 2017.
[19] E. Ozsoy, B. Soner, et al., "Disturbance Observer Based Power Control of DFIG Under Unbalanced Network Conditions," *Electric Power Components and Systems*, vol. 46, no. 13, pp. 1448-1461, 2018.
[20] M. Jahanpour-Dehkordi, S. Vaez-Zadeh, and J. Mohammadi, "Development of a Combined Control System to Improve the Performance of a PMSG-Based Wind Energy Conversion System Under Normal and Grid Fault Conditions," *IEEE Transactions on Energy Conversion*, vol. 34, no. 3, pp. 1287-1295, 2019.
[21] S. S. Lee, and Y. E. Heng, "Table-Based DPC for Grid Connected VSC under Unbalanced and Distorted Grid Voltages: Review and Optimal Method," *Renewable and Sustainable Energy Reviews*, vol. 76, pp. 51-61, 2017.
[22] A. Izanlo, S. A. Gholamian, and M. V. Kazemi, "Using of Four-Switch Three-Phase Converter in the Structure DPC of DFIG Under Unbalanced Grid Voltage Condition," *Electrical Engineering*, vol. 100, no. 3, pp. 1925-1938, 2018.
[23] J. Mohammadi, S. Vaez-Zadeh, S. Afsharnia, and E. Daryabeigi, "A Combined Vector and Direct Power Control for DFIG-Based Wind Turbines," *IEEE Transactions on Sustainable Energy*, vol. 5, no. 3, pp. 767-775, 2014.
[24] G. N. González, C. H. De Angelo, and D. A. Aligia, "A Control Strategy for DFIG-Based Systems Operating under Unbalanced Grid Voltage Conditions," *International Journal of Electrical Power & Energy Systems*, vol. 142, 108273, 2022.
[25] P. Cheng, C. Wu, F. Ning, and J. He, "Voltage Modulated DPC Strategy of DFIG Using Extended Power Theory under Unbalanced Grid Voltage Conditions," *Energies*, vol. 13, no. 22, p. 6077, 2020.
[26] E. G. Shehata, "Improved Power Control of DFIGs Driven by Wind Turbine under Unbalanced Grid Voltage," *Journal of Electrical Engineering & Technology*, vol. 19, no. 1, pp. 325-340, 2024.

[27] S. Gao, H. Zhao, et al., "Novel Direct Power Control for DFIG With Parallel Compensator under Unbalanced Grid Condition," *IEEE Transactions on Industrial Electronics*, vol. 68, no. 10, pp. 9607-9618, 2021.

[28] S. Das, and B. Singh, "Enhanced Control of DFIG Based Wind Energy Conversion System Under Unbalanced Grid Voltages Using Mixed Generalized Integrator," *IEEE Journal of Emerging and Selected Topics in Industrial Electronics*, vol. 3, no. 2, pp. 308-320, 2020.

[29] X. Ran, B. Xu, K. Liu, and J. Zhang, " An Improved Low-Complexity Model Predictive Direct Power Control with Reduced Power Ripples Under Unbalanced Grid Conditions" *IEEE Transactions on Power Electronics*, vol. 37, no. 5, pp. 5224-5234, 2022.

[30] L. Xu, and Y. Wang, "Dynamic Modeling and Control of DFIG-Based Wind Turbines Under Unbalanced Network Conditions," *IEEE Transactions on Power Systems*, vol. 22, no. 1, pp. 314-323, 2007.

[31] L. Xu, and P. Cartwright, "Direct Active and Reactive Power Control of DFIG for Wind Energy Generation," *IEEE Transactions on energy conversion*, vol 21, no. 3, pp. 750-758, 2006.

[32] G. Abad, J. Lopez, M. Rodriguez, L. Marroyo, and G. Iwanski, "Doubly fed induction machine: modeling and control for wind energy generation," vol. 85. *John Wiley & Sons*, 2011.

[33] Y. Zhang, C. Qu, Z. Li, and Y. Zhang, "Mechanism Analysis and Experimental Study of Table-Based Direct Power Control," *International Conference on Electrical Machines and Systems (ICEMS)*, pp. 2213-2218, 2013.

[34] F. Senani, A. Rahab, F. Louar, F. Bourourou, and H. Benalla, "Active and Reactive Power Control of DFIG using PI and DPC Controllers," *International Conference on Electrical Engineering (ICEE)*, pp. 1-6, 2015.

[35] M. Malinowski, M. P. Kazmierkowski, S. Hansen, F. Blaabjerg, and G. Marques. "Virtual Flux Based Direct Power Control of Three-Phase PWM Rectifiers," *IEEE Transactions on Industry Applications*, vol. 37, no. 4, pp. 1019-1027, 2001.

[36] J. Hu, J. Zhu, et al., "Predictive Direct Virtual Torque and Power Control of Doubly Fed Induction Generators for Fast and Smooth Grid Synchronization and Flexible Power Regulation," *IEEE Transactions on Power Electronics*, vol. 28, no. 7, pp. 3182-3194, 2012.

[37] G. Abad, M. Á. Rodríguez, and J. Poza, "Two-Level VSC Based Predictive Direct Torque Control of the Doubly Fed Induction Machine with Reduced Torque and Flux Ripples at Low Constant Switching Frequency," *IEEE transactions on power electronics*, vol. 23, no. 3, pp. 1050-1061, 2008.

[38] W. Wenjun, Z. Yanru, and W. Jianjun, "The Comparative Study of Different Methods About Constructing Switching Table in DPC for Three-Level Rectifier," *The 2nd International Symposium on Power Electronics for Distributed Generation Systems*, pp. 314-319, 2010.

[39] A. Hemdani, M. J. B. Ghorbal, M. W. Naouar, and I. Slama-Belkhodja, "Design of A Switching Table for Direct Power Control of a DFIG using Sliding Mode Theory," *Eighth International Multi-Conference on Systems, Signals & Devices*, pp. 1-7, 2011.

[40] J. Eloy-Garcia, and R. Alves, "DSP-Based Direct Power Control of a VSC with Voltage Angle Estimation," *IEEE/PES Transmission & Distribution Conference and Exposition: Latin America*, pp. 1-5, 2006.

[41] K. Kulikowski, and A. Sikorski, "New DPC Look-Up Table Methods for Three-Level AC/DC Converter," *IEEE Transactions on Industrial Electronics*, vol. 63, no. 12, pp. 7930-7938, 2016.

[42] Y. Zhang, and C. Qu, "Table-Based Direct Power Control for Three-Phase AC/DC Converters Under Unbalanced Grid Voltages," *IEEE Transactions on Power Electronics*, vol. 30, no. 12, pp. 7090-7099, 2015.

[43] A. Ben Amer, S. Belkacem, and T. Mahni, "Direct Torque Control of a Doubly Fed Induction Generator," *International Journal of Energetica*, vol. 2, no. 1, pp. 11-14, 2017.

[44] T. Noguchi, H. Tomiki, S. Kondo, and I. Takahashi, "Direct Power Control of PWM Converter without Power Source Voltage Sensors," *IAS'96. Conference Record of the 1996 IEEE Industry Applications Conference Thirty-First IAS Annual Meeting*, vol. 2, pp. 941-946, 1996.

[45] M. J. Zandzadeh, and A. Vahedi, "Modeling and Improvement of Direct Power Control of DFIG under Unbalanced Grid Voltage Condition," *International Journal of Electrical Power & Energy Systems*, vol. 59, pp. 58-65, 2014.

[46] T. Brekken, N. Mohan, and T. Undeland, "Control of a Doubly-Fed Induction Wind Generator Under Unbalanced Grid Voltage Conditions," *European Conference on Power Electronics and Applications*, pp. 10, 2005.
[47] F. Soares dos Reis, J. A. V. Alé, et al., "Active Shunt Filter for Harmonic Mitigation in Wind Turbines Generators," *37th IEEE Power Electronics Specialists Conference*, pp. 1-6, 2006.
[48] S. A. Papathanassiou, and M. P. Papadopoulos, "Harmonic Analysis in a Power System with Wind Generation," *IEEE Transactions on power delivery*, vol. 21, no. 4, pp. 2006-2016, 2006.
[49] S. K. Jain, and P. Agarwal, "Design Simulation and Experimental Investigations, on a Shunt Active Power Filter for Harmonics, and Reactive Power Compensation," *Electric Power Components and Systems*, vol. 31, no.7, pp.671-692, 2003.
[50] D. De Santis, and M. Chen, "Design of Active Low Pass Filters to Reduce Harmonic Current Emission," *IECON 2017-43rd Annual Conference of the IEEE Industrial Electronics Society*, pp. 1059-1065, 2017.
[51] A. Gaillard, P. Poure, S. Saadate, and M. Machmoum, "Variable Speed DFIG Wind Energy System for Power Generation and Harmonic Current Mitigation," *Renewable Energy*, vol. 34, no. 6, pp. 1545-1553, 2009.
[52] H. S. Song, H. G. Park, and K. Nam, "An Instantaneous Phase Angle Detection Algorithm under Unbalanced Line Voltage Condition," *Annual IEEE Power Electronics Specialists Conference. Record. (Cat. No.99CH36321),* pp. 533-537, 1999.
[53] F. Mulolani, "Performance of Direct Power Controlled Grid-Connected Voltage Source Converters," Ph.D. dissertation, Newcastle University, 2017.
[54] M. P. Kazmierkowski, R. Krishnan, F. Blaabjerg, and J. D. Irwin, Eds., "Control in Power Electronics: Selected Problems", Academic Press, 2002.
[55] S. Kouadria, E. M. Berkouk, Y. Messlem, and M. Denai, "Improved Control Strategy of DFIG-Based Wind Turbines using Direct Torque and Direct Power Control Techniques," *Journal of Renewable and Sustainable Energy*, vol. 10, no. 4, 2018.
[56] T. Sutikno, N. R. N. Idris, and A. Jidin, "A Review of Direct Torque Control of Induction Motors for Sustainable Reliability snd Energy Efficient Drives," *Renewable and sustainable energy reviews*, vol. 32, pp. 548-558, 2014.
[57] P. Gajewski, and K. Pieńkowski, "Advanced Control of Direct-Driven PMSG Generator in Wind Turbine System," *Archives of Electrical Engineering*, vol. 65, no. 4, pp.643-656, 2016.

Declaration of Competing Interest

The authors declare that they have no known competing financial interests or personal relationships that could have appeared to influence the work reported in this paper. The ethical issues, including plagiarism, informed consent, misconduct, data fabrication and/or falsification, double publication and/or submission, redundancy, have been completely observed by the authors.

Credit Authorship Contribution Statement

Mohammad Naser Hashemnia: Conceptualization, Formal analysis, Investigation, Methodology, Resources, Software, Supervision, Validation, Visualization, Roles/Writing-original draft, Writing-review & editing. **Ali Dehghan Nayeri:** Conceptualization, Software, Validation, Roles/Writing-original draft.

Bibliography

Mohammad Naser Hashemnia was born in Mashhad, Iran, in 1983. He received the B.S. degree in electrical power engineering from Ferdowsi University, Mashhad, Iran, in 2006 and the M.S. degree in electrical power engineering from the University of Tehran, Tehran, Iran, in 2008. He earned his Ph.D. degree in electrical power engineering from Sharif University of Technology, Tehran, Iran in 2013. Since 2015 he has been an assistant professor in Mashhad branch, Islamic Azad University, Mashhad, Iran. His primary research interests are electric machine analysis, modeling, and simulation, innovative electrical drive control approaches, and renewable energy systems.

Ali Dehghan Nayeri was born in Mashhad, Iran, in 1991. He received the B.S. degree in electronic engineering from Eqbal lahoori University, Mashhad, Iran, in 2014 and the M.S. degree in electrical power and renewable energy from Islamic Azad University, Mashhad, Iran, in 2019. His main research interests include analysis, programing and simulation of electric machines, automation and programming control and artificial intelligence.